

Search for continuous gravitational waves from known pulsars in the first part of the fourth LIGO-Virgo-KAGRA observing run

A. G. ABAC,¹ R. ABBOTT,² I. ABOUELFETTOUH,³ F. ACERNESE,^{4,5} K. ACKLEY,⁶ S. ADHICARY,⁷ N. ADHIKARI,⁸
R. X. ADHIKARI,² V. K. ADKINS,⁹ D. AGARWAL,^{10,11} M. AGATHOS,¹² M. AGHAEI ABCHOUYEH,¹³ O. D. AGUIAR,¹⁴
I. AGUILAR,¹⁵ L. AIELLO,^{16,17,18} A. AIN,¹⁹ P. AJITH,²⁰ T. AKUTSU,^{21,22} S. ALBANESI,^{23,24,25} R. A. ALFAIDI,²⁶
A. AL-JODAH,²⁷ C. ALLÉNÉ,²⁸ A. ALLOCCA,^{29,5} S. AL-SHAMMARI,¹⁸ P. A. ALTIN,³⁰ S. ALVAREZ-LOPEZ,³¹ A. AMATO,^{32,33}
L. AMEZ-DROZ,³⁴ A. AMOROSI,³⁴ C. AMRA,³⁵ A. ANANYEVA,² S. B. ANDERSON,² W. G. ANDERSON,² M. ANDIA,³⁶
M. ANDO,³⁷ T. ANDRADE,³⁸ N. ANDRES,²⁸ M. ANDRÉS-CARCASONA,³⁹ T. ANDRIĆ,^{40,41,1,42} J. ANGLIN,⁴³ S. ANSOLDI,^{44,45}
J. M. ANTELLIS,⁴⁶ S. ANTIER,⁴⁷ M. AOUMI,⁴⁸ E. Z. APPAVURAVTHER,^{49,50} S. APPERT,² S. K. APPLE,⁵¹ K. ARAI,²
A. ARAYA,³⁷ M. C. ARAYA,² J. S. AREEDA,⁵² L. ARGIANAS,⁵³ N. ARITOMI,³ F. ARMATO,^{54,55} N. ARNAUD,^{36,56}
M. AROGETI,⁵⁷ S. M. ARONSON,⁹ G. ASHTON,⁵⁸ Y. ASO,^{21,59} M. ASSIDUO,^{60,61} S. ASSIS DE SOUZA MELO,⁵⁶ S. M. ASTON,⁶²
P. ASTONE,⁶³ F. ATTADIO,^{64,63} F. AUBIN,⁶⁵ K. AULTONEAL,⁶⁶ G. AVALLONE,⁶⁷ S. BABAK,⁶⁸ F. BADARACCO,⁶⁴
C. BADGER,⁶⁹ S. BAE,⁷⁰ S. BAGNASCO,²³ E. BAGUI,⁷¹ J. G. BAIER,⁷² L. BAIOTTI,⁷³ R. BAJPAI,²¹ T. BAKA,⁷⁴ M. BALL,⁷⁵
G. BALLARDIN,⁵⁶ S. W. BALLMER,⁷⁶ S. BANAGIRI,⁷⁷ B. BANERJEE,⁴² D. BANKAR,¹¹ P. BARAL,⁸ J. C. BARAYOGA,²
B. C. BARISH,² D. BARKER,³ P. BARNEO,^{38,78} F. BARONE,^{79,5} B. BARR,²⁶ L. BARSOTTI,³¹ M. BARSUGLIA,⁶⁸ D. BARTA,⁸⁰
A. M. BARTOLETTI,⁸¹ M. A. BARTON,²⁶ I. BARTOS,⁴³ S. BASAK,²⁰ A. BASALAEV,⁸² R. BASSIRI,¹⁵ A. BASTI,^{83,84}
D. E. BATES,¹⁸ M. BAWAJ,^{85,49} P. BAXI,⁸⁶ J. C. BAYLEY,²⁶ A. C. BAYLOR,⁸ P. A. BAYNARD II,⁵⁷ M. BAZZAN,^{87,88}
V. M. BEDAKIHALE,⁸⁹ F. BEIRNAERT,⁹⁰ M. BEJGER,⁹¹ D. BELARDINELLI,¹⁷ A. S. BELL,²⁶ V. BENEDETTO,⁹² W. BENOIT,⁹³
J. D. BENTLEY,⁸² M. BEN YAALA,⁹⁴ S. BERA,⁹⁵ M. BERBEL,⁹⁶ F. BERGAMIN,^{40,41} B. K. BERGER,¹⁵ S. BERNUZZI,²⁴
M. BEROIZ,² D. BERSANETTI,⁵⁴ A. BERTOLINI,³³ J. BETZWIESER,⁶² D. BEVERIDGE,²⁷ N. BEVINS,⁵³ R. BHANDARE,⁹⁷
U. BHARDWAJ,^{98,33} R. BHATT,² D. BHATTACHARJEE,^{72,99} S. BHAUMIK,⁴³ S. BHOWMICK,¹⁰⁰ A. BIANCHI,^{33,101}
I. A. BILENKO,¹⁰² G. BILLINGSLEY,² A. BINETTI,¹⁰³ S. BINI,^{104,105} O. BIRNHOLTZ,¹⁰⁶ S. BISCOVEANU,⁷⁷ A. BISHT,⁴¹
M. BITOSSI,^{56,84} M.-A. BIZOUARD,⁴⁷ J. K. BLACKBURN,² L. A. BLAGG,⁷⁵ C. D. BLAIR,^{27,62} D. G. BLAIR,²⁷ F. BOBBA,^{67,107}
N. BODE,^{40,41} G. BOILEAU,^{19,47} M. BOLDRINI,^{64,63} G. N. BOLINGBROKE,¹⁰⁸ A. BOLLIAND,^{109,35} L. D. BONAVENTA,⁸⁷
R. BONDARESCU,³⁸ F. BONDU,¹¹⁰ E. BONILLA,¹⁵ M. S. BONILLA,⁵² A. BONINO,¹¹¹ R. BONNAND,²⁸ P. BOOKER,^{40,41}
A. BORCHERS,^{40,41} V. BOSCHI,⁸⁴ S. BOSE,¹¹² V. BOSSILKOV,⁶² V. BOUDART,¹¹³ A. BOUDON,¹¹⁴ A. BOZZI,⁵⁶
C. BRADASCHIA,⁸⁴ P. R. BRADY,⁸ M. BRAGLIA,¹¹⁵ A. BRANCH,⁶² M. BRANCHESI,^{42,116} J. BRANDT,⁵⁷ I. BRAUN,⁷²
M. BRESCHI,²⁴ T. BRIANT,¹¹⁷ A. BRILLET,⁴⁷ M. BRINKMANN,^{40,41} P. BROCKILL,⁸ E. BROCKMUELLER,^{40,41} A. F. BROOKS,²
B. C. BROWN,⁴³ D. D. BROWN,¹⁰⁸ M. L. BROZZETTI,^{85,49} S. BRUNETT,² G. BRUNO,¹⁰ R. BRUNTZ,¹¹⁸ J. BRYANT,¹¹¹
F. BUCCI,⁶¹ J. BUCHANAN,¹¹⁸ O. BULASHENKO,^{38,78} T. BULIK,¹¹⁹ H. J. BULTEN,³³ A. BUONANNO,^{120,1} K. BURTYNYK,³
R. BUSCICCHIO,^{121,122} D. BUSKULIC,²⁸ C. BUY,¹²³ R. L. BYER,¹⁵ G. S. CABOURN DAVIES,¹²⁴ G. CABRAS,^{44,45} R. CABRITA,¹⁰
V. CÁCERES-BARBOSA,⁷ L. CADONATI,⁵⁷ G. CAGNOLI,¹²⁵ C. CAHILLANE,⁷⁶ J. CALDERÓN BUSTILLO,¹²⁶ T. A. CALLISTER,¹²⁷
E. CALLONI,^{29,5} J. B. CAMP,¹²⁸ M. CANEPA,^{55,54} G. CANEVA SANTORO,³⁹ K. C. CANNON,³⁷ H. CAO,¹⁰⁸
L. A. CAPISTRAN,¹²⁹ E. CAPOCASA,⁶⁸ E. CAPOTE,⁷⁶ G. CARAPPELLA,^{67,107} F. CARBOGNANI,⁵⁶ M. CARLASSARA,^{40,41}
J. B. CARLIN,¹³⁰ M. CARPINELLI,^{121,131,56} G. CARRILLO,⁷⁵ J. J. CARTER,^{40,41} G. CARULLO,¹³² J. CASANUEVA DIAZ,⁵⁶
C. CASENTINI,^{133,16,17} S. Y. CASTRO-LUCAS,¹⁰⁰ S. CAUDILL,^{134,33,74} M. CAVAGLIÀ,⁹⁹ R. CAVALIERI,⁵⁶ G. CELLA,⁸⁴
P. CERDÁ-DURÁN,^{135,136} E. CESARINI,¹⁷ W. CHAIBI,⁴⁷ P. CHAKRABORTY,^{40,41} S. CHALATHADKA SUBRAHMANYA,⁸²
J. C. L. CHAN,¹³⁷ M. CHAN,¹³⁸ K. CHANDRA,⁷ R.-J. CHANG,¹³⁹ S. CHAO,^{140,141} E. L. CHARLTON,¹¹⁸ P. CHARLTON,¹⁴²
E. CHASSANDE-MOTTIN,⁶⁸ C. CHATTERJEE,¹⁴³ DEBARATI CHATTERJEE,¹¹ DEEP CHATTERJEE,³¹ M. CHATURVEDI,⁹⁷
S. CHATY,⁶⁸ A. CHEN,¹² A. H.-Y. CHEN,¹⁴⁴ D. CHEN,¹⁴⁵ H. CHEN,¹⁴⁰ H. Y. CHEN,¹⁴⁶ J. CHEN,³¹ K. H. CHEN,¹⁴¹
Y. CHEN,¹⁴⁰ YANBEI CHEN,¹⁴⁷ YITIAN CHEN,¹⁴⁸ H. P. CHENG,¹⁴⁹ P. CHESSA,^{85,49} H. T. CHEUNG,⁸⁶ S. Y. CHEUNG,¹⁵⁰
F. CHIADINI,^{151,107} G. CHIARINI,⁸⁸ R. CHERICI,¹¹⁴ A. CHINCARINI,⁵⁴ M. L. CHIOFALO,^{83,84} A. CHIUMMO,^{5,56} C. CHOU,¹⁴⁴
S. CHOUDHARY,²⁷ N. CHRISTENSEN,⁴⁷ S. S. Y. CHUA,³⁰ P. CHUGH,¹⁵⁰ G. CIANI,^{87,88} P. CIECIELAG,⁹¹ M. CIEŚLAR,¹¹⁹
M. CIFALDI,¹⁷ R. CIOLFI,^{152,88} F. CLARA,³ J. A. CLARK,^{2,57} J. CLARKE,¹⁸ T. A. CLARKE,¹⁵⁰ P. CLEARWATER,¹⁵³
S. CLESSE,⁷¹ E. COCCIA,^{42,116,39} E. CODAZZO,⁴² P.-F. COHADON,¹¹⁷ S. COLACE,⁵⁵ M. COLLEONI,⁹⁵ C. G. COLLETTE,³⁴
J. COLLINS,⁶² S. COLLOMS,²⁶ A. COLOMBO,^{121,122,154} M. COLPI,^{121,122} C. M. COMPTON,³ G. CONNOLLY,⁷⁵ L. CONTI,⁸⁸
T. R. CORBITT,⁹ I. CORDERO-CARRIÓN,¹⁵⁵ S. COREZZI,^{85,49} N. J. CORNISH,¹⁵⁶ A. CORSI,¹⁵⁷ S. CORTESE,⁵⁶ C. A. COSTA,¹⁴
R. COTTINGHAM,⁶² M. W. COUGHLIN,⁹³ A. COUINEAUX,⁶³ J.-P. COULON,⁴⁷ S. T. COUNTRYMAN,¹⁵⁸ J.-F. COUPECHOUX,¹¹⁴
P. COUVARES,^{2,57} D. M. COWARD,²⁷ M. J. COWART,⁶² R. COYNE,¹⁵⁹ K. CRAIG,⁹⁴ R. CREED,¹⁸ J. D. E. CREIGHTON,⁸
T. D. CREIGHTON,¹⁶⁰ P. CREMONESE,⁹⁵ A. W. CRISWELL,⁹³ J. C. G. CROCKETT-GRAY,⁹ S. CROOK,⁶² R. CROUCH,³
J. CSIZMAZIA,³ J. R. CUDELL,¹¹³ T. J. CULLEN,² A. CUMMING,²⁶ E. CUOCO,^{56,84} M. CUSINATO,¹³⁵ P. DABADIE,¹²⁵
T. DAL CANTON,³⁶ S. DALL'OSSO,⁶³ S. DAL PRA,⁶³ G. DÁLYA,¹²³ B. D'ANGELO,⁵⁴ S. DANILISHIN,^{32,33} S. D'ANTONIO,¹⁷
K. DANZMANN,^{41,40,41} K. E. DARROCH,¹¹⁸ L. P. DARTEZ,³ A. DASGUPTA,⁸⁹ S. DATTA,¹⁶¹ V. DATTILO,⁵⁶ A. DAUMAS,⁶⁸
N. DAVARI,^{162,131} I. DAVE,⁹⁷ A. DAVENPORT,¹⁰⁰ M. DAVIER,³⁶ T. F. DAVIES,²⁷ D. DAVIS,² L. DAVIS,²⁷ M. C. DAVIS,⁹³
P. J. DAVIS,^{163,164} M. DAX,¹ J. DE BOLLE,⁹⁰ M. DEENADAYALAN,¹¹ J. DEGALLAIX,¹⁶⁵ M. DE LAURENTIS,^{29,5}
S. DELÉGLISE,¹¹⁷ F. DE LILLO,¹⁰ D. DELL'AQUILA,^{162,131} W. DEL POZZO,^{83,84} F. DE MARCO,^{64,63} F. DE MATTEIS,^{16,17}
V. D'EMILIO,² N. DEMOS,³¹ T. DENT,¹²⁶ A. DEPASSE,¹⁰ N. DEPERGOLA,⁵³ R. DE PIETRI,^{166,167} R. DE ROSA,^{29,5}

- C. DE ROSSI,⁵⁶ R. DESALVO,¹⁶⁸ R. DE SIMONE,¹⁵¹ A. DHANI,¹ R. DIAB,⁴³ M. C. DÍAZ,¹⁶⁰ M. DI CESARE,²⁹ G. DIDERON,¹⁶⁹
 N. A. DIDIO,⁷⁶ T. DIETRICH,¹ L. DI FIORE,⁵ C. DI FRONZO,³⁴ M. DI GIOVANNI,^{64,63} T. DI GIROLAMO,^{29,5} D. DIKSHA,^{33,32}
 A. DI MICHELE,⁸⁵ J. DING,^{68,170} S. DI PACE,^{64,63} I. DI PALMA,^{64,63} F. DI RENZO,¹¹⁴ DIVYAJYOTI,¹⁷¹ A. DMITRIEV,¹¹¹
 Z. DOCTOR,⁷⁷ E. DOHMEN,³ P. P. DOLEVA,¹¹⁸ D. DOMINGUEZ,¹⁷² L. D'ONOFRIO,⁶³ F. DONOVAN,³¹ K. L. DOOLEY,¹⁸
 T. DOONEY,⁷⁴ S. DORAVARI,¹¹ O. DOROSH,¹⁷³ M. DRAGO,^{64,63} J. C. DRIGGERS,³ J.-G. DUCOIN,^{174,68} L. DUNN,¹³⁰
 U. DUPLETSA,⁴² D. D'URSO,^{162,131} H. DUVAL,¹⁷⁵ P.-A. DUVERNE,³⁶ S. E. DWYER,³ C. EASSA,³ M. EBERSOLD,²⁸
 T. ECKHARDT,⁸² G. EDDOLLS,⁷⁶ B. EDELMAN,⁷⁵ T. B. EDO,² O. EDY,¹²⁴ A. EFFLER,⁶² J. EICHHOLZ,³⁰ H. EINSLE,⁴⁷
 M. EISENMANN,²¹ R. A. EISENSTEIN,³¹ A. EJLLI,¹⁸ R. M. ELEVELD,¹⁷⁶ M. EMMA,⁵⁸ K. ENDO,¹⁷⁷ A. J. ENGL,¹⁵
 E. ENLOE,⁵⁷ L. ERRICO,^{29,5} R. C. ESSICK,¹⁷⁸ H. ESTELLÉS,¹ D. ESTEVEZ,⁶⁵ T. ETZEL,² M. EVANS,³¹ T. EVSTAFYEVA,¹⁷⁹
 B. E. EWING,⁷ J. M. EZQUIAGA,¹³⁷ F. FABRIZI,^{60,61} F. FAEDI,^{61,60} V. FAFONE,^{16,17} S. FAIRHURST,¹⁸ A. M. FARAH,¹²⁷
 B. FARR,⁷⁵ W. M. FARR,^{180,181} G. FAVARO,⁸⁷ M. FAVATA,¹⁸² M. FAYS,¹¹³ M. FAZIO,⁹⁴ J. FEICHT,² M. M. FEJER,¹⁵
 R. FELICETTI,¹⁸³ E. FENYVESI,^{80,184} D. L. FERGUSON,¹⁴⁶ S. FERRAIUOLO,^{185,64,63} I. FERRANTE,^{83,84} T. A. FERREIRA,⁹
 F. FIDECARO,^{83,84} P. FIGURA,⁹¹ A. FIORI,^{84,83} I. FIORI,⁵⁶ M. FISHBACH,¹⁷⁸ R. P. FISHER,¹¹⁸ R. FITTIPALDI,^{186,107}
 V. FIUMARA,^{187,107} R. FLAMINIO,²⁸ S. M. FLEISCHER,¹⁸⁸ L. S. FLEMING,¹⁸⁹ E. FLODEN,⁹³ E. M. FOLEY,⁹³ H. FONG,¹³⁸
 J. A. FONT,^{135,136} B. FORMAL,¹⁹⁰ P. W. F. FORSYTH,³⁰ K. FRANCESCHETTI,¹⁶⁶ N. FRANCHINI,⁶⁸ S. FRASCA,^{64,63}
 F. FRASCONI,⁸⁴ A. FRATTALE MASCIOLI,^{64,63} Z. FREI,¹⁹¹ A. FREISE,^{33,101} O. FREITAS,^{192,135} R. FREY,⁷⁵ W. FRISCHHERTZ,⁶²
 P. FRITSCHEL,³¹ V. V. FROLOV,⁶² G. G. FRONZÉ,²³ M. FUENTES-GARCIA,² S. FUJII,¹⁹³ T. FUJIMORI,¹⁹⁴ P. FULDA,⁴³
 M. FYFFE,⁶² B. GADRE,⁷⁴ J. R. GAIR,¹ S. GALAUDAGE,¹⁹⁵ V. GALDI,¹⁶⁸ H. GALLAGHER,¹⁹⁶ S. GALLARDO,¹⁹⁷
 B. GALLEGO,¹⁹⁷ R. GAMBA,²⁴ A. GAMBOA,¹ D. GANAPATHY,³¹ A. GANGULY,¹¹ B. GARAVENTA,^{54,55} J. GARCÍA-BELLIDO,¹¹⁵
 C. GARCÍA NÚÑEZ,¹⁸⁹ C. GARCÍA-QUIRÓS,¹⁹⁸ J. W. GARDNER,³⁰ K. A. GARDNER,¹³⁸ J. GARGIULO,⁵⁶ A. GARRON,⁹⁵
 F. GARUFI,^{29,5} C. GASBARRA,^{16,17} B. GATELEY,³ V. GAYATHRI,⁸ G. GEMME,⁵⁴ A. GENNAL,⁸⁴ V. GENNARI,¹²³ J. GEORGE,⁹⁷
 R. GEORGE,¹⁴⁶ O. GERBERDING,⁸² L. GERGELY,¹⁹⁹ ARCHISMAN GHOSH,⁹⁰ SAYANTAN GHOSH,²⁰⁰ SHAON GHOSH,¹⁸²
 SHROBANA GHOSH,^{40,41} SUPROVO GHOSH,¹¹ TATHAGATA GHOSH,¹¹ L. GIACOPPO,^{64,63} J. A. GIAIME,^{9,62} K. D. GIARDINA,⁶²
 D. R. GIBSON,¹⁸⁹ D. T. GIBSON,¹⁷⁹ C. GIER,⁹⁴ P. GIRI,^{84,83} F. GISSI,⁹² S. GKAITATZIS,^{83,84} J. GLANZER,⁹ F. GLOTIN,³⁶
 J. GODFREY,⁷⁵ P. GODWIN,² N. L. GOEBBELS,⁸² E. GOETZ,¹³⁸ J. GOLOMB,² S. GOMEZ LOPEZ,^{64,63} B. GONCHAROV,⁴²
 Y. GONG,²⁰¹ G. GONZÁLEZ,⁹ P. GOODARZI,²⁰² S. GOODE,¹⁵⁰ A. W. GOODWIN-JONES,²⁷ M. GOSSELIN,⁵⁶ A. S. GÖTTEL,¹⁸
 R. GOUATY,²⁸ D. W. GOULD,³⁰ K. GOVORKOVA,³¹ S. GOYAL,¹ B. GRACE,³⁰ A. GRADO,^{203,5} V. GRAHAM,²⁶
 A. E. GRANADOS,⁹³ M. GRANATA,¹⁶⁵ V. GRANATA,⁶⁷ S. GRAS,³¹ P. GRASSIA,² A. GRAY,⁹³ C. GRAY,³ R. GRAY,²⁶
 G. GRECO,⁴⁹ A. C. GREEN,^{33,101} S. M. GREEN,¹²⁴ S. R. GREEN,²⁰⁴ A. M. GRETARSSON,⁶⁶ E. M. GRETARSSON,⁶⁶
 D. GRIFFITH,² W. L. GRIFFITHS,¹⁸ H. L. GRIGGS,⁵⁷ G. GRIGNANI,^{85,49} A. GRIMALDI,^{104,105} C. GRIMAUD,²⁸ H. GROTE,¹⁸
 D. GUERRA,¹³⁵ D. GUETTA,^{205,63} G. M. GUIDI,^{60,61} A. R. GUIMARAES,⁹ H. K. GULATI,⁸⁹ F. GULMINELLI,^{163,164}
 A. M. GUNNY,³¹ H. GUO,¹⁹⁰ W. GUO,²⁷ Y. GUO,^{33,32} ANCHAL GUPTA,² ANURADHA GUPTA,²⁰⁶ ISH GUPTA,⁷
 N. C. GUPTA,⁸⁹ P. GUPTA,^{33,74} S. K. GUPTA,⁴³ T. GUPTA,¹⁵⁶ N. GUPTA,¹ J. GURS,⁸² N. GUTIERREZ,¹⁶⁵ F. GUZMAN,¹²⁹
 H.-Y. H,¹⁴⁰ D. HABA,¹⁷² M. HABERLAND,¹ S. HAINO,²⁰⁷ E. D. HALL,³¹ E. Z. HAMILTON,⁹⁵ G. HAMMOND,²⁶ W.-B. HAN,²⁰⁸
 M. HANEY,³³ J. HANKS,³ C. HANNA,⁷ M. D. HANNAM,¹⁸ O. A. HANNUKSELA,²⁰⁹ A. G. HANSELMAN,¹²⁷ H. HANSEN,³
 J. HANSON,⁶² R. HARADA,³⁷ A. R. HARDISON,²¹⁰ K. HARIS,^{33,74} T. HARMARK,¹³² J. HARMS,^{42,116} G. M. HARRY,²¹¹
 I. W. HARRY,¹²⁴ J. HART,⁷² B. HASKELL,⁹¹ C.-J. HASTER,²¹² J. S. HATHAWAY,¹⁹⁶ K. HAUGHIAN,²⁶ H. HAYAKAWA,⁴⁸
 K. HAYAMA,²¹³ R. HAYES,¹⁸ A. HEFFERNAN,⁹⁵ A. HEIDMANN,¹¹⁷ M. C. HEINTZE,⁶² J. HEINZE,¹¹¹ J. HEINZEL,³¹
 H. HEITMANN,⁴⁷ F. HELLMAN,²¹⁴ P. HELLO,³⁶ A. F. HELMLING-CORNEILL,⁷⁵ G. HEMMING,⁵⁶ O. HENDERSON-SAPIR,¹⁰⁸
 M. HENDRY,²⁶ I. S. HENG,²⁶ E. HENNES,³³ C. HENSHAW,⁵⁷ T. HERTOG,¹⁰³ M. HEURS,^{40,41} A. L. HEWITT,^{179,215} J. HEYNS,³¹
 S. HIGGINBOTHAM,¹⁸ S. HILD,^{32,33} S. HILL,²⁶ Y. HIMEMOTO,²¹⁶ N. HIRATA,²¹ C. HIROSE,²¹⁷ W. C. G. HO,²¹⁸ S. HOANG,³⁶
 S. HOCHHEIM,^{40,41} D. HOFMAN,¹⁶⁵ N. A. HOLLAND,^{33,101} K. HOLLEY-BOCKELMANN,¹⁴³ Z. J. HOLMES,¹⁰⁸ D. E. HOLZ,¹²⁷
 L. HONET,⁷¹ C. HONG,¹⁵ J. HORNUNG,⁷⁵ S. HOSHINO,²¹⁷ J. HOUGH,²⁶ S. HOURIHANE,² E. J. HOWELL,²⁷ C. G. HOY,¹²⁴
 C. A. HRISHIKESH,¹⁶ H.-F. HSIEH,¹⁴⁰ C. HSIUNG,²¹⁹ H. C. HSU,¹⁴¹ W.-F. HSU,¹⁰³ P. HU,¹⁴³ Q. HU,²⁶ H. Y. HUANG,¹⁴¹
 Y.-J. HUANG,⁷ A. D. HUDDART,²²⁰ B. HUGHEY,⁶⁶ D. C. Y. HUI,²²¹ V. HUI,²⁸ S. HUSA,⁹⁵ R. HUXFORD,⁷ T. HUYNH-DINH,⁶²
 L. IAMPieri,^{64,63} G. A. IANDOLO,³² M. IANNI,^{17,16} A. IESS,^{222,84} H. IMAFUKU,³⁷ K. INAYOSHI,²²³ Y. INOUE,¹⁴¹ G. IORIO,⁸⁷
 M. H. IQBAL,³⁰ J. IRWIN,²⁶ R. ISHIKAWA,²²⁴ M. ISI,^{180,181} M. A. ISMAIL,¹⁴¹ Y. ITOH,^{194,225} H. IWANAGA,¹⁹⁴ M. IWAYA,¹⁹³
 B. R. IYER,²⁰ V. JABERIANHAMEDAN,²⁷ C. JACQUET,¹²³ P.-E. JACQUET,¹¹⁷ S. J. JADHAV,²²⁶ S. P. JADHAV,¹⁵³ T. JAIN,¹⁷⁹
 A. L. JAMES,² P. A. JAMES,¹¹⁸ R. JAMSHIDI,³⁴ J. JANQUART,^{74,33} K. JANSSENS,^{19,47} N. N. JANTHALUR,²²⁶ S. JARABA,¹¹⁵
 P. JARANOWSKI,²²⁷ R. JAUME,⁹⁵ W. JAVED,¹⁸ A. JENNINGS,³ W. JIA,³¹ J. JIANG,⁴³ HONG-BO JIN,^{228,229} J. KUBISZ,²³⁰
 C. JOHANSON,¹³⁴ G. R. JOHNS,¹¹⁸ N. A. JOHNSON,⁴³ M. C. JOHNSTON,²¹² R. JOHNSTON,²⁶ N. JOHNY,^{40,41} D. H. JONES,³⁰
 D. I. JONES,²³¹ R. JONES,²⁶ S. JOSE,¹⁷¹ P. JOSHI,⁷ L. JU,²⁷ K. JUNG,²³² J. JUNKER,³⁰ V. JUSTE,⁷¹ T. KAJITA,²³³
 I. KAKU,¹⁹⁴ C. KALAGHATGI,^{74,33,234} V. KALOGERA,⁷⁷ M. KAMIZUMI,⁴⁸ N. KANDA,^{225,194} S. KANDHASAMY,¹¹ G. KANG,²³⁵
 J. B. KANNER,² S. J. KAPADIA,¹¹ D. P. KAPASI,³⁰ S. KARAT,² C. KARATHANASIS,³⁹ R. KASHYAP,⁷ M. KASPRZACK,²
 W. KASTAUN,^{40,41} T. KATO,¹⁹³ E. KATSAVOUNIDIS,³¹ W. KATZMAN,⁶² R. KAUSHIK,⁹⁷ K. KAWABE,³ R. KAWAMOTO,¹⁹⁴
 A. KAZEMI,⁹³ D. KEITEL,⁹⁵ J. KELLEY-DERZON,⁴³ J. KENNINGTON,⁷ R. KESHARWANI,¹¹ J. S. KEY,²³⁶ R. KHADELA,^{40,41}
 S. KHADKA,¹⁵ F. Y. KHALILI,¹⁰² F. KHAN,^{40,41} I. KHAN,^{237,35} T. KHANAM,¹⁵⁷ M. KHURSHEED,⁹⁷ N. M. KHUSID,^{180,181}
 W. KIENDREBEOGO,^{47,238} N. KIJBUNCHOO,¹⁰⁸ C. KIM,²³⁹ J. C. KIM,²⁴⁰ K. KIM,²⁴¹ M. H. KIM,²⁴² S. KIM,²²¹ Y.-M. KIM,²⁴¹
 C. KIMBALL,⁷⁷ M. KINLEY-HANLON,²⁶ M. KINNEAR,¹⁸ J. S. KISSEL,³ S. KLIMENKO,⁴³ A. M. KNEE,¹³⁸ N. KNUST,^{40,41}
 K. KOBAYASHI,¹⁹³ P. KOCH,^{40,41} S. M. KOEHLERBECK,¹⁵ G. KOEKOEK,^{33,32} K. KOHRI,^{243,244} K. KOKEYAMA,¹⁸ S. KOLEY,⁴²
 P. KOLITSIDOU,¹¹¹ M. KOLSTEIN,³⁹ K. KOMORI,³⁷ A. K. H. KONG,¹⁴⁰ A. KONTOS,²⁴⁵ M. KOROBKO,⁸² R. V. KOSSAK,^{40,41}
 X. Kou,⁹³ A. Koushik,¹⁹ N. KOUVATOS,⁶⁹ M. KOVALAM,²⁷ D. B. KOZAK,² S. L. KRANZHOFF,^{32,33} V. KRINGEL,^{40,41}

N. V. KRISHNENDU,²⁰ A. KRÓLAK,^{246,173} K. KRUSKA,^{40,41} G. KUEHN,^{40,41} P. KUIJER,³³ S. KULKARNI,²⁰⁶
 A. KULUR RAMAMOCHAN,³⁰ A. KUMAR,²²⁶ PRAVEEN KUMAR,¹²⁶ PRAYUSH KUMAR,²⁰ RAHUL KUMAR,³ RAKESH KUMAR,⁸⁹
 J. KUME,^{87,88,37} K. KUNS,³¹ N. KUNTIMADDI,¹⁸ S. KUROYANAGI,^{115,247} N. J. KURTH,⁹ S. KUWAHARA,³⁷ K. KWAK,²³²
 K. KWAN,³⁰ J. KWOK,¹⁷⁹ G. LACAILE,²⁶ P. LAGABBE,²⁸ D. LAGHI,¹²³ S. LAI,¹⁴⁴ A. H. LAITY,¹⁵⁹ M. H. LAKKIS,³⁴
 E. LALANDE,²⁴⁸ M. LALLEMAN,¹⁹ P. C. LALREMUAUATI,²⁴⁹ M. LANDRY,³ B. B. LANE,³¹ R. N. LANG,³¹ J. LANGE,¹⁴⁶
 B. LANTZ,¹⁵ A. LA RANA,⁶³ I. LA ROSA,⁹⁵ A. LARTAUD-VOLLARD,³⁶ P. D. LASKY,¹⁵⁰ J. LAWRENCE,¹⁵⁷ M. N. LAWRENCE,⁹
 M. LAXEN,⁶² A. LAZZARINI,² C. LAZZARO,^{87,88} P. LEACI,^{64,63} Y. K. LECOEUICHE,¹³⁸ H. M. LEE,²⁴⁰ H. W. LEE,²⁵⁰
 K. LEE,²⁴² R.-K. LEE,¹⁴⁰ R. LEE,³¹ S. LEE,²⁴¹ Y. LEE,¹⁴¹ I. N. LEGRED,² J. LEHMANN,^{40,41} L. LEHNER,¹⁶⁹ M. LE JEAN,¹⁶⁵
 A. LEMAÎTRE,²⁵¹ M. LENTI,^{61,252} M. LEONARDI,^{104,105,21} M. LEQUIME,³⁵ N. LEROY,³⁶ M. LESOVSKY,² N. LETENDRE,²⁸
 M. LETHUILLIER,¹¹⁴ S. E. LEVIN,²⁰² Y. LEVIN,¹⁵⁰ K. LEYDE,⁶⁸ A. K. Y. LI,² K. L. LI,¹³⁹ T. G. F. LI,^{209,103} X. LI,¹⁴⁷
 Z. LI,²⁶ A. LIHOS,¹¹⁸ C.-Y. LIN,²⁵³ C.-Y. LIN,¹⁴¹ E. T. LIN,¹⁴⁰ F. LIN,¹⁴¹ H. LIN,¹⁴¹ L. C.-C. LIN,¹³⁹ Y.-C. LIN,¹⁴⁰
 F. LINDE,^{234,33} S. D. LINKER,¹⁹⁷ T. B. LITTENBERG,²⁵⁴ A. LIU,²⁰⁹ G. C. LIU,²¹⁹ JIAN LIU,²⁷ F. LLAMAS VILLARREAL,¹⁶⁰
 J. LLOBERA-QUEROL,⁹⁵ R. K. L. LO,¹³⁷ J.-P. LOCQUET,¹⁰³ L. T. LONDON,^{69,31,98} A. LONGO,^{60,61} D. LOPEZ,¹¹³
 M. LOPEZ PORTILLA,⁷⁴ M. LORENZINI,^{16,17} A. LORENZO-MEDINA,¹²⁶ V. LORLETTE,³⁶ M. LORMAND,⁶² G. LOSURDO,⁸⁴
 T. P. LOTT IV,⁵⁷ J. D. LOUGH,^{40,41} H. A. LOUGHLIN,³¹ C. O. LOUSTO,¹⁹⁶ M. J. LOWRY,¹¹⁸ N. LU,³⁰ H. LÜCK,^{41,40,41}
 D. LUMACA,¹⁷ A. P. LUNDRÉN,¹²⁴ A. W. LUSSIER,²⁴⁸ L.-T. MA,¹⁴⁰ S. MA,¹⁶⁹ M. MA'ARIF,¹⁴¹ R. MACAS,¹²⁴
 A. MACEDO,⁵² M. MACINNIS,³¹ R. R. MACIY,^{40,41} D. M. MACLEOD,¹⁸ I. A. O. MACMILLAN,² A. MACQUET,³⁶ D. MACRI,³¹
 K. MAEDA,¹⁷⁷ S. MAENAUT,¹⁰³ I. MAGAÑA HERNANDEZ,⁸ S. S. MAGARE,¹¹ C. MAGAZZÙ,⁸⁴ R. M. MAGEE,² E. MAGGIO,¹
 R. MAGGIORE,^{33,101} M. MAGNOZZI,^{54,55} M. MAHESH,⁸² S. MAHESH,²⁵⁵ M. MAINI,¹⁵⁹ S. MAJHI,¹¹ E. MAJORANA,^{64,63}
 C. N. MAKAREM,² E. MAKELELE,⁷² J. A. MALAQUIAS-REIS,¹⁴ U. MALI,¹⁷⁸ S. MALIAKAL,² A. MALIK,⁹⁷ N. MAN,⁴⁷
 V. MANDIC,⁹³ V. MANGANO,^{63,64} B. MANNIX,⁷⁵ G. L. MANSELL,^{76,31} G. MANSINGH,²¹¹ M. MANSKE,⁸ M. MANTOVANI,⁵⁶
 M. MAPELLI,^{87,88,256} F. MARCHESONI,^{50,49,257} D. MARÍN PINA,^{38,78,258} F. MARION,²⁸ S. MÁRKA,¹⁵⁸ Z. MÁRKA,¹⁵⁸
 A. S. MARKOSYAN,¹⁵ A. MARKOWITZ,² E. MAROS,² S. MARSAT,¹²³ F. MARTELLI,^{60,61} I. W. MARTIN,²⁶ R. M. MARTIN,¹⁸²
 B. B. MARTINEZ,¹²⁹ M. MARTINEZ,^{39,259} V. MARTINEZ,¹²⁵ A. MARTINI,^{104,105} K. MARTINOVIC,⁶⁹ J. C. MARTINS,¹⁴
 D. V. MARTYNOV,¹¹¹ E. J. MARX,³¹ L. MASSARO,^{32,33} A. MASSEROT,²⁸ M. MASSO-REID,²⁶ M. MASTRODICASA,^{63,64}
 S. MASTROGIOVANNI,⁶³ T. MATCOVICH,⁴⁹ M. MATIUSHECHKINA,^{40,41} M. MATSUYAMA,¹⁹⁴ N. MAVALVALA,³¹ N. MAXWELL,³
 G. MCCARROL,⁶² R. MCCARTHY,³ D. E. MCCLELLAND,³⁰ S. MCCORMICK,⁶² L. MCCULLER,² S. MCEACHIN,¹¹⁸
 C. MCELHENNY,¹¹⁸ G. I. MCGHEE,²⁶ J. MCGINN,²⁶ K. B. M. MCGOWAN,¹⁴³ J. MCIVER,¹³⁸ A. MCLEOD,²⁷ T. MCRAE,³⁰
 D. MEACHER,⁸ Q. MEIJER,⁷⁴ A. MELATOS,¹³⁰ S. MELLAERTS,¹⁰³ A. MENENDEZ-VAZQUEZ,³⁹ C. S. MENONI,¹⁰⁰ F. MERA,³
 R. A. MERCER,⁸ L. MERENI,¹⁶⁵ K. MERFELD,¹⁵⁷ E. L. MERILH,⁶² J. R. MÉROU,⁹⁵ J. D. MERRITT,⁷⁵ M. MERZOUGUI,⁴⁷
 C. MESSENGER,²⁶ C. MESSICK,⁸ Z. METZLER,^{120,128,260} M. MEYER-CONDE,¹⁹⁴ F. MEYLAHN,^{40,41} A. MHASKE,¹¹
 A. MIANI,^{104,105} H. MIAO,²⁶¹ I. MICHALOLIAKOS,⁴³ C. MICHEL,¹⁶⁵ Y. MICHIMURA,^{2,37} H. MIDDLETON,¹¹¹ A. L. MILLER,³³
 S. MILLER,² M. MILLHOUSE,⁵⁷ E. MILOTTI,^{183,45} V. MILOTTI,⁸⁷ Y. MINENKOV,¹⁷ N. MIO,³⁷ LL. M. MIR,³⁹
 L. MIRASOLA,^{262,63} M. MIRAVET-TENÉS,¹³⁵ C.-A. MIRITESCU,³⁹ A. K. MISHRA,²⁰ A. MISHRA,¹¹ C. MISHRA,¹⁷¹
 T. MISHRA,⁴³ A. L. MITCHELL,^{33,101} J. G. MITCHELL,⁶⁶ S. MITRA,¹¹ V. P. MITROFANOV,¹⁰² R. MITTLEMAN,³¹
 O. MIYAKAWA,⁴⁸ S. MIYAMOTO,¹⁹³ S. MIYOKI,⁴⁸ G. MO,³¹ L. MOBILIA,^{60,61} S. R. P. MOHAPATRA,² S. R. MOHITE,⁷
 M. MOLINA-RUIZ,²¹⁴ C. MONDAL,¹⁶³ M. MONDIN,¹⁹⁷ M. MONTANI,^{60,61} C. J. MOORE,¹⁷⁹ D. MORARU,³ A. MORE,¹¹
 S. MORE,¹¹ G. MORENO,³ C. MORGAN,¹⁸ S. MORISAKI,^{37,193} Y. MORIWAKI,¹⁷⁷ G. MORRAS,¹¹⁵ A. MOSCATELLO,⁸⁷
 P. MOURIER,⁹⁵ B. MOURS,⁶⁵ C. M. MOW-LOWRY,^{33,101} F. MUCIACCIA,^{64,63} ARUNAVA MUKHERJEE,²⁶³ D. MUKHERJEE,²⁵⁴
 SAMANWAYA MUKHERJEE,¹¹ SOMA MUKHERJEE,¹⁶⁰ SUBROTO MUKHERJEE,⁸⁹ SUVODIP MUKHERJEE,^{264,169,98} N. MUKUND,³¹
 A. MULLAVEY,⁶² J. MUNCH,¹⁰⁸ J. MUNDI,²¹¹ C. L. MUNGIOLO,²⁷ W. R. MUNN OBERG,²⁶⁵ Y. MURAKAMI,¹⁹³
 M. MURAKOSHI,²²⁴ P. G. MURRAY,²⁶ S. MUUSSE,³⁰ D. NABARI,^{104,105} S. L. NADJI,^{40,41} A. NAGAR,^{23,266} N. NAGARAJAN,²⁶
 K. N. NAGLER,⁶⁶ K. NAKAGAKI,⁴⁸ K. NAKAMURA,²¹ H. NAKANO,²⁶⁷ M. NAKANO,² D. NANDI,⁹ V. NAPOLANO,⁵⁶
 P. NARAYAN,²⁰⁶ I. NARDECCHIA,¹⁷ T. NARIKAWA,¹⁹³ H. NAROLA,⁷⁴ L. NATICCHIONI,⁶³ R. K. NAYAK,²⁴⁹ J. NEILSON,^{92,107}
 A. NELSON,¹²⁹ T. J. N. NELSON,⁶² M. NERY,^{40,41} A. NEUNZERT,³ S. NG,⁵² L. NGUYEN QUYNH,²⁶⁸ S. A. NICHOLS,⁹
 A. B. NIELSEN,²⁶⁹ G. NIERADKA,⁹¹ A. NIKO,¹⁴¹ Y. NISHINO,^{21,37} A. NISHIZAWA,²⁷⁰ S. NISSANKE,^{98,33} E. NITOGLIA,¹¹⁴
 W. NIU,⁷ F. NOCERA,⁵⁶ M. NORMAN,¹⁸ C. NORTH,¹⁸ J. NOVAK,^{109,271,272,273} J. F. NUÑO SILES,¹¹⁵ L. K. NUTTALL,¹²⁴
 K. OBAYASHI,²²⁴ J. OBERLING,³ J. O'DELL,²²⁰ M. OERTEL,^{109,271,272,274,273} A. OFFERMANS,¹⁰³ G. OGANESYAN,^{42,116}
 J. J. OH,²⁷⁵ K. OH,²²¹ T. O'HANLON,⁶² M. OHASHI,⁴⁸ M. OHKAWA,²¹⁷ F. OHME,^{40,41} A. S. OLIVEIRA,¹⁵⁸
 R. OLIVERI,^{109,271,272} B. O'NEAL,¹¹⁸ K. OOHARA,^{276,277} B. O'REILLY,⁶² N. D. ORMSBY,¹¹⁸ M. ORSELLI,^{49,85}
 R. O'SHAUGHNESSY,¹⁹⁶ S. O'SHEA,²⁶ Y. OSHIMA,³⁷ S. OSHINO,⁴⁸ S. OSSOKINE,¹ C. OSTHELDER,² I. OTA,⁹
 D. J. OTTAWAY,¹⁰⁸ A. OUZRIAT,¹¹⁴ H. OVERMIER,⁶² B. J. OWEN,¹⁵⁷ A. E. PACE,⁷ R. PAGANO,⁹ M. A. PAGE,²¹ A. PAI,²⁰⁰
 A. PAL,²⁷⁸ S. PAL,²⁴⁹ M. A. PALAIA,^{84,83} M. PÁLFI,¹⁹¹ P. P. PALMA,^{64,16,17} C. PALOMBA,⁶³ P. PALUD,⁶⁸ H. PAN,¹⁴⁰
 J. PAN,²⁷ K. C. PAN,¹⁴⁰ R. PANAI,^{262,87} P. K. PANDA,²²⁶ S. PANDEY,⁷ L. PANEBIANCO,^{60,61} P. T. H. PANG,^{33,74}
 F. PANNARALE,^{64,63} K. A. PANNONE,⁵² B. C. PANT,⁹⁷ F. H. PANTHER,²⁷ F. PAOLETTI,⁸⁴ A. PAOLONE,^{63,279}
 E. E. PAPALEXAKIS,²⁰² L. PAPALINI,^{84,83} G. PAPIGIOTIS,²⁸⁰ A. PAQUIS,³⁶ A. PARISI,^{85,49} B.-J. PARK,²⁴¹ J. PARK,²⁸¹
 W. PARKER,⁶² G. PASCALE,^{40,41} D. PASCUCCI,⁹⁰ A. PASQUALETTI,⁵⁶ R. PASSAQUIETI,^{83,84} L. PASSENGER,¹⁵⁰
 D. PASSUELLO,⁸⁴ O. PATANE,³ D. PATHAK,¹¹ M. PATHAK,¹⁰⁸ A. PATRA,¹⁸ B. PATRICELLI,^{83,84} A. S. PATRÓN,⁹ K. PAUL,¹⁷¹
 S. PAUL,⁷⁵ E. PAYNE,² T. PEARCE,¹⁸ M. PEDRAZA,² R. PEGNA,⁸⁴ A. PELE,² F. E. PEÑA ARELLANO,⁴⁶ S. PENN,²⁶⁵
 M. D. PENULIAR,⁵² A. PEREGO,^{104,105} Z. PEREIRA,¹³⁴ J. J. PEREZ,⁴³ C. PÉRIGOIS,^{152,88,87} G. PERNA,⁸⁷ A. PERRECA,^{104,105}
 J. PERRET,⁶⁸ S. PERRIÈS,¹¹⁴ J. W. PERRY,^{33,101} D. PESIOS,²⁸⁰ S. PETRACCA,¹⁶⁸ C. PETRILLO,⁸⁵ H. P. PFEIFFER,¹
 H. PHAM,⁶² K. A. PHAM,⁹³ K. S. PHUKON,^{111,33,234} H. PHURAILATPAM,²⁰⁹ M. PIARULLI,¹²³ L. PICCARI,^{64,63}

- O. J. PICCINI,³⁹ M. PICHOT,⁴⁷ M. PIENDIBENE,^{83,84} F. PIERGIOVANNI,^{60,61} L. PIERINI,⁶³ G. PIERRA,¹¹⁴ V. PIERRO,^{92,107}
M. PIETRZAK,⁹¹ M. PILLAS,⁴⁷ F. PILO,⁸⁴ L. PINARD,¹⁶⁵ I. M. PINTO,^{92,107,282,29} M. PINTO,⁵⁶ B. J. PIOTRZKOWSKI,⁸
M. PIRELLO,³ M. D. PITKIN,^{179,215} A. PLACIDI,⁶¹ E. PLACIDI,^{64,63} M. L. PLANAS,⁹⁵ W. PLASTINO,^{283,17} R. POGGIANI,^{83,84}
E. POLINI,²⁸ L. POMPILI,¹ J. POON,²⁰⁹ E. PORCELLI,³³ E. K. PORTER,⁶⁸ C. POSNANSKY,⁷ R. POULTON,⁵⁶ J. POWELL,¹⁵³
M. PRACCHIA,¹¹³ B. K. PRADHAN,¹¹ T. PRADIER,⁶⁵ A. K. PRAJAPATI,⁸⁹ K. PRASAI,¹⁵ R. PRASANNA,²²⁶ P. PRASIA,¹¹
G. PRATTEN,¹¹¹ G. PRINCIPE,^{183,45} M. PRINCIPE,^{168,92,282,107} G. A. PRODI,^{104,105} L. PROKHOROV,¹¹¹ P. PROSPITO,^{16,17}
A. PUECHER,^{33,74} J. PULLIN,⁹ M. PUNTURO,⁴⁹ P. PUPPO,⁶³ M. PÜRNER,¹⁵⁹ H. QI,¹² J. QIN,³⁰ G. QUÉMÉNER,^{164,109}
V. QUETSCHKE,¹⁶⁰ C. QUIGLEY,¹⁸ P. J. QUINONEZ,⁶⁶ F. J. RAAB,³ S. S. RAABITH,⁹ G. RAALJMAKERS,^{98,33} S. RAJA,⁹⁷
C. RAJAN,⁹⁷ B. RAJBHANDARI,¹⁹⁶ K. E. RAMIREZ,⁶² F. A. RAMIS VIDAL,⁹⁵ A. RAMOS-BUADES,³³ D. RANA,¹¹ S. RANJAN,⁵⁷
K. RANSOM,⁶² P. RAPAGNANI,^{64,63} B. RATTO,⁶⁶ S. RAWAT,⁹³ A. RAY,⁸ V. RAYMOND,¹⁸ M. RAZZANO,^{83,84} J. READ,⁵²
M. RECAMAN PAYO,¹⁰³ T. REGIMBAU,²⁸ L. REI,⁵⁴ S. REID,⁹⁴ D. H. REITZE,² P. RELTON,¹⁸ A. I. RENZINI,²
P. RETTEGNO,²³ B. REVENU,^{284,68} R. REYES,¹⁹⁷ A. S. REZAEI,^{63,64} F. RICCI,^{64,63} M. RICCI,^{63,64} A. RICCIARDONE,^{83,84}
J. W. RICHARDSON,²⁰² M. RICHARDSON,¹⁰⁸ A. RIJAL,⁶⁶ K. RILES,⁸⁶ H. K. RILEY,¹⁸ S. RINALDI,^{256,87} J. RITTMAYER,⁸²
C. ROBERTSON,²²⁰ F. ROBINET,³⁶ M. ROBINSON,³ A. ROCCHI,¹⁷ L. ROLLAND,²⁸ J. G. ROLLINS,² A. E. ROMANO,²⁸⁵
R. ROMANO,^{4,5} A. ROMERO,¹⁷⁵ I. M. ROMERO-SHAW,¹⁷⁹ J. H. ROMIE,⁶² S. RONCHINI,^{42,116} T. J. ROOKE,¹⁰⁸ L. ROSA,^{5,29}
T. J. ROSAUER,²⁰² C. A. ROSE,⁸ D. ROSIŃSKA,¹¹⁹ M. P. ROSS,⁵¹ M. ROSSELLO,⁹⁵ S. ROWAN,²⁶ S. K. ROY,^{180,181} S. C. ROY,⁷⁴
D. ROZZA,^{121,122} P. RUGGI,⁵⁶ N. RUHAMA,²³² E. RUIZ MORALES,^{286,115} K. RUIZ-ROCHA,¹⁴³ S. SACHDEV,⁵⁷ T. SADECKI,³
J. SADIQ,¹²⁶ P. SAFFARIEH,^{33,101} M. R. SAH,²⁶⁴ S. S. SAHA,¹⁴⁰ S. SAHA,¹⁴⁰ T. SAINRAT,⁶⁵ S. SAJITH MENON,^{205,64,63}
K. SAKAI,²⁸⁷ M. SAKELLARIADOU,⁶⁹ S. SAKON,⁷ O. S. SALAFIA,^{154,122,121} F. SALCES-CARCOBA,² L. SALCONI,⁵⁶
M. SALEEM,⁹³ F. SALEMI,^{64,63} M. SALLÉ,³³ S. SALVADOR,^{164,163,109} A. SANCHEZ,³ E. J. SANCHEZ,² J. H. SANCHEZ,⁷⁷
L. E. SANCHEZ,² N. SANCHIS-GUAL,¹³⁵ J. R. SANDERS,²¹⁰ E. M. SÄNGER,¹ F. SANTOLIUQUIDO,⁴² T. R. SARAVANAN,¹¹
N. SARIN,¹⁵⁰ S. SASAOKA,¹⁷² A. SASLI,²⁸⁰ P. SASSI,^{49,85} B. SASSOLAS,¹⁶⁵ H. SATARI,²⁷ R. SATO,²¹⁷ Y. SATO,¹⁷⁷
O. SAUTER,⁴³ R. L. SAVAGE,³ T. SAWADA,⁴⁸ H. L. SAWANT,¹¹ S. SAYAH,²⁸ V. SCACCO,^{16,17} D. SCHAETZL,² M. SCHEEL,¹⁴⁷
A. SCHIEBELBEIN,¹⁷⁸ M. G. SCHIWORSKI,¹⁰⁸ P. SCHMIDT,¹¹¹ S. SCHMIDT,⁷⁴ R. SCHNABEL,⁸² M. SCHNEEWIND,^{40,41}
R. M. S. SCHOFIELD,⁷⁵ K. SCHOUTEDEN,¹⁰³ B. W. SCHULTE,^{40,41} B. F. SCHUTZ,^{18,40,41} E. SCHWARTZ,¹⁸ M. SCIALPI,²⁸⁸
J. SCOTT,²⁶ S. M. SCOTT,³⁰ T. C. SEETHARAMU,²⁶ M. SEGLAR-ARROYO,³⁹ Y. SEKIGUCHI,²⁸⁹ D. SELLERS,⁶²
A. S. SENGUPTA,²⁹⁰ D. SENTENAC,⁵⁶ E. G. SEO,²⁶ J. W. SEO,¹⁰³ V. SEQUINO,^{29,5} M. SERRA,⁶³ G. SERVIGNAT,²⁷¹
A. SEVRIN,¹⁷⁵ T. SHAFFER,³ U. S. SHAH,⁵⁷ M. A. SHAIKH,²⁴⁰ L. SHAO,²²³ A. K. SHARMA,²⁰ P. SHARMA,⁹⁷
S. SHARMA-CHAUDHARY,⁹⁹ M. R. SHAW,¹⁸ P. SHAWHAN,¹²⁰ N. S. SHCHEBLANOV,^{291,251} E. SHERIDAN,¹⁴³ Y. SHIKANO,^{292,293}
M. SHIKAUCHI,³⁷ K. SHIMODE,⁴⁸ H. SHINKAI,²⁹⁴ J. SHIOTA,²²⁴ D. H. SHOEMAKER,³¹ D. M. SHOEMAKER,¹⁴⁶ R. W. SHORT,³
S. SHYAMSUNDAR,⁹⁷ A. SIDER,³⁴ H. SIEGEL,^{180,181} M. SIENIAWSKA,¹⁰ D. SIGG,³ L. SILENZI,^{49,50} M. SIMMONS,¹⁰⁸
L. P. SINGER,¹²⁸ A. SINGH,²⁰⁶ D. SINGH,⁷ M. K. SINGH,²⁰ S. SINGH,^{21,59} A. SINGHA,^{32,33} A. M. SINTES,⁹⁵ V. SIPALA,^{162,131}
V. SKLIRIS,¹⁸ B. J. J. SLAGMOLEN,³⁰ T. J. SLAVEN-BLAIR,²⁷ J. SMETANA,¹¹¹ J. R. SMITH,⁵² L. SMITH,²⁶ R. J. E. SMITH,¹⁵⁰
W. J. SMITH,¹⁴³ J. SOLDATESCHI,^{252,295,61} K. SOMIYA,¹⁷² I. SONG,¹⁴⁰ K. SONI,¹¹ S. SONI,³¹ V. SORDINI,¹¹⁴ F. SORRENTINO,⁵⁴
N. SORRENTINO,^{83,84} H. SOTANI,²⁹⁶ R. SOULARD,⁴⁷ A. SOUTHGATE,¹⁸ V. SPAGNUOLO,^{32,33} A. P. SPENCER,²⁶
M. SPERA,^{45,297} P. SPINICELLI,⁵⁶ J. B. SPOON,⁹ C. A. SPRAGUE,²⁶⁸ A. K. SRIVASTAVA,⁸⁹ F. STACHURSKI,²⁶ D. A. STEER,⁶⁸
J. STEINLECHNER,^{32,33} S. STEINLECHNER,^{32,33} N. STERGIOLAS,²⁸⁰ P. STEVENS,³⁶ M. STPIERRE,¹⁵⁹ G. STRATTA,^{298,133,63,299}
M. D. STRONG,⁹ A. STRUNK,³ R. STURANI,³⁰⁰ A. L. STUVER,^{53,*} M. SUCHENEK,⁹¹ S. SUDHAGAR,⁹¹ N. SUELTSMANN,⁸²
L. SULEIMAN,⁵² K. L. SULLIVAN,⁹ L. SUN,³⁰ S. SUNIL,⁸⁹ J. SURESH,¹⁰ P. J. SUTTON,¹⁸ T. SUZUKI,²¹⁷ Y. SUZUKI,²²⁴
B. L. SWINKELS,³³ A. SYX,⁶⁵ M. J. SZCZEPAŃCZYK,^{301,43} P. SZEWCZYK,¹¹⁹ M. TACCA,³³ H. TAGOSHI,¹⁹³ S. C. TAIT,²
H. TAKAHASHI,³⁰² R. TAKAHASHI,²¹ A. TAKAMORI,³⁷ T. TAKASE,⁴⁸ K. TAKATANI,¹⁹⁴ H. TAKEDA,³⁰³ K. TAKESHITA,¹⁷²
C. TALBOT,¹²⁷ M. TAMAKI,¹⁹³ N. TAMANINI,¹²³ D. TANABE,¹⁴¹ K. TANAKA,⁴⁸ S. J. TANAKA,²²⁴ T. TANAKA,³⁰³ D. TANG,²⁷
S. TANIOKA,⁷⁶ D. B. TANNER,⁴³ L. TAO,⁴³ R. D. TAPIA,⁷ E. N. TAPIA SAN MARTÍN,³³ R. TARAFDER,² C. TARANTO,^{16,17,64}
A. TARUYA,³⁰⁴ J. D. TASSON,¹⁷⁶ M. TELOI,³⁴ R. TENORIO,⁹⁵ H. THEMANN,¹⁹⁷ A. THEODOROPOULOS,¹³⁵
M. P. THIRUGNANASAMBANDAM,¹¹ L. M. THOMAS,² M. THOMAS,⁶² P. THOMAS,³ J. E. THOMPSON,¹⁴⁷ S. R. THONDAPU,⁹⁷
K. A. THORNE,⁶² E. THRANE,¹⁵⁰ J. TISSINO,⁴² A. TIWARI,¹¹ P. TIWARI,⁴² S. TIWARI,¹⁹⁸ V. TIWARI,¹¹¹ M. R. TODD,⁷⁶
A. M. TOIVONEN,⁹³ K. TOLAND,²⁶ A. E. TOLLEY,¹²⁴ T. TOMAR,²¹ K. TOMITA,¹⁹⁴ T. TOMURA,⁴⁸ C. TONG-YU,¹⁴¹
A. TORIYAMA,²²⁴ N. TOROPOV,¹¹¹ A. TORRES-FORNÉ,^{135,136} C. I. TORRIE,² M. TOSCANI,¹²³ I. TOSTA E MELO,³⁰⁵
E. TOURNEFIER,²⁸ A. TRAPANANTI,^{50,49} F. TRAVASSO,^{50,49} G. TRAYLOR,⁶² M. TREVOR,¹²⁰ M. C. TRINGALI,⁵⁶
A. TRIPATHEE,⁸⁶ G. TROIAN,¹⁸³ L. TROIANO,^{306,107} A. TROVATO,^{183,45} L. TROZZO,⁵ R. J. TRUDEAU,² T. T. L. TSANG,¹⁸
R. TSO,^{147,†} S. TSUCHIDA,³⁰⁷ L. TSUKADA,⁷ T. TSUTSUI,³⁷ K. TURBANG,^{175,19} M. TURCONI,⁴⁷ C. TURSKI,⁹⁰ H. UBACH,^{38,78}
T. UCHIYAMA,⁴⁸ R. P. UDALL,² T. UEHARA,³⁰⁸ M. UEMATSU,¹⁹⁴ K. UENO,³⁷ S. UENO,²²⁴ V. UNDHEIM,²⁶⁹ T. USHIBA,⁴⁸
M. VACATELLO,^{84,83} H. VAHLBRUCH,^{40,41} N. VAIDYA,² G. VAJENTE,² A. VAJPEYI,¹⁵⁰ G. VALDES,¹²⁹ J. VALENCIA,⁹⁵
M. VALENTINI,^{101,33} S. A. VALLEJO-PEÑA,²⁸⁵ S. VALLERO,²³ V. VALSAN,⁸ N. VAN BAKEL,³³ M. VAN BEUZEKOM,³³
M. VAN DAEL,^{33,309} J. F. J. VAN DEN BRAND,^{32,101,33} C. VAN DEN BROECK,^{74,33} D. C. VANDER-HUYDE,⁷⁶
M. VAN DER SLUYS,^{33,74} A. VAN DE WALLE,³⁶ J. VAN DONGEN,^{33,101} K. VANDRA,⁵³ H. VAN HAEVERMAET,¹⁹
J. V. VAN HEIJNINGEN,^{33,101} P. VAN HOVE,⁶⁵ M. VANKEUREN,⁷² J. VANOSKY,² M. H. P. M. VAN PUTTEN,¹³
Z. VAN RANST,^{32,33} N. VAN REMORTEL,¹⁹ M. VARDARO,^{32,33} A. F. VARGAS,¹³⁰ J. J. VARGHESE,⁶⁶ V. VARMA,¹³⁴
M. VASÚTH,^{80,‡} A. VECCHIO,¹¹¹ G. VEDOVATO,⁸⁸ J. VEITCH,²⁶ P. J. VEITCH,¹⁰⁸ S. VENIKOUDIS,¹⁰ J. VENNEBERG,^{40,41}
P. VERDIER,¹¹⁴ D. VERKINDT,²⁸ B. VERMA,¹³⁴ P. VERMA,¹⁷³ Y. VERMA,⁹⁷ S. M. VERMEULEN,² F. VETRANO,⁶⁰
A. VEUTRO,^{63,64} A. M. VIBHUTE,³ A. VICERÉ,^{60,61} S. VIDYANT,⁷⁶ A. D. VIETS,⁸¹ A. VIJAYKUMAR,¹⁷⁸ A. VILKHA,¹⁹⁶
V. VILLA-ORTEGA,¹²⁶ E. T. VINCENT,⁵⁷ J.-Y. VINET,⁴⁷ S. VIRET,¹¹⁴ A. VIRTUOSO,^{183,45} S. VITALE,³¹ A. VIVES,⁷⁵

H. VOCCA,^{85,49} D. VOIGT,⁸² E. R. G. VON REIS,³ J. S. A. VON WRANGLER,^{40,41} S. P. VYATCHANIN,¹⁰² L. E. WADE,⁷² M. WADE,⁷² K. J. WAGNER,¹⁹⁶ A. WAJID,^{54,55} M. WALKER,¹¹⁸ G. S. WALLACE,⁹⁴ L. WALLACE,² H. WANG,³⁷ J. Z. WANG,⁸⁶ W. H. WANG,¹⁶⁰ Z. WANG,¹⁴¹ G. WARATKAR,²⁰⁰ J. WARNER,³ M. WAS,²⁸ T. WASHIMI,²¹ N. Y. WASHINGTON,² D. WATARAI,³⁷ K. E. WAYT,⁷² B. R. WEAVER,¹⁸ B. WEAVER,³ C. R. WEAVING,¹²⁴ S. A. WEBSTER,²⁶ M. WEINERT,^{40,41} A. J. WEINSTEIN,² R. WEISS,³¹ F. WELLMANN,^{40,41} L. WEN,²⁷ P. WESSELS,^{40,41} K. WETTE,³⁰ J. T. WHELAN,¹⁹⁶ B. F. WHITING,⁴³ C. WHITTLE,² J. B. WILDBERGER,¹ O. S. WILK,⁷² D. WILKEN,^{40,41,41} A. T. WILKIN,²⁰² D. J. WILLADSEN,⁸¹ K. WILLETTS,¹⁸ D. WILLIAMS,²⁶ M. J. WILLIAMS,¹²⁴ N. S. WILLIAMS,¹¹¹ J. L. WILLIS,² B. WILLKE,^{41,40,41} M. WILS,¹⁰³ J. WINTERFLOOD,²⁷ C. C. WIPF,² G. WOAN,²⁶ J. WOELLER,^{32,33} J. K. WOFFORD,¹⁹⁶ N. E. WOLFE,³¹ H. T. WONG,¹⁴¹ H. W. Y. WONG,²⁰⁹ I. C. F. WONG,² W. WONG,²⁰⁹ J. L. WRIGHT,³⁰ M. WRIGHT,²⁶ C. WU,¹⁴⁰ D. S. WU,^{40,41} H. WU,¹⁴⁰ E. WUCHNER,⁵² D. M. WYSOCKI,⁸ V. A. XU,³¹ Y. XU,¹⁹⁸ N. YADAV,⁹¹ H. YAMAMOTO,² K. YAMAMOTO,¹⁷⁷ T. S. YAMAMOTO,²⁴⁷ T. YAMAMOTO,⁴⁸ S. YAMAMURA,¹⁹³ R. YAMAZAKI,²²⁴ S. YAN,¹⁵ T. YAN,¹¹¹ F. W. YANG,¹⁹⁰ F. YANG,¹⁵⁸ K. Z. YANG,⁹³ Y. YANG,¹⁴⁴ Z. YARBROUGH,⁹ H. YASUI,⁴⁸ S.-W. YEH,¹⁴⁰ A. B. YELIKAR,¹⁹⁶ X. YIN,³¹ J. YOKOYAMA,^{310,37} T. YOKOZAWA,⁴⁸ J. YOO,¹⁴⁸ H. YU,¹⁴⁷ S. YUAN,²⁷ H. YUZURIHARA,⁴⁸ A. ZADROŻNY,¹⁷³ M. ZANOLIN,⁶⁶ M. ZEESHAN,¹⁹⁶ T. ZELENKOVA,⁵⁶ J.-P. ZENDRI,⁸⁸ M. ZEOLI,^{113,10} M. ZERRAD,³⁵ M. ZEVIN,⁷⁷ A. C. ZHANG,¹⁵⁸ L. ZHANG,² R. ZHANG,⁴³ T. ZHANG,¹¹¹ Y. ZHANG,³⁰ C. ZHAO,²⁷ YUE ZHAO,¹⁹⁰ YUHANG ZHAO,⁶⁸ Y. ZHENG,⁹⁹ H. ZHONG,⁹³ R. ZHOU,²¹⁴ X.-J. ZHU,³¹¹ Z.-H. ZHU,^{311,201} A. B. ZIMMERMAN,¹⁴⁶ M. E. ZUCKER,^{31,2} J. ZWEIZIG,² S. B. ARAUJO FURLAN,³¹² Z. ARZOUமானIAN,³¹³ A. BASU,³¹⁴ A. CASSITY,³¹⁵ I. COGNARD,^{316,317} K. CROWTER,³¹⁵ S. DEL PALACIO,^{312,318} C. M. ESPINOZA,^{319,320} E. FONSECA,^{321,322} C. M. L. FLYNN,¹⁵³ G. GANCIO,³¹² F. GARCÍA,^{312,323} K. C. GENDREAU,³¹³ D. C. GOOD,^{324,325} L. GUILLEMOT,^{316,317} S. GUILLOT,^{326,327} M. J. KEITH,³¹⁴ L. KUIPER,³²⁸ M. E. LOWER,^{329,153} A. G. LYNE,³¹⁴ J. W. MCKEE,³³⁰ B. W. MEYERS,^{315,331} J. L. PALFREYMAN,³³² A. B. PEARLMAN,^{333,334,§} G. E. ROMERO,^{312,323} R. M. SHANNON,¹⁵³ B. SHAW,³¹⁴ I. H. STAIRS,³¹⁵ B. W. STAPPERS,³¹⁴ C. M. TAN,^{333,334,331} G. THEUREAU,^{316,317,335} M. THOMPSON,³¹⁵ P. WELTEVREDE,³¹⁴ AND E. ZUBIETA,^{312,323}

¹Max Planck Institute for Gravitational Physics (Albert Einstein Institute), D-14476 Potsdam, Germany

²LIGO Laboratory, California Institute of Technology, Pasadena, CA 91125, USA

³LIGO Hanford Observatory, Richland, WA 99352, USA

⁴Dipartimento di Farmacia, Università di Salerno, I-84084 Fisciano, Salerno, Italy

⁵INFN, Sezione di Napoli, I-80126 Napoli, Italy

⁶University of Warwick, Coventry CV4 7AL, United Kingdom

⁷The Pennsylvania State University, University Park, PA 16802, USA

⁸University of Wisconsin-Milwaukee, Milwaukee, WI 53201, USA

⁹Louisiana State University, Baton Rouge, LA 70803, USA

¹⁰Université catholique de Louvain, B-1348 Louvain-la-Neuve, Belgium

¹¹Inter-University Centre for Astronomy and Astrophysics, Pune 411007, India

¹²Queen Mary University of London, London E1 4NS, United Kingdom

¹³Department of Physics and Astronomy, Sejong University, 209 Neungdong-ro, Gwangjin-gu, Seoul 143-747, Republic of Korea

¹⁴Instituto Nacional de Pesquisas Espaciais, 12227-010 São José dos Campos, São Paulo, Brazil

¹⁵Stanford University, Stanford, CA 94305, USA

¹⁶Università di Roma Tor Vergata, I-00133 Roma, Italy

¹⁷INFN, Sezione di Roma Tor Vergata, I-00133 Roma, Italy

¹⁸Cardiff University, Cardiff CF24 3AA, United Kingdom

¹⁹Universiteit Antwerpen, 2000 Antwerpen, Belgium

²⁰International Centre for Theoretical Sciences, Tata Institute of Fundamental Research, Bengaluru 560089, India

²¹Gravitational Wave Science Project, National Astronomical Observatory of Japan, 2-21-1 Osawa, Mitaka City, Tokyo 181-8588, Japan

²²Advanced Technology Center, National Astronomical Observatory of Japan, 2-21-1 Osawa, Mitaka City, Tokyo 181-8588, Japan

²³INFN Sezione di Torino, I-10125 Torino, Italy

²⁴Theoretisch-Physikalisches Institut, Friedrich-Schiller-Universität Jena, D-07743 Jena, Germany

²⁵Dipartimento di Fisica, Università degli Studi di Torino, I-10125 Torino, Italy

²⁶SUPA, University of Glasgow, Glasgow G12 8QQ, United Kingdom

²⁷OzGrav, University of Western Australia, Crawley, Western Australia 6009, Australia

²⁸Univ. Savoie Mont Blanc, CNRS, Laboratoire d'Annecy de Physique des Particules - IN2P3, F-74000 Annecy, France

²⁹Università di Napoli "Federico II", I-80126 Napoli, Italy

³⁰OzGrav, Australian National University, Canberra, Australian Capital Territory 0200, Australia

³¹LIGO Laboratory, Massachusetts Institute of Technology, Cambridge, MA 02139, USA

³²Maastricht University, 6200 MD Maastricht, Netherlands

³³Nikhef, 1098 XG Amsterdam, Netherlands

³⁴Université Libre de Bruxelles, Brussels 1050, Belgium

³⁵Aix Marseille Univ, CNRS, Centrale Med, Institut Fresnel, F-13013 Marseille, France

³⁶Université Paris-Saclay, CNRS/IN2P3, IJCLab, 91405 Orsay, France

- ³⁷ *University of Tokyo, Tokyo, 113-0033, Japan.*
- ³⁸ *Institut de Ciències del Cosmos (ICCUB), Universitat de Barcelona (UB), c. Martí i Franquès, 1, 08028 Barcelona, Spain*
- ³⁹ *Institut de Física d'Altes Energies (IFAE), The Barcelona Institute of Science and Technology, Campus UAB, E-08193 Bellaterra (Barcelona), Spain*
- ⁴⁰ *Max Planck Institute for Gravitational Physics (Albert Einstein Institute), D-30167 Hannover, Germany*
- ⁴¹ *Leibniz Universität Hannover, D-30167 Hannover, Germany*
- ⁴² *Gran Sasso Science Institute (GSSI), I-67100 L'Aquila, Italy*
- ⁴³ *University of Florida, Gainesville, FL 32611, USA*
- ⁴⁴ *Dipartimento di Scienze Matematiche, Informatiche e Fisiche, Università di Udine, I-33100 Udine, Italy*
- ⁴⁵ *INFN, Sezione di Trieste, I-34127 Trieste, Italy*
- ⁴⁶ *Tecnológico de Monterrey Campus Guadalajara, 45201 Zapopan, Jalisco, Mexico*
- ⁴⁷ *Université Côte d'Azur, Observatoire de la Côte d'Azur, CNRS, Artemis, F-06304 Nice, France*
- ⁴⁸ *Institute for Cosmic Ray Research, KAGRA Observatory, The University of Tokyo, 238 Higashi-Mozumi, Kamioka-cho, Hida City, Gifu 506-1205, Japan*
- ⁴⁹ *INFN, Sezione di Perugia, I-06123 Perugia, Italy*
- ⁵⁰ *Università di Camerino, I-62032 Camerino, Italy*
- ⁵¹ *University of Washington, Seattle, WA 98195, USA*
- ⁵² *California State University Fullerton, Fullerton, CA 92831, USA*
- ⁵³ *Villanova University, Villanova, PA 19085, USA*
- ⁵⁴ *INFN, Sezione di Genova, I-16146 Genova, Italy*
- ⁵⁵ *Dipartimento di Fisica, Università degli Studi di Genova, I-16146 Genova, Italy*
- ⁵⁶ *European Gravitational Observatory (EGO), I-56021 Cascina, Pisa, Italy*
- ⁵⁷ *Georgia Institute of Technology, Atlanta, GA 30332, USA*
- ⁵⁸ *Royal Holloway, University of London, London TW20 0EX, United Kingdom*
- ⁵⁹ *Astronomical course, The Graduate University for Advanced Studies (SOKENDAI), 2-21-1 Osawa, Mitaka City, Tokyo 181-8588, Japan*
- ⁶⁰ *Università degli Studi di Urbino "Carlo Bo", I-61029 Urbino, Italy*
- ⁶¹ *INFN, Sezione di Firenze, I-50019 Sesto Fiorentino, Firenze, Italy*
- ⁶² *LIGO Livingston Observatory, Livingston, LA 70754, USA*
- ⁶³ *INFN, Sezione di Roma, I-00185 Roma, Italy*
- ⁶⁴ *Università di Roma "La Sapienza", I-00185 Roma, Italy*
- ⁶⁵ *Université de Strasbourg, CNRS, IPHC UMR 7178, F-67000 Strasbourg, France*
- ⁶⁶ *Embry-Riddle Aeronautical University, Prescott, AZ 86301, USA*
- ⁶⁷ *Dipartimento di Fisica "E.R. Caianiello", Università di Salerno, I-84084 Fisciano, Salerno, Italy*
- ⁶⁸ *Université Paris Cité, CNRS, Astroparticule et Cosmologie, F-75013 Paris, France*
- ⁶⁹ *King's College London, University of London, London WC2R 2LS, United Kingdom*
- ⁷⁰ *Korea Institute of Science and Technology Information, Daejeon 34141, Republic of Korea*
- ⁷¹ *Université libre de Bruxelles, 1050 Bruxelles, Belgium*
- ⁷² *Kenyon College, Gambier, OH 43022, USA*
- ⁷³ *International College, Osaka University, 1-1 Machikaneyama-cho, Toyonaka City, Osaka 560-0043, Japan*
- ⁷⁴ *Institute for Gravitational and Subatomic Physics (GRASP), Utrecht University, 3584 CC Utrecht, Netherlands*
- ⁷⁵ *University of Oregon, Eugene, OR 97403, USA*
- ⁷⁶ *Syracuse University, Syracuse, NY 13244, USA*
- ⁷⁷ *Northwestern University, Evanston, IL 60208, USA*
- ⁷⁸ *Departament de Física Quàntica i Astrofísica (FQA), Universitat de Barcelona (UB), c. Martí i Franquès, 1, 08028 Barcelona, Spain*
- ⁷⁹ *Dipartimento di Medicina, Chirurgia e Odontoiatria "Scuola Medica Salernitana", Università di Salerno, I-84081 Baronissi, Salerno, Italy*
- ⁸⁰ *HUN-REN Wigner Research Centre for Physics, H-1121 Budapest, Hungary*
- ⁸¹ *Concordia University Wisconsin, Mequon, WI 53097, USA*
- ⁸² *Universität Hamburg, D-22761 Hamburg, Germany*
- ⁸³ *Università di Pisa, I-56127 Pisa, Italy*
- ⁸⁴ *INFN, Sezione di Pisa, I-56127 Pisa, Italy*
- ⁸⁵ *Università di Perugia, I-06123 Perugia, Italy*
- ⁸⁶ *University of Michigan, Ann Arbor, MI 48109, USA*
- ⁸⁷ *Università di Padova, Dipartimento di Fisica e Astronomia, I-35131 Padova, Italy*
- ⁸⁸ *INFN, Sezione di Padova, I-35131 Padova, Italy*
- ⁸⁹ *Institute for Plasma Research, Bhat, Gandhinagar 382428, India*
- ⁹⁰ *Universiteit Gent, B-9000 Gent, Belgium*

- ⁹¹ *Nicolaus Copernicus Astronomical Center, Polish Academy of Sciences, 00-716, Warsaw, Poland*
- ⁹² *Dipartimento di Ingegneria, Università del Sannio, I-82100 Benevento, Italy*
- ⁹³ *University of Minnesota, Minneapolis, MN 55455, USA*
- ⁹⁴ *SUPA, University of Strathclyde, Glasgow G1 1XQ, United Kingdom*
- ⁹⁵ *IAC3-IIEEC, Universitat de les Illes Balears, E-07122 Palma de Mallorca, Spain*
- ⁹⁶ *Departamento de Matemáticas, Universitat Autònoma de Barcelona, 08193 Bellaterra (Barcelona), Spain*
- ⁹⁷ *RRCAT, Indore, Madhya Pradesh 452013, India*
- ⁹⁸ *GRAPPA, Anton Pannekoek Institute for Astronomy and Institute for High-Energy Physics, University of Amsterdam, 1098 XH Amsterdam, Netherlands*
- ⁹⁹ *Missouri University of Science and Technology, Rolla, MO 65409, USA*
- ¹⁰⁰ *Colorado State University, Fort Collins, CO 80523, USA*
- ¹⁰¹ *Department of Physics and Astronomy, Vrije Universiteit Amsterdam, 1081 HV Amsterdam, Netherlands*
- ¹⁰² *Lomonosov Moscow State University, Moscow 119991, Russia*
- ¹⁰³ *Katholieke Universiteit Leuven, Oude Markt 13, 3000 Leuven, Belgium*
- ¹⁰⁴ *Università di Trento, Dipartimento di Fisica, I-38123 Povo, Trento, Italy*
- ¹⁰⁵ *INFN, Trento Institute for Fundamental Physics and Applications, I-38123 Povo, Trento, Italy*
- ¹⁰⁶ *Bar-Ilan University, Ramat Gan, 5290002, Israel*
- ¹⁰⁷ *INFN, Sezione di Napoli, Gruppo Collegato di Salerno, I-80126 Napoli, Italy*
- ¹⁰⁸ *OzGrav, University of Adelaide, Adelaide, South Australia 5005, Australia*
- ¹⁰⁹ *Centre national de la recherche scientifique, 75016 Paris, France*
- ¹¹⁰ *Univ Rennes, CNRS, Institut FOTON - UMR 6082, F-35000 Rennes, France*
- ¹¹¹ *University of Birmingham, Birmingham B15 2TT, United Kingdom*
- ¹¹² *Washington State University, Pullman, WA 99164, USA*
- ¹¹³ *Université de Liège, B-4000 Liège, Belgium*
- ¹¹⁴ *Université Claude Bernard Lyon 1, CNRS, IP2I Lyon / IN2P3, UMR 5822, F-69622 Villeurbanne, France*
- ¹¹⁵ *Instituto de Física Teórica UAM-CSIC, Universidad Autónoma de Madrid, 28049 Madrid, Spain*
- ¹¹⁶ *INFN, Laboratori Nazionali del Gran Sasso, I-67100 Assergi, Italy*
- ¹¹⁷ *Laboratoire Kastler Brossel, Sorbonne Université, CNRS, ENS-Université PSL, Collège de France, F-75005 Paris, France*
- ¹¹⁸ *Christopher Newport University, Newport News, VA 23606, USA*
- ¹¹⁹ *Astronomical Observatory Warsaw University, 00-478 Warsaw, Poland*
- ¹²⁰ *University of Maryland, College Park, MD 20742, USA*
- ¹²¹ *Università degli Studi di Milano-Bicocca, I-20126 Milano, Italy*
- ¹²² *INFN, Sezione di Milano-Bicocca, I-20126 Milano, Italy*
- ¹²³ *L2IT, Laboratoire des 2 Infinis - Toulouse, Université de Toulouse, CNRS/IN2P3, UPS, F-31062 Toulouse Cedex 9, France*
- ¹²⁴ *University of Portsmouth, Portsmouth, PO1 3FX, United Kingdom*
- ¹²⁵ *Université de Lyon, Université Claude Bernard Lyon 1, CNRS, Institut Lumière Matière, F-69622 Villeurbanne, France*
- ¹²⁶ *IGFAE, Universidad de Santiago de Compostela, 15782 Spain*
- ¹²⁷ *University of Chicago, Chicago, IL 60637, USA*
- ¹²⁸ *NASA Goddard Space Flight Center, Greenbelt, MD 20771, USA*
- ¹²⁹ *Texas A&M University, College Station, TX 77843, USA*
- ¹³⁰ *OzGrav, University of Melbourne, Parkville, Victoria 3010, Australia*
- ¹³¹ *INFN, Laboratori Nazionali del Sud, I-95125 Catania, Italy*
- ¹³² *Niels Bohr Institute, Copenhagen University, 2100 København, Denmark*
- ¹³³ *Istituto di Astrofisica e Planetologia Spaziali di Roma, 00133 Roma, Italy*
- ¹³⁴ *University of Massachusetts Dartmouth, North Dartmouth, MA 02747, USA*
- ¹³⁵ *Departamento de Astronomía y Astrofísica, Universitat de València, E-46100 Burjassot, València, Spain*
- ¹³⁶ *Observatori Astronòmic, Universitat de València, E-46980 Paterna, València, Spain*
- ¹³⁷ *Niels Bohr Institute, University of Copenhagen, 2100 København, Denmark*
- ¹³⁸ *University of British Columbia, Vancouver, BC V6T 1Z4, Canada*
- ¹³⁹ *Department of Physics, National Cheng Kung University, No.1, University Road, Tainan City 701, Taiwan*
- ¹⁴⁰ *National Tsing Hua University, Hsinchu City 30013, Taiwan*
- ¹⁴¹ *National Central University, Taoyuan City 320317, Taiwan*
- ¹⁴² *OzGrav, Charles Sturt University, Wagga Wagga, New South Wales 2678, Australia*
- ¹⁴³ *Vanderbilt University, Nashville, TN 37235, USA*
- ¹⁴⁴ *Department of Electrophysics, National Yang Ming Chiao Tung University, 101 Univ. Street, Hsinchu, Taiwan*
- ¹⁴⁵ *Kamioka Branch, National Astronomical Observatory of Japan, 238 Higashi-Mozumi, Kamioka-cho, Hida City, Gifu 506-1205, Japan*
- ¹⁴⁶ *University of Texas, Austin, TX 78712, USA*

- ¹⁴⁷ *CaRT, California Institute of Technology, Pasadena, CA 91125, USA*
- ¹⁴⁸ *Cornell University, Ithaca, NY 14850, USA*
- ¹⁴⁹ *Northeastern University, Boston, MA 02115, USA*
- ¹⁵⁰ *OzGrav, School of Physics & Astronomy, Monash University, Clayton 3800, Victoria, Australia*
- ¹⁵¹ *Dipartimento di Ingegneria Industriale (DIIN), Università di Salerno, I-84084 Fisciano, Salerno, Italy*
- ¹⁵² *INAF, Osservatorio Astronomico di Padova, I-35122 Padova, Italy*
- ¹⁵³ *OzGrav, Swinburne University of Technology, Hawthorn VIC 3122, Australia*
- ¹⁵⁴ *INAF, Osservatorio Astronomico di Brera sede di Merate, I-23807 Merate, Lecco, Italy*
- ¹⁵⁵ *Departamento de Matemáticas, Universitat de València, E-46100 Burjassot, València, Spain*
- ¹⁵⁶ *Montana State University, Bozeman, MT 59717, USA*
- ¹⁵⁷ *Texas Tech University, Lubbock, TX 79409, USA*
- ¹⁵⁸ *Columbia University, New York, NY 10027, USA*
- ¹⁵⁹ *University of Rhode Island, Kingston, RI 02881, USA*
- ¹⁶⁰ *The University of Texas Rio Grande Valley, Brownsville, TX 78520, USA*
- ¹⁶¹ *Chennai Mathematical Institute, Chennai 603103, India*
- ¹⁶² *Università degli Studi di Sassari, I-07100 Sassari, Italy*
- ¹⁶³ *Université de Normandie, ENSICAEN, UNICAEN, CNRS/IN2P3, LPC Caen, F-14000 Caen, France*
- ¹⁶⁴ *Laboratoire de Physique Corpusculaire Caen, 6 boulevard du maréchal Juin, F-14050 Caen, France*
- ¹⁶⁵ *Université Claude Bernard Lyon 1, CNRS, Laboratoire des Matériaux Avancés (LMA), IP2I Lyon / IN2P3, UMR 5822, F-69622 Villeurbanne, France*
- ¹⁶⁶ *Dipartimento di Scienze Matematiche, Fisiche e Informatiche, Università di Parma, I-43124 Parma, Italy*
- ¹⁶⁷ *INFN, Sezione di Milano Bicocca, Gruppo Collegato di Parma, I-43124 Parma, Italy*
- ¹⁶⁸ *University of Sannio at Benevento, I-82100 Benevento, Italy and INFN, Sezione di Napoli, I-80100 Napoli, Italy*
- ¹⁶⁹ *Perimeter Institute, Waterloo, ON N2L 2Y5, Canada*
- ¹⁷⁰ *Corps des Mines, Mines Paris, Université PSL, 60 Bd Saint-Michel, 75272 Paris, France*
- ¹⁷¹ *Indian Institute of Technology Madras, Chennai 600036, India*
- ¹⁷² *Graduate School of Science, Tokyo Institute of Technology, 2-12-1 Ookayama, Meguro-ku, Tokyo 152-8551, Japan*
- ¹⁷³ *National Center for Nuclear Research, 05-400 Świerk-Otwock, Poland*
- ¹⁷⁴ *Institut d'Astrophysique de Paris, Sorbonne Université, CNRS, UMR 7095, 75014 Paris, France*
- ¹⁷⁵ *Vrije Universiteit Brussel, 1050 Brussel, Belgium*
- ¹⁷⁶ *Carleton College, Northfield, MN 55057, USA*
- ¹⁷⁷ *Faculty of Science, University of Toyama, 3190 Gofuku, Toyama City, Toyama 930-8555, Japan*
- ¹⁷⁸ *Canadian Institute for Theoretical Astrophysics, University of Toronto, Toronto, ON M5S 3H8, Canada*
- ¹⁷⁹ *University of Cambridge, Cambridge CB2 1TN, United Kingdom*
- ¹⁸⁰ *Stony Brook University, Stony Brook, NY 11794, USA*
- ¹⁸¹ *Center for Computational Astrophysics, Flatiron Institute, New York, NY 10010, USA*
- ¹⁸² *Montclair State University, Montclair, NJ 07043, USA*
- ¹⁸³ *Dipartimento di Fisica, Università di Trieste, I-34127 Trieste, Italy*
- ¹⁸⁴ *HUN-REN Institute for Nuclear Research, H-4026 Debrecen, Hungary*
- ¹⁸⁵ *Centre de Physique des Particules de Marseille, 163, avenue de Luminy, 13288 Marseille cedex 09, France*
- ¹⁸⁶ *CNR-SPIN, I-84084 Fisciano, Salerno, Italy*
- ¹⁸⁷ *Scuola di Ingegneria, Università della Basilicata, I-85100 Potenza, Italy*
- ¹⁸⁸ *Western Washington University, Bellingham, WA 98225, USA*
- ¹⁸⁹ *SUPA, University of the West of Scotland, Paisley PA1 2BE, United Kingdom*
- ¹⁹⁰ *The University of Utah, Salt Lake City, UT 84112, USA*
- ¹⁹¹ *Eötvös University, Budapest 1117, Hungary*
- ¹⁹² *Centro de Física das Universidades do Minho e do Porto, Universidade do Minho, PT-4710-057 Braga, Portugal*
- ¹⁹³ *Institute for Cosmic Ray Research, KAGRA Observatory, The University of Tokyo, 5-1-5 Kashiwa-no-Ha, Kashiwa City, Chiba 277-8582, Japan*
- ¹⁹⁴ *Department of Physics, Graduate School of Science, Osaka Metropolitan University, 3-3-138 Sugimoto-cho, Sumiyoshi-ku, Osaka City, Osaka 558-8585, Japan*
- ¹⁹⁵ *Université Côte d'Azur, Observatoire de la Côte d'Azur, CNRS, Lagrange, F-06304 Nice, France*
- ¹⁹⁶ *Rochester Institute of Technology, Rochester, NY 14623, USA*
- ¹⁹⁷ *California State University, Los Angeles, Los Angeles, CA 90032, USA*
- ¹⁹⁸ *University of Zurich, Winterthurerstrasse 190, 8057 Zurich, Switzerland*
- ¹⁹⁹ *University of Szeged, Dóm tér 9, Szeged 6720, Hungary*
- ²⁰⁰ *Indian Institute of Technology Bombay, Powai, Mumbai 400 076, India*

- ²⁰¹ *School of Physics and Technology, Wuhan University, Bayi Road 299, Wuchang District, Wuhan, Hubei, 430072, China*
- ²⁰² *University of California, Riverside, Riverside, CA 92521, USA*
- ²⁰³ *INAF, Osservatorio Astronomico di Capodimonte, I-80131 Napoli, Italy*
- ²⁰⁴ *University of Nottingham NG7 2RD, UK*
- ²⁰⁵ *Ariel University, Ramat HaGolan St 65, Ari'el, Israel*
- ²⁰⁶ *The University of Mississippi, University, MS 38677, USA*
- ²⁰⁷ *Institute of Physics, Academia Sinica, 128 Sec. 2, Academia Rd., Nankang, Taipei 11529, Taiwan*
- ²⁰⁸ *Shanghai Astronomical Observatory, Chinese Academy of Sciences, 80 Nandan Road, Shanghai 200030, China*
- ²⁰⁹ *The Chinese University of Hong Kong, Shatin, NT, Hong Kong*
- ²¹⁰ *Marquette University, Milwaukee, WI 53233, USA*
- ²¹¹ *American University, Washington, DC 20016, USA*
- ²¹² *University of Nevada, Las Vegas, Las Vegas, NV 89154, USA*
- ²¹³ *Department of Applied Physics, Fukuoka University, 8-19-1 Nanakuma, Jonan, Fukuoka City, Fukuoka 814-0180, Japan*
- ²¹⁴ *University of California, Berkeley, CA 94720, USA*
- ²¹⁵ *University of Lancaster, Lancaster LA1 4YW, United Kingdom*
- ²¹⁶ *College of Industrial Technology, Nihon University, 1-2-1 Izumi, Narashino City, Chiba 275-8575, Japan*
- ²¹⁷ *Faculty of Engineering, Niigata University, 8050 Ikarashi-2-no-cho, Nishi-ku, Niigata City, Niigata 950-2181, Japan*
- ²¹⁸ *Department of Physics and Astronomy, Haverford College, 370 Lancaster Avenue, Haverford, PA 19041, USA*
- ²¹⁹ *Department of Physics, Tamkang University, No. 151, Yingzhuan Rd., Danshui Dist., New Taipei City 25137, Taiwan*
- ²²⁰ *Rutherford Appleton Laboratory, Didcot OX11 0DE, United Kingdom*
- ²²¹ *Department of Astronomy and Space Science, Chungnam National University, 9 Daehak-ro, Yuseong-gu, Daejeon 34134, Republic of Korea*
- ²²² *Scuola Normale Superiore, I-56126 Pisa, Italy*
- ²²³ *Kavli Institute for Astronomy and Astrophysics, Peking University, Yiheyuan Road 5, Haidian District, Beijing 100871, China*
- ²²⁴ *Department of Physical Sciences, Aoyama Gakuin University, 5-10-1 Fuchinobe, Sagami-hara City, Kanagawa 252-5258, Japan*
- ²²⁵ *Nambu Yoichiro Institute of Theoretical and Experimental Physics (NITEP), Osaka Metropolitan University, 3-3-138 Sugimoto-cho, Sumiyoshi-ku, Osaka City, Osaka 558-8585, Japan*
- ²²⁶ *Directorate of Construction, Services & Estate Management, Mumbai 400094, India*
- ²²⁷ *University of Białystok, 15-424 Białystok, Poland*
- ²²⁸ *National Astronomical Observatories, Chinese Academic of Sciences, 20A Datun Road, Chaoyang District, Beijing, China*
- ²²⁹ *School of Astronomy and Space Science, University of Chinese Academy of Sciences, 20A Datun Road, Chaoyang District, Beijing, China*
- ²³⁰ *Astronomical Observatory, Jagiellonian University, 31-007 Cracow, Poland*
- ²³¹ *University of Southampton, Southampton SO17 1BJ, United Kingdom*
- ²³² *Department of Physics, Ulsan National Institute of Science and Technology (UNIST), 50 UNIST-gil, Ulsu-gun, Ulsan 44919, Republic of Korea*
- ²³³ *Institute for Cosmic Ray Research, The University of Tokyo, 5-1-5 Kashiwa-no-Ha, Kashiwa City, Chiba 277-8582, Japan*
- ²³⁴ *Institute for High-Energy Physics, University of Amsterdam, 1098 XH Amsterdam, Netherlands*
- ²³⁵ *Chung-Ang University, Seoul 06974, Republic of Korea*
- ²³⁶ *University of Washington Bothell, Bothell, WA 98011, USA*
- ²³⁷ *Aix Marseille Université, Jardin du Pharo, 58 Boulevard Charles Livon, 13007 Marseille, France*
- ²³⁸ *Laboratoire de Physique et de Chimie de l'Environnement, Université Joseph KI-ZERBO, 9GH2+3V5, Ouagadougou, Burkina Faso*
- ²³⁹ *Ewha Womans University, Seoul 03760, Republic of Korea*
- ²⁴⁰ *Seoul National University, Seoul 08826, Republic of Korea*
- ²⁴¹ *Korea Astronomy and Space Science Institute, Daejeon 34055, Republic of Korea*
- ²⁴² *Sungkyunkwan University, Seoul 03063, Republic of Korea*
- ²⁴³ *Institute of Particle and Nuclear Studies (IPNS), High Energy Accelerator Research Organization (KEK), 1-1 Oho, Tsukuba City, Ibaraki 305-0801, Japan*
- ²⁴⁴ *Division of Science, National Astronomical Observatory of Japan, 2-21-1 Osawa, Mitaka City, Tokyo 181-8588, Japan*
- ²⁴⁵ *Bard College, Annandale-On-Hudson, NY 12504, USA*
- ²⁴⁶ *Institute of Mathematics, Polish Academy of Sciences, 00656 Warsaw, Poland*
- ²⁴⁷ *Department of Physics, Nagoya University, ES building, Furocho, Chikusa-ku, Nagoya, Aichi 464-8602, Japan*
- ²⁴⁸ *Université de Montréal/Polytechnique, Montreal, Quebec H3T 1J4, Canada*
- ²⁴⁹ *Indian Institute of Science Education and Research, Kolkata, Mohanpur, West Bengal 741252, India*
- ²⁵⁰ *Inje University Gimhae, South Gyeongsang 50834, Republic of Korea*
- ²⁵¹ *NAVIER, École des Ponts, Univ Gustave Eiffel, CNRS, Marne-la-Vallée, France*
- ²⁵² *Università di Firenze, Sesto Fiorentino I-50019, Italy*

- ²⁵³ *National Center for High-performance Computing, National Applied Research Laboratories, No. 7, R&D 6th Rd., Hsinchu Science Park, Hsinchu City 30076, Taiwan*
- ²⁵⁴ *NASA Marshall Space Flight Center, Huntsville, AL 35811, USA*
²⁵⁵ *West Virginia University, Morgantown, WV 26506, USA*
- ²⁵⁶ *Institut fuer Theoretische Astrophysik, Zentrum fuer Astronomie Heidelberg, Universitaet Heidelberg, Albert Ueberle Str. 2, 69120 Heidelberg, Germany*
²⁵⁷ *School of Physics Science and Engineering, Tongji University, Shanghai 200092, China*
²⁵⁸ *Institut d'Estudis Espacials de Catalunya, c. Gran Capità, 2-4, 08034 Barcelona, Spain*
- ²⁵⁹ *Institucio Catalana de Recerca i Estudis Avançats (ICREA), Passeig de Lluís Companys, 23, 08010 Barcelona, Spain*
²⁶⁰ *Center for Research and Exploration in Space Science and Technology, NASA/GSFC, Greenbelt, MD 20771*
²⁶¹ *Tsinghua University, Beijing 100084, China*
- ²⁶² *INFN Cagliari, Physics Department, Università degli Studi di Cagliari, Cagliari 09042, Italy*
²⁶³ *Saha Institute of Nuclear Physics, Bidhannagar, West Bengal 700064, India*
²⁶⁴ *Tata Institute of Fundamental Research, Mumbai 400005, India*
²⁶⁵ *Hobart and William Smith Colleges, Geneva, NY 14456, USA*
²⁶⁶ *Institut des Hautes Etudes Scientifiques, F-91440 Bures-sur-Yvette, France*
- ²⁶⁷ *Faculty of Law, Ryukoku University, 67 Fukakusa Tsukamoto-cho, Fushimi-ku, Kyoto City, Kyoto 612-8577, Japan*
²⁶⁸ *Department of Physics and Astronomy, University of Notre Dame, 225 Nieuwland Science Hall, Notre Dame, IN 46556, USA*
²⁶⁹ *University of Stavanger, 4021 Stavanger, Norway*
- ²⁷⁰ *Physics Program, Graduate School of Advanced Science and Engineering, Hiroshima University, 1-3-1 Kagamiyama, Higashihiroshima City, Hiroshima 903-0213, Japan*
²⁷¹ *Laboratoire Univers et Théories, Observatoire de Paris, 92190 Meudon, France*
²⁷² *Observatoire de Paris, 75014 Paris, France*
²⁷³ *Université PSL, 75006 Paris, France*
²⁷⁴ *Université de Paris Cité, 75006 Paris, France*
²⁷⁵ *National Institute for Mathematical Sciences, Daejeon 34047, Republic of Korea*
- ²⁷⁶ *Graduate School of Science and Technology, Niigata University, 8050 Ikarashi-2-no-cho, Nishi-ku, Niigata City, Niigata 950-2181, Japan*
²⁷⁷ *Niigata Study Center, The Open University of Japan, 754 Ichibancho, Asahimachi-dori, Chuo-ku, Niigata City, Niigata 951-8122, Japan*
²⁷⁸ *CSIR-Central Glass and Ceramic Research Institute, Kolkata, West Bengal 700032, India*
²⁷⁹ *Consiglio Nazionale delle Ricerche - Istituto dei Sistemi Complessi, I-00185 Roma, Italy*
²⁸⁰ *Department of Physics, Aristotle University of Thessaloniki, 54124 Thessaloniki, Greece*
- ²⁸¹ *Department of Astronomy, Yonsei University, 50 Yonsei-Ro, Seodaemun-Gu, Seoul 03722, Republic of Korea*
²⁸² *Museo Storico della Fisica e Centro Studi e Ricerche "Enrico Fermi", I-00184 Roma, Italy*
²⁸³ *Dipartimento di Ingegneria Industriale, Eletttronica e Meccanica, Università degli Studi Roma Tre, I-00146 Roma, Italy*
- ²⁸⁴ *Subatech, CNRS/IN2P3 - IMT Atlantique - Nantes Université, 4 rue Alfred Kastler BP 20722 44307 Nantes CÉDEX 03, France*
²⁸⁵ *Universidad de Antioquia, Medellín, Colombia*
²⁸⁶ *Departamento de Física - ETSIDI, Universidad Politécnica de Madrid, 28012 Madrid, Spain*
- ²⁸⁷ *Department of Electronic Control Engineering, National Institute of Technology, Nagaoka College, 888 Nishikataki, Nagaoka City, Niigata 940-8532, Japan*
²⁸⁸ *Università Degli Studi Di Ferrara, Via Savonarola, 9, 44121 Ferrara FE, Italy*
²⁸⁹ *Faculty of Science, Toho University, 2-2-1 Miyama, Funabashi City, Chiba 274-8510, Japan*
²⁹⁰ *Indian Institute of Technology, Palaj, Gandhinagar, Gujarat 382355, India*
- ²⁹¹ *Laboratoire MSME, Cité Descartes, 5 Boulevard Descartes, Champs-sur-Marne, 77454 Marne-la-Vallée Cedex 2, France*
²⁹² *Institute of Systems and Information Engineering, University of Tsukuba, 1-1-1, Tennodai, Tsukuba, Ibaraki 305-8573, Japan*
²⁹³ *Institute for Quantum Studies, Chapman University, 1 University Dr., Orange, CA 92866, USA*
- ²⁹⁴ *Faculty of Information Science and Technology, Osaka Institute of Technology, 1-79-1 Kitayama, Hirakata City, Osaka 573-0196, Japan*
²⁹⁵ *INAF, Osservatorio Astrofisico di Arcetri, I-50125 Firenze, Italy*
- ²⁹⁶ *THEMS (Interdisciplinary Theoretical and Mathematical Sciences Program), RIKEN, 2-1 Hirosawa, Wako, Saitama 351-0198, Japan*
²⁹⁷ *Scuola Internazionale Superiore di Studi Avanzati, Via Bonomea, 265, I-34136, Trieste TS, Italy*
- ²⁹⁸ *Institut für Theoretische Physik, Johann Wolfgang Goethe-Universität, Max-von-Laue-Str. 1, 60438 Frankfurt am Main, Germany*
²⁹⁹ *INAF, Osservatorio di Astrofisica e Scienza dello Spazio, I-40129 Bologna, Italy*
³⁰⁰ *Universidade Estadual Paulista, 01140-070 São Paulo, Brazil*
- ³⁰¹ *Faculty of Physics, University of Warsaw, Ludwika Pasteura 5, 02-093 Warszawa, Poland*
³⁰² *Research Center for Space Science, Advanced Research Laboratories, Tokyo City University, 3-3-1 Ushikubo-Nishi, Tsuzuki-Ku, Yokohama, Kanagawa 224-8551, Japan*

- ³⁰³ *Department of Physics, Kyoto University, Kita-Shirakawa Oiwake-cho, Sakyou-ku, Kyoto City, Kyoto 606-8502, Japan*
- ³⁰⁴ *Yukawa Institute for Theoretical Physics (YITP), Kyoto University, Kita-Shirakawa Oiwake-cho, Sakyou-ku, Kyoto City, Kyoto 606-8502, Japan*
- ³⁰⁵ *University of Catania, Department of Physics and Astronomy, Via S. Sofia, 64, 95123 Catania CT, Italy*
- ³⁰⁶ *Dipartimento di Scienze Aziendali - Management and Innovation Systems (DISA-MIS), Università di Salerno, I-84084 Fisciano, Salerno, Italy*
- ³⁰⁷ *National Institute of Technology, Fukui College, Geshi-cho, Sabae-shi, Fukui 916-8507, Japan*
- ³⁰⁸ *Department of Communications Engineering, National Defense Academy of Japan, 1-10-20 Hashirimizu, Yokosuka City, Kanagawa 239-8686, Japan*
- ³⁰⁹ *Eindhoven University of Technology, 5600 MB Eindhoven, Netherlands*
- ³¹⁰ *Kavli Institute for the Physics and Mathematics of the Universe, WPI, The University of Tokyo, 5-1-5 Kashiwa-no-Ha, Kashiwa City, Chiba 277-8583, Japan*
- ³¹¹ *Department of Astronomy, Beijing Normal University, Xijiekouwai Street 19, Haidian District, Beijing 100875, China*
- ³¹² *Instituto Argentino de Radioastronomía (CCT La Plata, CONICET; CICPBA; UNLP), C.C.5, (1894) Villa Elisa, Buenos Aires, Argentina*
- ³¹³ *X-Ray Astrophysics Laboratory, NASA Goddard Space Flight Center, Greenbelt, MD 20771, USA*
- ³¹⁴ *Jodrell Bank Centre for Astrophysics, School of Physics and Astronomy, University of Manchester, Manchester, UK, M13 9PL*
- ³¹⁵ *Department of Physics and Astronomy, University of British Columbia, 6224 Agricultural Road, Vancouver, BC V6T 1Z1 Canada*
- ³¹⁶ *LPC2E, OSUC, Univ Orleans, CNRS, CNES, Observatoire de Paris, F-45071 Orleans, France*
- ³¹⁷ *Observatoire Radioastronomique de Nançay, Observatoire de Paris, Université PSL, Université d'Orléans, CNRS, 18330 Nançay, France*
- ³¹⁸ *Department of Space, Earth and Environment, Chalmers University of Technology, SE-412 96 Gothenburg, Sweden*
- ³¹⁹ *Departamento de Física, Universidad de Santiago de Chile (USACH), Av. Víctor Jara 3493, Estación Central, Chile*
- ³²⁰ *Center for Interdisciplinary Research in Astrophysics and Space Sciences (CIRAS), Universidad de Santiago de Chile, Chile*
- ³²¹ *Department of Physics and Astronomy, West Virginia University, PO Box 6315, Morgantown, WV 26506, USA*
- ³²² *Center for Gravitational Waves and Cosmology, West Virginia University, Chestnut Ridge Research Building, Morgantown, WV, USA*
- ³²³ *Facultad de Ciencias Astronómicas y Geofísicas, Universidad Nacional de La Plata, Paseo del Bosque, B1900FWA La Plata, Argentina*
- ³²⁴ *Center for Computational Astrophysics, Flatiron Institute, 162 5th Avenue, New York, New York, 10010, USA*
- ³²⁵ *Department of Physics, University of Connecticut, 196 Auditorium Road, U-3046, Storrs, CT 06269-3046, USA*
- ³²⁶ *IRAP, CNRS, 9 avenue du Colonel Roche, BP 44346, F-31028 Toulouse Cedex 4, France*
- ³²⁷ *Université de Toulouse, CNES, UPS-OMP, F-31028 Toulouse, France*
- ³²⁸ *SRON-Netherlands Institute for Space Research, Niels Bohrweg 4, 2333 CA, Leiden, Netherlands*
- ³²⁹ *CSIRO, Space and Astronomy, PO Box 76, Epping, NSW 1710, Australia*
- ³³⁰ *Canadian Institute for Theoretical Astrophysics, University of Toronto, 60 St. George Street, Toronto, ON M5S 3H8, Canada*
- ³³¹ *International Centre for Radio Astronomy Research, Curtin University, Bentley, WA 6102, Australia*
- ³³² *School of Natural Sciences, University of Tasmania, Hobart, Australia*
- ³³³ *Department of Physics, McGill University, 3600 rue University, Montréal, QC H3A 2T8, Canada*
- ³³⁴ *McGill Space Institute, McGill University, 3550 rue University, Montréal, QC H3A 2A7, Canada*
- ³³⁵ *LUTH, Observatoire de Paris, PSL Research University, CNRS, Université Paris Diderot, Sorbonne Paris Cité, F-92195 Meudon, France*

(Dated: January 6, 2025)

ABSTRACT

Continuous gravitational waves (CWs) emission from neutron stars carries information about their internal structure and equation of state, and it can provide tests of General Relativity. We present a search for CWs from a set of 45 known pulsars in the first part of the fourth LIGO–Virgo–KAGRA observing run, known as O4a. We conducted a targeted search for each pulsar using three independent analysis methods considering the single-harmonic and the dual-harmonic emission models. We find no evidence of a CW signal in O4a data for both models and set upper limits on the signal amplitude and on the ellipticity, which quantifies the asymmetry in the neutron star mass distribution. For the single-harmonic emission model, 29 targets have the upper limit on the amplitude below the theoretical spin-down limit. The lowest upper limit on the amplitude is 6.4×10^{-27} for the young energetic pulsar J0537–6910, while the lowest constraint on the ellipticity is 8.8×10^{-9} for the bright nearby millisecond pulsar J0437–4715. Additionally, for a subset of 16 targets we performed a narrowband search that is

more robust regarding the emission model, with no evidence of a signal. We also found no evidence of non-standard polarizations as predicted by the Brans-Dicke theory.

1. INTRODUCTION

Since their discovery in 1967, pulsars have been crucial in advancing our understanding of fundamental physics. These extremely dense and compact objects possess strong magnetic fields and rotate rapidly, emitting beams of electromagnetic (EM) radiation from hot spots near the poles or from the higher magnetosphere (Philippov & Kramer 2022). EM observations across various wavelengths (radio, X-rays, and gamma rays) have provided detailed insights into pulsar properties, allowing precise measurements of pulsar parameters. Given their stability and predictability, pulsars present an excellent opportunity for the search of continuous gravitational waves (CWs) in the LIGO–Virgo–KAGRA (LVK) data.

In contrast to transient gravitational waves (GWs) emitted by binary black hole (and neutron star) mergers (Abbott et al. 2021a,b, 2023), CWs have yet to be observed. These signals should be nearly monochromatic, with amplitude and frequency exhibiting small variations over year-long timescales.

CWs are expected from a time-varying non-axisymmetric mass distribution in rotating neutron stars (Zimmermann & Szedenits 1979). This could be the result of strain in the elastic crust (Ushomirsky et al. 2000), accretion from a companion star (Bildsten 1998; Melatos & Payne 2005; Gittins & Andersson 2021), or a strong inner magnetic field (Bonazzola & Gourgoulhon 1996; Cutler 2002). Alternatively, the deformation could be caused by fluid oscillations, such as those due to r-modes (Andersson 1998; Friedman & Morsink 1998). However, the sources of CWs are likely to possess smaller mass quadrupoles compared to the sources of transient GWs, resulting in a weaker signal. Therefore, for signals to be detectable with current detectors, we need to consider nearby sources integrating long stretches (months or years worth) of detector data.

Observation of CWs from a neutron star would yield crucial insights into the star’s structure and its equation of state (Haskell & Bejger 2023; Gittins 2024). Moreover, the form of the signal can be employed to test general relativity by measuring (or constraining) the pres-

ence of non-standard polarizations (Isi et al. 2017; Abbott et al. 2019a). Possible mechanisms of CW emission from neutron stars are discussed in greater detail by Riles (2023) and Glampedakis & Gualtieri (2018).

The primary challenge for CW searches lies in accurately accounting for the various modulations that affect the signal received on the Earth. These include the Doppler effect due to the Earth’s motion, the pulsar’s rotational evolution (i.e., the slow spin-down) and relativistic effects. EM observations provide accurate measurements of the sky position and rotation parameters that allow us to predict and correct these modulations, thereby enhancing the search sensitivity.

Based on the knowledge of the source parameters, different strategies can be used to search for CW signals in LVK data (see Wette 2023, for a complete review of search methods). *Targeted searches*, the primary subject of this paper, aim to detect CWs from known pulsars, whose timing solutions can be calculated from known rotation phases and spin-down rates. Targeted searches use full-coherent methods that integrate data over long observation times maintaining phase coherence over time. By assuming that the GW phase evolution follows the EM solution, the parameter space can be reduced to the unknown signal amplitude and polarization parameters. This assumption is relaxed in *narrowband searches*, which are performed in a narrow band around the frequency and spin-down rate (e.g., Abbott et al. 2017a, 2019b; Abbott et al. 2022). However, because these searches decrease the sensitivity and increase the computational cost, they are often performed on fewer targets.

Although several CW searches have been conducted in the last years targeting both isolated pulsars and those in binary systems, so far none of these searches have produced evidence of CWs (e.g., Abbott et al. 2017b, 2019c, 2020, 2021c, 2022; Ashok et al. 2021; Nieder et al. 2019, 2020). In the absence of a signal, these searches set upper limits on the GW amplitude and on the ellipticity, the physical parameter that quantifies the asymmetry in the mass distribution. In many cases, these limits are more stringent than (it is said to have “surpassed”) the so-called *spin-down limit*; the theoretical limit calculated by assuming 100% of each pulsar’s spin-down luminosity to be radiated through GWs. In the most recent targeted search (Abbott et al. 2021c, 2022) considering O3 data, 24 pulsars surpassed their spin-down limits, including the Crab and Vela pulsars, J0537–6910 and two millisecond pulsars, J0437–4715 and J0711–6830. Ad-

* Deceased, September 2024.

† Deceased, July 2023.

‡ Deceased, February 2024.

§ Banting Fellow, McGill Space Institute (MSI) Fellow, and FRQNT Postdoctoral Fellow.

ditionally, searches for an r-mode emission are described in Rajbhandari et al. (2021) for the Crab and in Fesik & Papa (2020); Rajbhandari et al. (2021); Abbott et al. (2021d) for J0537–6910. Continuous improvements in detector sensitivity and data analysis techniques are progressively enhancing our ability to detect these faint signals.

In this paper, we present a targeted search for CWs from a set of 45 known pulsars, considering LIGO data from the initial part, O4a, of the most recent LVK observing run. Pulsar selection is based on the available EM observations (see Section 4.2) and on the anticipated sensitivity for targeted searches near or below the spin-down limit. Considering two different emission models, we find no evidence of CW signals in the data, and we set upper limits on the amplitude and on the ellipticity for each target. Additionally, we perform a narrowband search for a subset of 16 targets and a search for non-standard polarizations as predicted by the Brans-Dicke theory (Brans & Dicke 1961).

The paper is structured as follows. In Section 2, we briefly describe the expected signal for the emission models that we considered. The data analysis methods used in the paper are discussed in Section 3, while in Section 4 we describe the EM and GW data used for the analysis. The results are summarized and discussed in detail in Sections 5 and 6. Conclusions are reported in Section 7.

2. SIGNAL MODEL

2.1. *Standard signal*

For the targeted search, we assume that the GW signal is locked to the rotational phase of the pulsar obtained through EM observations. For an isolated triaxial star, rotating steadily about one of its principal axes of inertia, the GW emission frequency is twice the pulsar’s spin frequency, f_{rot} . For the single-harmonic emission model, we search for signals at $2f_{\text{rot}}$. However, there are additional mechanisms which could emit GWs at other frequencies. A superfluid component beneath the crust, rotating with a spin axis misaligned to the star’s rotation axis would produce an additional emission at the rotation frequency, so that overall we have a dual-harmonic emission at both once and twice the rotation frequency (Jones 2010). This would not impact the EM signature. Therefore, a dual-harmonic search is performed at both f_{rot} and $2f_{\text{rot}}$. Additionally, a single-harmonic narrowband search is performed around $2f_{\text{rot}}$, allowing for the possibility of a difference in rotation rate between the pulsation-producing magnetosphere and the part of the star responsible for the CW emission.

For the general dual-harmonic emission model, the signals h_{21} and h_{22} at f_{rot} and $2f_{\text{rot}}$ can be defined as (Pitkin et al. 2015):

$$h_{21} = -\frac{C_{21}}{2} \left[F_+^D(\alpha, \delta, \psi; t) \sin \iota \cos \iota \cos(\Phi(t) + \Phi_{21}^C) + F_\times^D(\alpha, \delta, \psi; t) \sin \iota \sin(\Phi(t) + \Phi_{21}^C) \right], \quad (1)$$

$$h_{22} = -C_{22} \left[F_+^D(\alpha, \delta, \psi; t)(1 + \cos^2 \iota) \cos(2\Phi(t) + \Phi_{22}^C) + 2F_\times^D(\alpha, \delta, \psi; t) \cos \iota \sin(2\Phi(t) + \Phi_{22}^C) \right], \quad (2)$$

where C_{21} and C_{22} are the dimensionless constants that give the component amplitudes, the angles (α, δ) are the right ascension and declination of the source, the angles (ι, ψ) describe the orientation of the source’s spin axis with respect to the observer in terms of inclination and polarization, Φ_{21}^C and Φ_{22}^C are phase angles at a defined epoch and $\Phi(t)$ is the rotational phase of the source. The antenna functions F_+^D and F_\times^D describe how the two polarization components (plus and cross) are projected onto the detector. These waveforms are detailed in Jones (2010) and used in Abbott et al. (2022).

For the triaxial star described earlier, which only emits GWs at $2f_{\text{rot}}$, C_{21} in Equation (1) is 0, which leaves only Equation (2) which contains C_{22} . The amplitude h_0 is defined as the amplitude of the circularly polarized signal observable for a source directly above or below the plane of the detector with its spin axis pointed directly toward or away from the detector. It can be calculated as:

$$h_0 = 2C_{22} = \frac{16\pi^2 G I_{zz} \varepsilon f_{\text{rot}}^2}{c^4 d}, \quad (3)$$

where d is the distance of the source. The equatorial ellipticity ε for the triaxial star emitting GWs at only $2f_{\text{rot}}$ is defined as

$$\varepsilon \equiv \frac{|I_{xx} - I_{yy}|}{I_{zz}}, \quad (4)$$

where I_{xx} , I_{yy} and I_{zz} are the source’s principle moments of inertia, with the star rotating about the z -axis. From the ellipticity, the pulsar’s mass quadrupole, Q_{22} can be calculated using (Owen 2005)

$$Q_{22} = I_{zz} \varepsilon \sqrt{\frac{15}{8\pi}}. \quad (5)$$

The spin-down limit h_0^{sd} of a source is given by:

$$h_0^{\text{sd}} = \frac{1}{d} \left(\frac{5GI_{zz} |\dot{f}_{\text{rot}}|}{2c^3 f_{\text{rot}}} \right)^{1/2} \quad (6)$$

where \dot{f}_{rot} is the rotation frequency derivative, or spin-down rate. This limit is the maximum GW amplitude

allowed assuming all the lost rotational energy of the star is due to conversion into GW energy. It should be noted that there are two types of spin-down rates: observed, which can be affected by the transverse velocity of the source (e.g. the Shklovskii effect, described in Shklovskii (1970)), and intrinsic. Therefore, where possible, the intrinsic spin-down rate is used in calculating the spin-down limit.

2.2. Non-standard polarization signal

In this paper, similar to the analysis in Abbott et al. (2022), we search for gravitational waves (GWs) with polarizations predicted by the Brans-Dicke modification of General Relativity (GR). Brans-Dicke theory includes two tensor polarizations, like in GR, and an additional scalar polarization. The dominant scalar radiation stems from the time-dependent dipole moment D . The dipole radiation occurs at the pulsar’s rotational frequency f_{rot} . Assuming the dipole moment is along the x -axis the amplitude h_0^d of the signal is given by

$$h_0^d = \frac{4\pi G}{c^3} \zeta \frac{Df_{\text{rot}}}{d}, \quad (7)$$

where ζ is the parameter of the Brans-Dicke theory (see Verma 2021, for details).

3. METHODS

In this Section, we describe the data analysis methods used in this work: three independent pipelines for the targeted searches, one pipeline for the narrowband searches and one pipeline for the non-standard polarizations searches. We use three targeted pipelines to compare independent results as our methods rely on different statistical approaches (Bayesian or frequentist) and on different pre-processings and handling of non-stationary or non-gaussian noise disturbances in the data.

3.1. Time-domain Bayesian Method

The Continuous (gravitational) Wave Inference in Python (CWInPy) package is used to perform the Bayesian analysis (Pitkin 2022) following the method described in Abbott et al. (2019c) and summarized here.

First, a complex, slowly evolving heterodyne is used to remove the phase evolution of the source. This includes corrections for the relative motion of the source with respect to the detector and relativistic effects (Dupuis & Woan 2005). Then, a low-pass anti-aliasing filter is applied to the data to remove the upper sideband produced from the heterodyne and limit the possibility of disturbances from spectral lines. Next, the data is down-sampled, centered about the expected signal frequency which has been shifted to 0 Hz by the heterodyne. For

the dual-harmonic search, this method is repeated so that time series centered at both f_{rot} and $2f_{\text{rot}}$ are obtained.

There are several unknown signal parameters, with the amplitude being of primary interest. Bayesian inference is used to estimate these parameters as well as the evidence for the signal model. The priors used are the same as those detailed in Appendix 2 of Abbott et al. (2017b) except for the amplitude priors, for which we use flat priors with an upper cut off much higher than the detector sensitivity. This value is 1.0×10^{-21} for all pulsars. The Bayesian stochastic sampling algorithm used is DYNESTY (Skilling 2004, 2006), as wrapped with BILBY (Ashton et al. 2019), with 1024 live points (the number of points drawn from the prior). In the absence of a signal, we calculate 95% credible upper bounds derived from the posterior probability distributions.

3.1.1. Restricted priors

For some pulsars, there is sufficient information to restrict our uninformative prior assumptions on their inclination and polarisation angles, for example if we have EM observations of their pulsar wind nebulae or, in the case of J1952+3252, from proper motion measurements and observations of H α lobes bracketing the bow shock (Ng & Romani 2004). In these cases, the parameter estimation is repeated and used along with the results from the original uninformed priors. Table 1 shows the pulsars for which we could restrict the priors and the values used for the restrictions. These values were obtained using the data from Table 2 of Ng & Romani (2008) and the methods described in Appendix B of Abbott et al. (2017b). Each prior range is assumed to be Gaussian about the given mean and standard deviation. The two values for ι are to incorporate the unknown rotation direction in the search by using a bimodal distribution. The additional ι_2 is simply $\pi - \iota_1$ radians.

3.1.2. Glitches

Glitches are transient events, where the normally stable pulsar spin suddenly increases in both rotation frequency and spin-down rate (Espinoza et al. 2011; Yu et al. 2013; Basu et al. 2022). These events are most common in younger, non-recycled pulsars with rarer glitches seen in some millisecond pulsars (Cognard & Backer 2004; McKee et al. 2016). Some searches (e.g., Keitel et al. 2019; Abbott et al. 2022; Abac et al. 2024a) look for transient GWs in the aftermath of glitches.

When a glitch occurs in a pulsar during the course of a GW observing run, we assume that the GW phase is affected in the same way as the EM phase. However, since the phase offset is unknown at the time of the glitch, it is incorporated into the parameter inference for the

Table 1. Pulsars for which we can restrict their orientation priors using electromagnetic observations. Ψ is the polarisation angle and ι is the inclination angle, with $\iota_2 = \pi - \iota_1$.

PSR	Ψ (rad)	ι_1 (rad)	ι_2 (rad)
J0205+6449	1.5760 ± 0.0078	1.5896 ± 0.0219	1.5519 ± 0.0219
J0534+2200 (Crab)	2.1844 ± 0.0016	1.0850 ± 0.0149	2.0566 ± 0.0149
J0537–6910	2.2864 ± 0.0383	1.6197 ± 0.0165	1.5219 ± 0.0165
J0540–6919	2.5150 ± 0.0144	1.6214 ± 0.0106	1.5202 ± 0.0106
J0835–4510 (Vela)	2.2799 ± 0.0015	1.1048 ± 0.0105	2.0368 ± 0.0105
J1952+3252	0.2007 ± 0.1501
J2021+3651	0.7854 ± 0.0250	1.3788 ± 0.0390	1.7628 ± 0.0390
J2229+6114	1.7977 ± 0.0454	0.8029 ± 0.1100	2.3387 ± 0.1100

Bayesian method. This adjustment is not necessary for pulsars that glitch before or after the observation period. Only two of the pulsars in our sample experienced glitches during the length of O4a: J0537–6910 with an epoch of \sim MJD 60223 and J0540–6919 with an epoch of \sim MJD 60150 (see, e.g., Espinoza et al. (2024); Tuo et al. (2024)).

3.2. 5-vector targeted pipeline

The 5-vector method is a frequentist data-analysis approach (Astone et al. 2010), which has been used in the last decade in several LVK searches (Abbott et al. 2022, 2020, 2019c, 2017b). The 5-vector targeted pipeline relies on the Band-Sample Data (BSD) (Piccinni et al. 2018) framework, i.e. a database of sub-sampled complex time-domain files (so-called BSD files) that covers 10 Hz and spans 1 month of the original dataset that allows to reduce the computational cost of the analysis.

To correct for the signal phase modulations due to, for example, the pulsar spin-down and the Doppler effect, a heterodyne method is used. Recently (D’Onofrio et al. 2023), the 5-vector method has been also applied to pulsars in binary systems with the implementation of the Doppler correction due to the orbital motion (Leaci & Prix 2015; Leaci et al. 2017). After the spin-down and Doppler/relativistic corrections, there is a residual modulation at the detector due to the Earth sidereal motion that splits the frequency of the expected CW signal.

Assuming the single-harmonic emission scenario, the central peak at twice the pulsar rotation frequency has four sidebands whose distance to the central peak is $\pm 1, \pm 2f_{\oplus}$ where f_{\oplus} is the Earth’s sidereal rotation frequency. A 5-vector consists of a complex array with five components corresponding to the Fourier transform of the detector’s data (*data 5-vector*) or of the antenna patterns (*template 5-vectors* for the plus and cross component) at the five signal frequencies. The 5-vector method defines two matched filters in the frequency domain, defined by the normalized scalar product between the data 5-vector and the two template 5-vectors. To extend the

analysis to n detectors, the data 5-vector from each detector are combined together with coefficients that take into account the detector’s sensitivity and observation time to construct the $5n$ -vectors (D’Onofrio et al. 2024). The two matched filters are linearly combined to define a detection statistic (D’Onofrio et al. 2023). To assess the significance of a candidate, a p-value is computed from the noise distribution of the detection statistic using off-source frequencies as the noise background in the analyzed frequency bands. In case of no detection, a mixed Bayesian-frequentist upper limit procedure (described in Abbott et al. (2019c)) is used to set the upper limit on the amplitude, assuming a uniform prior and considering informative priors on the polarization parameters, if present (see Table 1).

It is not straightforward to generalize the 5-vector method to the dual-harmonic emission model due to the complexity of the expected CW signal. In this case, an additional analysis considering the emission at only the rotation frequency is performed; this would be a good approximation if the star’s moment of inertia tensor is biaxial, with a small misalignment angle between its symmetry axis and the rotation axis (see Jones (2010)).

3.3. $\mathcal{F}/\mathcal{G}/\mathcal{D}$ -statistic method

The time-domain $\mathcal{F}/\mathcal{G}/\mathcal{D}$ -statistic method utilizes the \mathcal{F} -statistic derived in Jaranowski et al. (1998) and the \mathcal{G} -statistic derived in Jaranowski & Królak (2010). The input data for this analysis are the heterodyned data used in time-domain Bayesian analysis. The \mathcal{F} -statistic is employed when the amplitude, phase, and polarization of the signal are unknown, whereas the \mathcal{G} -statistic is applied when only the amplitude and phase are unknown, and the polarization is known (as described in Section 3.1.1). These methods have been used in several analyses of LIGO and Virgo data (Abadie et al. 2011; Aasi et al. 2014; Abbott et al. 2017b, 2020, 2022). Additionally, the method incorporates the \mathcal{D} -statistic developed in Verma (2021) to search for dipole radiation in Brans-Dicke theory. The \mathcal{D} -statistic search was first

performed in the LIGO and Virgo analysis presented in [Abbott et al. \(2022\)](#).

The three statistics are derived by calculating the maximum likelihood estimators of the signal’s constant amplitude parameters. This is done by maximizing the likelihood function and then substituting the amplitude values with their respective maximum likelihood estimators. As a result, we obtain statistics that are independent of the amplitudes. In this method, a signal is detected if the value of the \mathcal{F} -, \mathcal{G} - or \mathcal{D} statistic exceeds a certain threshold corresponding to an acceptable false-alarm probability. We consider a false-alarm probability of 1% for a signal to be deemed significant. The \mathcal{F} -, \mathcal{G} -, and \mathcal{D} -statistics are computed for each detector and each inter-glitch period separately. The results from different detectors or inter-glitch periods are then combined incoherently by summing the respective statistics. When the values of the statistics are not statistically significant, we set an upper limit with a frequentist approach on the amplitude of the GW signal.

3.4. $5n$ -vector narrowband pipeline

The $5n$ -vector narrowband pipeline makes use of the $5n$ -vector as in [Astone et al. \(2014a\)](#) and follows the same principle of the method described in Section 3.2.

While the former searches for a CW tightly locked to the EM emission, this assumption is here relaxed searching for CWs in a narrow frequency and spin-down range around twice the values inferred from EM observations, namely

$$f \in 2f_{\text{rot}}[1 - \delta, 1 + \delta] \quad (8)$$

with $\delta = 10^{-3}$ ([Abbott et al. 2022](#)), and an analogous expression for \dot{f} .

The method makes use of the Short Fourier Data Base (SFDB) ([Astone et al. 2005](#)), which is a collection of short-duration (2048 s) Fast Fourier Transforms (FFTs) overlapped by half.

For every target, data are Doppler corrected in the time domain with a non-uniform resampling that is independent of the CW frequency, then they are subsampled at 1 Hz. At this point, the time series are match-filtered (using 5 -vectors as for the targeted search) to estimate the two CW polarizations using a template bank in the $f - \dot{f}$ space. We build the template bank considering bin widths equal to the inverse of the time series duration for the frequency, while its inverse squared for the spin-down grid. Higher-order spin-down terms, if provided in the ephemerides, are fixed at twice the rotation terms to track the GW frequency evolution over time, without exploring any additional template ([Astone et al. 2014b](#)).

Then, the matched filter results from different detectors are coherently combined ([Mastrogiovanni et al.](#)

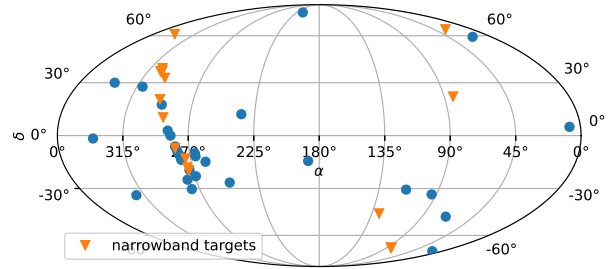


Figure 1. Sky location in equatorial coordinates of the analyzed targets. All targets are selected for the targeted search, while the triangles are the targets analyzed also with the narrowband search.

2017) to evaluate the detection statistic. From the collection of statistic values, we order them along the frequency axis to select the maximum every 10^{-4} Hz, marginalizing over the spin-down. We use a p-value threshold (i.e., the tail probability of the noise-only distribution) of 1% to determine whether a selected point has to be considered an outlier. The noise-only distribution is inferred from the tail of the histogrammed non-maxima values which is fitted with an exponential ([Singhal et al. 2019](#)). We use here a threshold of 1%, similar to previous searches (e.g., [Abbott et al. \(2022\)](#)), after taking into account the trial factor.

If CW detection is not claimed, we set the 95% confidence level upper limit $h_0^{95\%}$ through software-injection campaigns.

4. DATASETS

4.1. GW dataset

The considered dataset is the first part of the fourth observing run, known as O4a, of the LIGO Livingston (L1) and LIGO Hanford (H1) detectors¹. The O4a run took place between May 24, 2023 15:00:00 UTC and ended January 16, 2024 16:00:00 UTC. The duty factors for L1 and H1 were 69.0% and 67.5%, respectively. The Virgo detector has not been considered since it joined the O4 run on April 10, 2024 while the KAGRA detector is planned to join O4 by the end of the run. For a description of the upgrades to the Advanced LIGO ([Capote et al. 2024](#)), Advanced Virgo, and KAGRA detectors in preparation to the O4 run, we refer to Appendix A in [Abac et al. \(2024b\)](#).

The LIGO detectors are calibrated using photon radiation pressure actuation, where an amplitude-

¹ We considered L1:GDS-CALIB-STRAIN-CLEAN_AR and H1:GDS-CALIB-STRAIN-CLEAN_AR frame channels with CAT1 vetoes for L1 and H1, respectively.

modulated laser beam is directed onto the end test masses, causing a known change in the arm length from the equilibrium position (Karki et al. (2016), Viets et al. (2018)). For the O4a data used in this analysis, the worst 1σ calibration uncertainty is within 10% in amplitude, and 10 degrees in phase, over the range 10–2000 Hz. The uncertainty at specific frequencies or times can be significantly smaller.

The dataset used underwent cleaning processes depending on the data framework used by each pipeline (we refer to Soni et al. (2024) for more details on data quality for CW searches). For the Bayesian pipeline, outliers are removed before the heterodyne using a median-absolute-deviation (MAD) method as described in Chapter 3 of Iglewicz & Hoaglin (1993) with a threshold of 3.5. Concerning the 5-vector targeted pipeline, two cleaning steps are applied. First, short duration time-domain disturbances are identified and subtracted from the data when the SFDB database - from which BSD files are built - are created (this cleaning step is shared with the 5-vector narrowband search, which also starts from the SFDB Astone et al. (2005)). A second cleaning step is applied on the BSD files (Piccinni et al. 2018), removing large time-domain outliers, which were not visible in the full band time series, with quadratic value larger than ten times the quadratic sum of the medians of the data real and imaginary parts (computed over non-zero samples). The \mathcal{F} -, \mathcal{G} - or \mathcal{D} statistic method performs further cleaning of the fine heterodyne data through the Grubbs test (see Appendix D of Abadie et al. (2011)).

4.2. EM dataset

The timing solutions used as inputs for the GW search were produced with EM data in the gamma rays, X-rays and radio wavelengths. The gamma ray timing solutions were obtained from Fermi-LAT (Atwood et al. 2009); X-ray timing solutions were obtained from Chandra (Weiskopf et al. 2002) and the Neutron Star Interior Composition Explorer (NICER, Gendreau et al. 2016), while the radio timing solutions were obtained from the Nancy Radio Telescope (NRT, Guillemot, L. et al. 2023), the Jodrell Bank Observatory (JBO), the Argentine Institute of Radio astronomy (IAR, Gancio et al. 2020), the Mount Pleasant Radio Observatory (Lewis et al. 2003), the Five-hundred-meter Aperture Spherical Telescope (FAST, Smits et al. 2009) and the Canadian Hydrogen Intensity Mapping Experiment (CHIME, Amiri et al. 2021).

For the radio-emitting pulsars, we used PAZI or RIFIND tasks in PSRCHIVE (van Straten et al. 2012) and PRESTO (Ransom 2011) packages respectively to

mitigate Radio-frequency interferences (RFIs). Next, we folded observations with PREPFOLD or FOLD_PSRFITS tasks in PRESTO and PSRFITS UTILS (Hotan et al. 2004) packages. We then cross-correlated the folded profiles with a noise-free template profile with high signal-to-noise ratio to obtain the Times of Arrivals (ToAs). Next, we select ToAs during the course of O4a run, so the solutions are valid for this time range. We use TEMPO (Nice et al. 2015), TEMPO2 (Edwards et al. 2006; Hobbs et al. 2006, 2009) or PINT (Luo et al. 2019, 2021) to characterise the rotation of each pulsar by fitting the ToAs to a Taylor series expansion:

$$\phi(t) = \phi_0 + f_{\text{rot}}(t-t_0) + \frac{1}{2}\dot{f}_{\text{rot}}(t-t_0)^2 + \frac{1}{6}\ddot{f}_{\text{rot}}(t-t_0)^3 + \dots, \quad (9)$$

where t_0 is the reference epoch and ϕ_0 is the phase at t_0 , and f_{rot} , \dot{f}_{rot} , and \ddot{f}_{rot} are the rotation frequency of the pulsar, and its first and second derivatives, respectively. If higher-order derivatives are measured, we also include the corresponding terms in the Taylor expansion.

During a glitch, the rotation frequency abruptly increases. This glitch-induced alteration in the rotational phase can be taken into account in the timing model as (Yu et al. 2013):

$$\begin{aligned} \phi_g(t) = & \Delta\phi + \Delta f_{\text{rot}}^p(t-t_g) + \frac{1}{2}\Delta\dot{f}_{\text{rot}}^p(t-t_g)^2 + \\ & \frac{1}{6}\Delta\ddot{f}_{\text{rot}}^p(t-t_g)^3 + \sum_i \left[1 - \exp\left(-\frac{t-t_g}{\tau_d^i}\right) \right] \Delta f_{\text{rot}}^{d,i} \tau_d^i. \end{aligned} \quad (10)$$

The uncertainty on the glitch epoch t_g is counteracted here by $\Delta\phi$, and the step changes in f_{rot} , \dot{f}_{rot} and \ddot{f}_{rot} at t_g are represented by Δf_{rot}^p , $\Delta\dot{f}_{\text{rot}}^p$, and $\Delta\ddot{f}_{\text{rot}}^p$. Finally, $\Delta f_{\text{rot}}^{d,i}$ denotes temporal frequency increases that decay in τ_d^i days.

The ToA fitting process also provides the astrometric parameters of each pulsar and the orbital parameters for binary pulsars (Lorimer & Kramer 2004). Uncertainties in the values of the pulsar and orbital parameters derived from fitting the ToAs are not taken into account in targeted/narrowband searches.

For many pulsars, their distances (Hobbs et al. 2004) are based on the observed dispersion measure using the Galactic electron density distribution model YMW16 (Yao et al. 2017). The uncertainties in these measurements can be as large as a factor of two. For other pulsars, the distance can be determined by measuring the parallax with the timing solution (Smits et al. 2011) or, if the pulsar is in a binary system, the orbital period derivative (Verbiest et al. 2008). The first method usually results in an uncertainty ranging from 5% to 50%

(Shamohammadi et al. 2024). The second one offers significantly higher accuracy, achieving uncertainties as low as 0.1% (Verbiest et al. 2008; Reardon et al. 2016). Other methods such as Very Long Baseline Interferometry (Lin et al. 2023) were also used to determine pulsar distances.

For this analysis, we selected pulsars with a rotation frequency close to or greater than 10 Hz, to lie in the bandwidth of the LIGO detectors, and with an expected targeted search sensitivity for the strain amplitude within a factor 3 of the spin-down limit (see Figure 1 for the pulsars’ sky locations and Table 2 for the list of analyzed pulsars). Out of the 45 pulsars analyzed in this work, 11 pulsars belong to binary systems and there are 10 millisecond pulsars with frequencies higher than 100 Hz.

5. RESULTS

5.1. Targeted searches

We found no statistical evidence of a CW signal in the O4a data for any of the analyzed targets. In this section, we present the results of the targeted search conducted using three different analysis methods across the full set of 45 pulsars.

The results are shown in Table 2. The 95% upper limit $h_0^{95\%}$ is given for the single-harmonic search along with the mass quadrupole $Q_{22}^{95\%}$ and ellipticity $\epsilon^{95\%}$ upper limits calculated using the distance listed in the table and a fiducial moment of inertia $I_{zz} = 10^{38} \text{ kg m}^2$. Uncertainties on these parameters are not taken into account, and for reference, we report the used best-fit distance values in Table 2 provided by the EM observation. However, for pulsars that did not surpass their spin-down limits, these Q_{22} and ϵ upper limits are unphysical since they would lead to spin-down rates that are greater than their measured values. From the upper limit on the amplitude, we also compute the spin-down ratio as $h_0^{95\%}/h_0^{\text{sd}}$ with h_0^{sd} defined in Equation (6). The upper limits for the dual-harmonic search are included as $C_{21}^{95\%}$ and $C_{22}^{95\%}$. Finally, for the Bayesian method, the odds of a coherent signal versus incoherent noise are given for both the single $\mathcal{O}_{m=2}^{l=2}$ and dual-harmonic $\mathcal{O}_{m=1,2}^{l=2}$ searches. For the \mathcal{F} -statistic and for the 5-vector method, to assess the statistical significance of a candidate and quantify the consistency with the assumption of just noise, we report the p-value.

For the two glitching pulsars, J0537–6910 and J0540–6919, the Bayesian results are produced when incorporating an additional phase offset in the parameter inference while for the \mathcal{F} -statistic and the 5-vector method, an incoherent approach is used summing the statistics from the inter-glitch periods. In cases with

sufficient observations of the pulsar wind nebulae, results using restricted priors of inclination and polarisation angles are listed in parentheses.

Figure 2 shows the upper limits from the Bayesian analysis for the single-harmonic search against an estimate of the sensitivity of the search using both detectors during O4a. The results for each pulsar are compared with the corresponding spin-down limit. The results from this analysis for each pulsar are represented by the blue dots, with their corresponding spin-down limit shown by the grey triangles at the same frequency. The sensitivity curve is shown as a pink line. Some highlighted results for individual pulsars include the Crab pulsar (J0534+2200) which had the lowest spin-down ratio of 0.00783, the Vela pulsar (J0835–4510), J2021+3651 which had the highest odds of coherent signal versus incoherent noise with -3.1 , J0537–6910 which had the most constraining amplitude upper limit of 6.38×10^{-27} , and J0437–4715 which had the most constraining ellipticity upper limit of 8.8×10^{-9} . The distribution of spin-down ratios for these results is shown in Figure 3 with 29 targets that surpass the spin-down limit and the remaining targets, which all have a spin-down ratio below 5.

In Figure 4, the ellipticity $\epsilon^{95\%}$ and mass quadrupole $Q_{22}^{95\%}$ upper limits are plotted against the GW frequency and compared with the corresponding spin-down limits for the ellipticity. The contours of equal characteristic age have been calculated using $\tau = P/4\dot{P}$ which can be derived with the assumption that GW emission alone is driving the spin-down.

As shown in Table 2, there is broad agreement among the different pipelines, despite these pipelines being largely independent, and the statistical procedures used to derive the upper limits are different. The data frameworks and pre-processing procedures used by each pipeline account for the differences found in the upper limit results.

5.2. Narrowband results

In this section, we detail the results obtained with the narrowband pipeline, presented in Section 3.4. The search did not highlight, for any of the 16 considered targets, outliers with a False-Alarm Probability $\text{FAP} < 10^{-2}$ after taking into account the trial factor.

For the narrowband search, we consider only those targets with h_0^{sd} above the expected sensitivity that is typically worse by a factor of two (Astone et al. 2014a) than that of targeted pipelines due to the trial factor. In this way, we selected 16 pulsars out of which 8 have not been analyzed in O3 (Abbott et al. 2022). Our dataset includes the two pulsars that glitched, J0537-6910 and

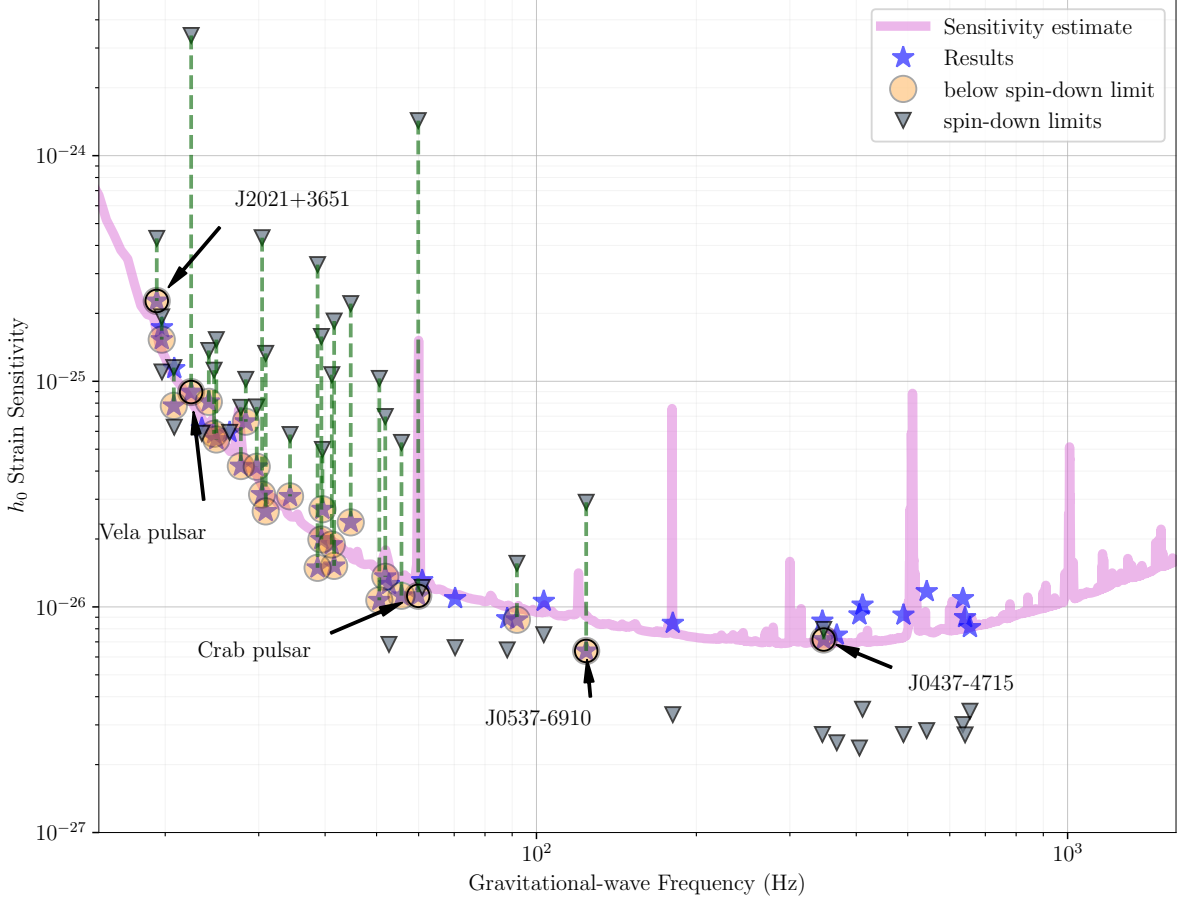


Figure 2. Upper limits on h_0 for the 45 pulsars in this analysis using the time-domain Bayesian method and considering the single-harmonic emission model. The blue stars show 95% credible upper limits on the amplitudes of h_0 . Grey triangles represent the spin-down limits for each pulsar (based on the distance measurement stated in Table 2 and assuming the canonical moment of inertia). The pink curve gives an estimate of the expected strain sensitivity of both detectors combined during the course of O4a. The upper limits from the other two pipelines are broadly consistent, as shown in Table 2.

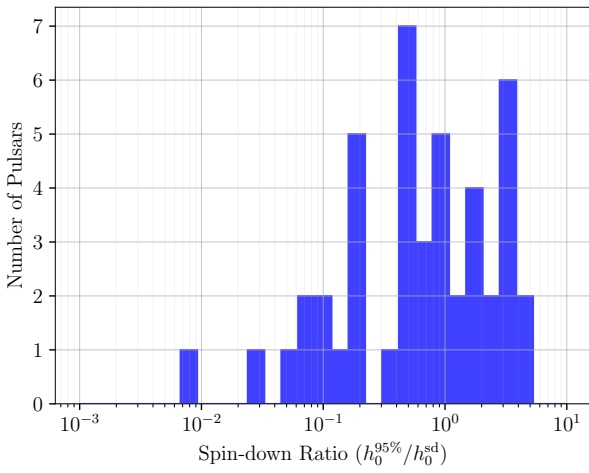


Figure 3. A histogram of the spin-down ratio considering the single-harmonic emission model for 45 pulsars from the Bayesian analysis.

J0540-6919. Similar to O3, for these pulsars we split O4a data into two segments that exclude from the analysis the period around $[t_g - 1 \text{ d}, t_g + 2 \text{ d}]$, with t_g the glitch epoch. The segments are then analyzed independently.

The search did not highlight any statistically significant outlier since the measured p-values are well above the threshold set by a FAP of 10^{-2} corrected for the trial factor. In Table 3, we report for each target the lowest p-value found during the analysis and the threshold.

In the absence of any detections, we have calculated upper limits at the 95% CL for each of the analyzed targets. Our results are listed in Table 3 and shown in Figure 5 comparing them with the expected sensitivity.

5.3. Brans-Dicke theory

Table 4 shows the results for the analyses on 45 pulsars using the \mathcal{D} -statistic to search for dipole radiation predicted by Brans-Dicke theory. No outliers have been found in the analysis and we set upper limits on the ex-

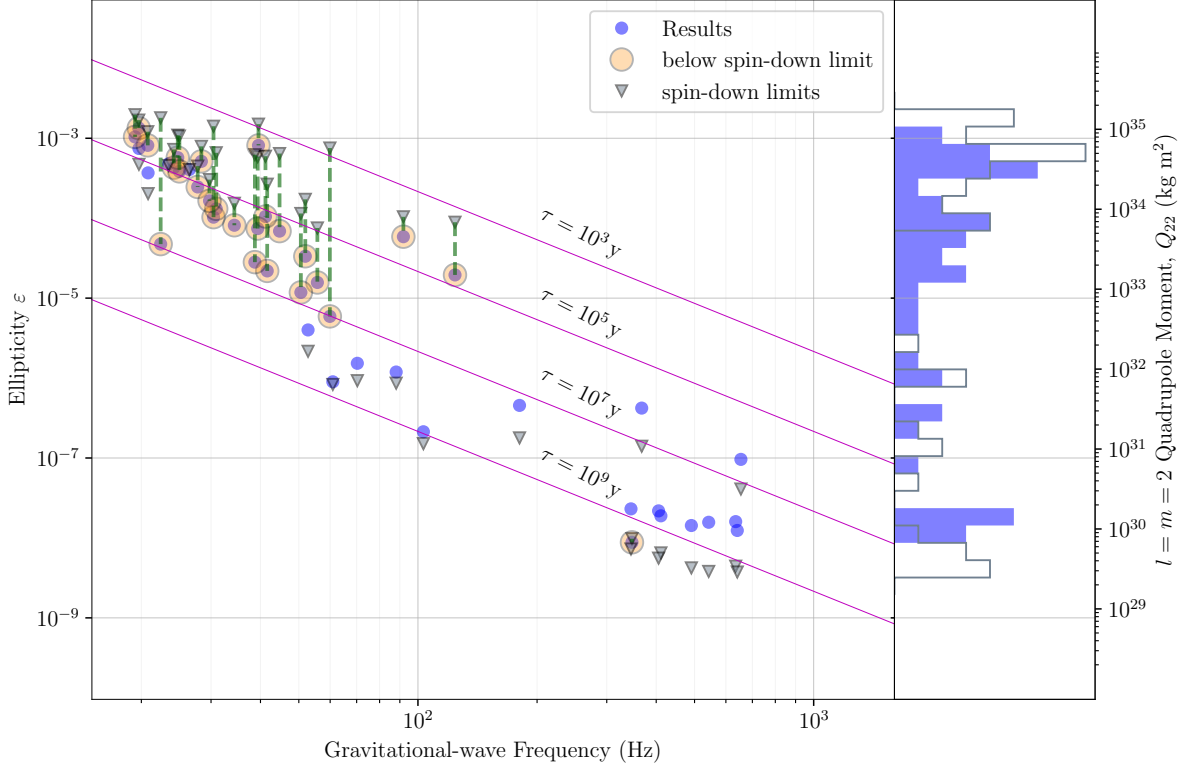


Figure 4. 95% credible upper limits on ellipticity $\varepsilon^{95\%}$ and mass quadrupole $Q_{22}^{95\%}$ for all 45 pulsars using the Bayesian analysis method and considering the single-harmonic emission model. The upper limits for each pulsar are represented by blue circles while their spin-down limits are shown as grey triangles. Also included are purple contour lines of equal characteristic age $\tau = P/4\dot{P}$ assuming that GW emission alone is causing spin-down. Only the results for pulsars which surpassed their spin-down are physically meaningful. The histogram on the right shows the distribution of the ellipticities obtained from the results (blue filled bars) and in the spin-down limit (grey bars).

pected amplitude defined in Equation (7). The upper limits in brackets shows the results using informative priors on the polarization parameters for the pulsars in Table 1.

6. DISCUSSION

In this section, we discuss the results in Table 2. Motivated by the comparable results among the three pipelines, we consider the Bayesian pipeline as a reference. As described in the previous section, we have no evidence of a CW signal in any of the searches we conducted.

We compare the O4a results with previous targeted searches by the LVK Collaboration (Abbott et al. 2022, 2020, 2019c, 2017b), considering the first three observing runs. The ratio between the O4a upper limits on h_0 and C_{21} and the corresponding upper limits set in previous searches is shown in Figure 6.

34 pulsars out of the 45 considered targets in Table 2 have been already analyzed in the joint O2 plus O3 analysis (Abbott et al. 2022). Overall the corresponding upper limits on the GW amplitude are comparable for

the single-harmonic search, with some targets showing better results in O4a and some targets having worse results than those in Abbott et al. (2022), see Figure 6. This is expected since the targeted search sensitivity of the O2–O3 dataset is comparable to the O4a one, except at very low frequencies. The targeted search sensitivity can be expressed in terms of minimum detectable amplitude (D’Onofrio et al. 2024), h_{\min} . For a multi-detector analysis considering n detectors and averaging over the sky position and polarization parameters,

$$h_{\min} \approx C \sqrt{\left(\sum_{i=1}^n \frac{T_i}{S_i} \right)^{-1}}, \quad (11)$$

where the factor $C \simeq 11$ (the exact value depending on the considered pipeline), while T_i and S_i are respectively the effective observation time and the average power spectral density (PSD) for the i -th detector. For the O4a targeted search sensitivity (with an observation time of approximately 1.3×10^7 seconds for both detectors), see the pink curve in Figure 2.

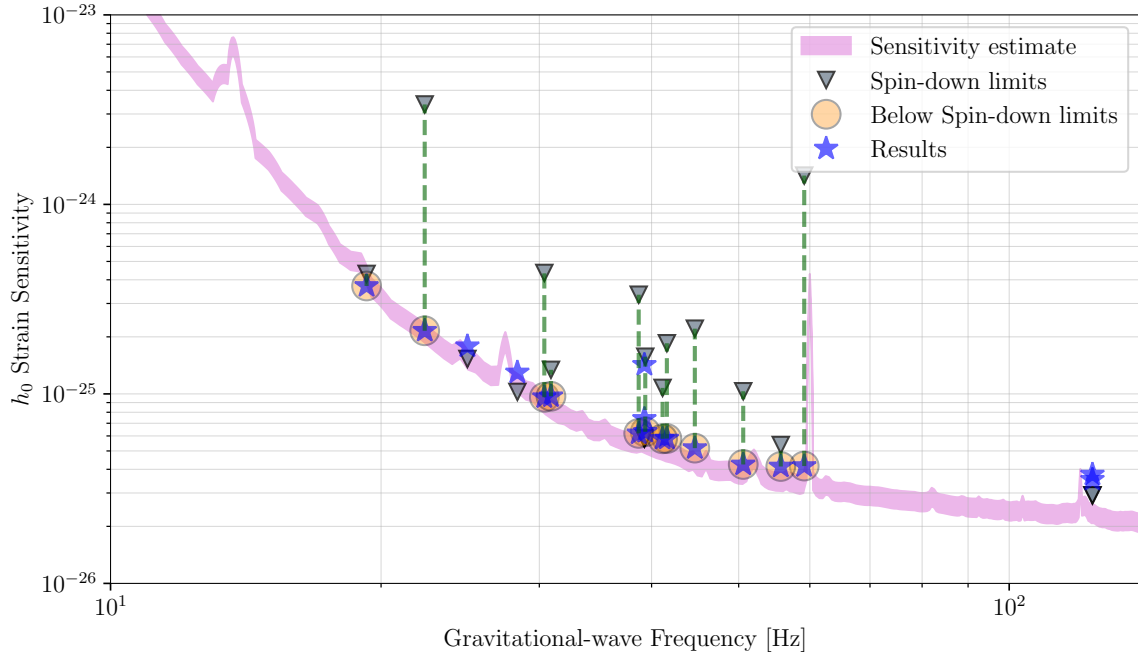


Figure 5. Expected sensitivity of the narrowband search using O4a (shaded pink region) dataset from the two LIGO detectors considering the single-harmonic emission model. The curve is compared with the spin-down limits (triangles) and the upper limits (stars) averaged over all the 10^{-4} Hz bands for each source. Upper limits below the spin-down limit are highlighted with orange circles.

The O4a PSDs for the two LIGO detectors are generally better, by almost a factor of 1.5 to 2, compared to the corresponding O3 PSD² depending on the considered frequency band. However, the effective observation time for O4a is reduced by a factor of approximately 1.6, which diminishes the benefit of the improved detector sensitivity in O4a. As a result, we expect the sensitivity of the O4a search to be comparable to that of the combined O2+O3 search. Upper limits on C_{21} , on the other hand, are lower on average than the corresponding O2+O3 results due to a better search sensitivity at frequencies below 20 Hz.

For the remaining targets, 5 pulsars (J0205+6449, J0737–3039A, J1813–1246, J1831–0952, and J1837–0604) have been analyzed in the O2 search (Abbott et al. 2019c), and J1826–1334 has been analyzed in the O1 search (Abbott et al. 2017b). For these pulsars, we have a clear improvement in the upper limits, as shown in Figure 6. The remaining targets (J0058–7218, J1811–1925, J2016+3711, J2021+3651, J2022+3842) have not been analyzed in recent targeted searches and we surpass the spin-down limit for all these targets.

² For this estimation, we only consider the O3 run for simplicity since it dominates the combined datasets.

Many studies have been dedicated to illustrate how a future successful detection of CW will provide a wealth of information about neutron stars (see e.g. Sieniawska & Jones (2022); Lu et al. (2023)), and even help to constrain the nuclear equation of state (see e.g. Idrisy et al. (2015); Ghosh et al. (2023); Ghosh (2023)). It is interesting to note that with improving sensitivity of the searches with each observing run, even non-detection of a CW signal sets more and more stringent upper limits on the ellipticity and possible sources of non-axisymmetric deformations in rotating neutron stars. This may lead to a better understanding of properties of the crust, internal magnetic fields, and accretion physics (Bildsten 1998; Melatos & Payne 2005; Ciolfi & Rezzolla 2013), and even rule out certain scenarios related to r-modes or limit their maximum saturation amplitudes (Abbott et al. 2021d).

Theoretical estimates of the *maximum* mountain sizes that an elastically deformed neutron star can sustain are subject to significant uncertainties, with estimates for the ellipticity ϵ ranging from $\sim 10^{-6}$ for conventional neutron stars, to as large as $\sim 10^{-3}$ for stars with exotic solid phases (see e.g. Ushomirsky et al. (2000); Owen (2005); Haskell et al. (2007); Johnson-McDaniel & Owen (2013); Gittins & Andersson (2021); Morales & Horowitz (2022)). Comparison with the results given in Figure 4 and Table 2 show that our observationally-obtained up-

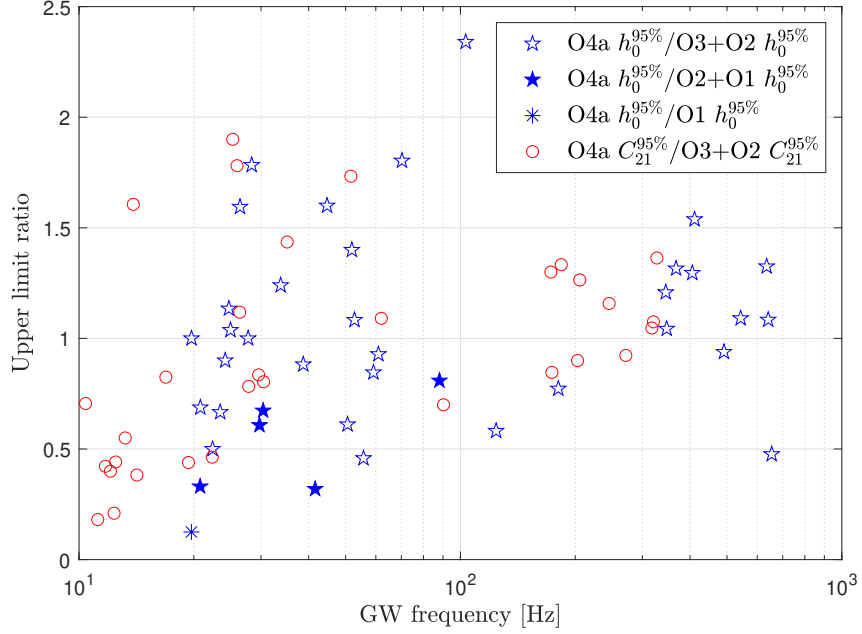


Figure 6. Blue stars show the ratio between the O4a h_0 upper limits for the analyzed targets (excluding the glitching pulsars) assuming the single-harmonic model divided by the corresponding h_0 upper limits in Abbott et al. (2022) for the Bayesian method as a function of the corresponding frequency at twice the rotation frequency (red circles refer instead to the C_{21} parameter at the rotation frequency assuming the dual-harmonic model). Blue filled stars show the h_0 upper limit ratios considering the targets (J0205+6449, J0737–3039A, J1813–1246, J1831–0952, J1837–0604) analyzed using O2 (Abbott et al. 2019c) and O1 data (blue asterisk for J1826–1334, Abbott et al. (2017b)).

per limits overlap with these ranges, confirming we are continuing to push into the regime of astrophysical interest. Estimates for magnetically-induced ellipticities are similarly uncertain (see e.g. Haskell et al. (2008); Glampedakis et al. (2012); Fujisawa et al. (2022)). Nevertheless, to give a concrete example, Dall’Osso & Perna (2017) (see however Lander & Jones (2018)) have suggested that the apparent gradual increase in the angle between the spin axis and magnetic axis of the Crab pulsar provides evidence for a magnetically-induced ellipticity $\epsilon \sim (3-10) \times 10^{-6}$. This to be compared with our upper limit of $\epsilon \approx 6 \times 10^{-6}$ for the Crab, again confirming we are probing a regime for astrophysical interest.

Theoretical estimates of the *minimum* mountain sizes are presented in Woan et al. (2018), which provides population-based evidence for millisecond pulsars having a minimum ellipticity of $\epsilon \approx 10^{-9}$.

We stress that our upper limits are subject to the uncertainties from the detector calibration as described in Section 4.1, as well as statistical uncertainties that are dependent on the particular analysis method.

The narrowband results in Table 3 and in Figure 5 show no evidence of a CW signal for the considered subset of pulsars. No outlier was found for any of the tar-

gets. Out of the 16 analyzed targets, 12 searches report an upper limit below the corresponding spin-down limit (see Table 3), ranging from a factor of 1.16 for J2021+3651 to 33 for J0534+2200. As for other methods, the targets analyzed with O3 data (Abbott et al. 2022) report upper limits comparable to those in Table 3. We stress that the narrowband search sensitivity is worse by at least a factor of 2 compared to the targeted search sensitivity as it depends on the number of templates explored for each target (Mastrogiovanni et al. 2017).

The search for non-GR polarizations as predicted by the Brans-Dicke theory shows no evidence of a dipole radiation. The most constraining upper limit for dipole radiation is obtained for the millisecond pulsar J1719–1438. Together with results from the O3 targeted search analysis (Abbott et al. 2022) the obtained upper limits constitute the first constraints on the dipole radiation from the pulsar gravitational wave observations.

7. CONCLUSION

In this work, we present a search for CW signals from a set of 45 known pulsars using O4a data from the two LIGO detectors. Pulsars are chosen considering an expected sensitivity for the amplitude below or slightly

above the theoretical spin-down limit with a rotation frequency close to or greater than 10 Hz. EM observations were employed to constrain the pulsars’ sky positions and rotational parameters covering the O4a data period.

We performed a targeted search utilizing three independent data analysis methods and two different emission models. No evidence of a CW signal was found for any of the targets. The upper limit results show that 29 targets surpass the theoretical spin-down limit. For 11 of the 45 pulsars not analyzed in the last LVK targeted search, we have a notable improvement in detection sensitivity compared to previous searches. For these targets, we surpass or equal the theoretical spin-down limit for the single-harmonic emission model. We also have, on average, an improvement in the upper limits for the low frequency component of the dual-harmonic search for all analyzed pulsars. For the remaining targets, the O4a upper limits are comparable to the results of the joint O2–O3 analysis described in [Abbott et al. \(2022\)](#), which considered data with lower sensitivity but a longer observation time.

We also conducted a narrowband search for 16 pulsars and a search for non-GR polarization as predicted by Brans-Dicke theory. No evidence of a CW signal was found in any of these searches.

The analysis of the full O4 dataset will improve the sensitivity of targeted/narrowband searches for some of the pulsars analyzed in [Abbott et al. \(2022\)](#) and here, including the Crab and Vela pulsars.

ACKNOWLEDGEMENT

This material is based upon work supported by NSF’s LIGO Laboratory, which is a major facility fully funded by the National Science Foundation. The authors also gratefully acknowledge the support of the Science and Technology Facilities Council (STFC) of the United Kingdom, the Max-Planck-Society (MPS), and the State of Niedersachsen/Germany for support of the construction of Advanced LIGO and construction and operation of the GEO 600 detector. Additional support for Advanced LIGO was provided by the Australian Research Council. The authors gratefully acknowledge the Italian Istituto Nazionale di Fisica Nucleare (INFN), the French Centre National de la Recherche Scientifique (CNRS) and the Netherlands Organization for Scientific Research (NWO) for the construction and operation of the Virgo detector and the creation and support of the EGO consortium. The authors also gratefully acknowledge research support from these agen-

cies as well as by the Council of Scientific and Industrial Research of India, the Department of Science and Technology, India, the Science & Engineering Research Board (SERB), India, the Ministry of Human Resource Development, India, the Spanish Agencia Estatal de Investigación (AEI), the Spanish Ministerio de Ciencia, Innovación y Universidades, the European Union NextGenerationEU/PRTR (PRTR-C17.I1), the ICSC - Centro Nazionale di Ricerca in High Performance Computing, Big Data and Quantum Computing, funded by the European Union NextGenerationEU, the Comunitat Autònoma de les Illes Balears through the Conselleria d’Educació i Universitats, the Conselleria d’Innovació, Universitats, Ciència i Societat Digital de la Generalitat Valenciana and the CERCA Programme Generalitat de Catalunya, Spain, the Polish National Agency for Academic Exchange, the National Science Centre of Poland and the European Union - European Regional Development Fund; the Foundation for Polish Science (FNP), the Polish Ministry of Science and Higher Education, the Swiss National Science Foundation (SNSF), the Russian Science Foundation, the European Commission, the European Social Funds (ESF), the European Regional Development Funds (ERDF), the Royal Society, the Scottish Funding Council, the Scottish Universities Physics Alliance, the Hungarian Scientific Research Fund (OTKA), the French Lyon Institute of Origins (LIO), the Belgian Fonds de la Recherche Scientifique (FRS-FNRS), Actions de Recherche Concertées (ARC) and Fonds Wetenschappelijk Onderzoek – Vlaanderen (FWO), Belgium, the Paris Île-de-France Region, the National Research, Development and Innovation Office of Hungary (NKFIH), the National Research Foundation of Korea, the Natural Sciences and Engineering Research Council of Canada (NSERC), the Canadian Foundation for Innovation (CFI), the Brazilian Ministry of Science, Technology, and Innovations, the International Center for Theoretical Physics South American Institute for Fundamental Research (ICTP-SAIFR), the Research Grants Council of Hong Kong, the National Natural Science Foundation of China (NSFC), the Israel Science Foundation (ISF), the US-Israel Binational Science Fund (BSF), the Leverhulme Trust, the Research Corporation, the National Science and Technology Council (NSTC), Taiwan, the United States Department of Energy, and the Kavli Foundation. The authors gratefully acknowledge the support of the NSF, STFC, INFN and CNRS for provision of computational resources.

This work was supported by MEXT, the JSPS Leading-edge Research Infrastructure Program, JSPS Grant-in-Aid for Specially Promoted Research

26000005, JSPS Grant-in-Aid for Scientific Research on Innovative Areas 2905: JP17H06358, JP17H06361 and JP17H06364, JSPS Core-to-Core Program A, Advanced Research Networks, JSPS Grants-in-Aid for Scientific Research (S) 17H06133 and 20H05639, JSPS Grant-in-Aid for Transformative Research Areas (A) 20A203: JP20H05854, the joint research program of the Institute for Cosmic Ray Research, the University of Tokyo, the National Research Foundation (NRF), the Computing Infrastructure Project of Global Science experimental Data hub Center (GSDC) at KISTI, the Korea Astronomy and Space Science Institute (KASI), the Ministry of Science and ICT (MSIT) in Korea, Academia Sinica (AS), the AS Grid Center (ASGC) and the National Science and Technology Council (NSTC) in Taiwan under grants including the Rising Star Program and Science Vanguard Research Program, the Advanced Technology Center (ATC) of NAOJ, and the Mechanical Engineering Center of KEK.

C.M.E. acknowledges support from ANID/FONDECYT, grant 1211964. S.G. acknowledges the support of the CNES. W.C.G.H. acknowledges support through grant 80NSSC22K1305 from NASA. This work is supported by NASA through the NICER mission and the Astrophysics Explorers Program and uses data and software provided by the High Energy Astrophysics Science Archive Research Center (HEASARC), which is a service of the Astrophysics Science Division at

NASA/GSFC and High Energy Astrophysics Division of the Smithsonian Astrophysical Observatory.

The Nançay radio Observatory is operated by the Paris Observatory, associated with the French Centre National de la Recherche Scientifique (CNRS), and partially supported by the Region Centre in France. We acknowledge financial support from “Programme National de Cosmologie and Galaxies” (PNCG), and “Programme National Hautes Energies” (PNHE) funded by CNRS/INSU-IN2P3-INP, CEA and CNES, France.

A.B.P. is a Banting Fellow, a McGill Space Institute (MSI) Fellow, and a Fonds de Recherche du Québec – Nature et Technologies (FRQNT) postdoctoral fellow.

E.F. is supported by the NSF grant AST-2407399.

The activities at the Instituto Argentino de Radioastronomía (IAR) are supported by the national agency CONICET, the Province of Buenos Aires agency CIC, and the National University of La Plata (UNLP).

Software: The 5-vector method is based on the BSD framework (Piccinni et al. 2018) while the narrow-band method makes use of the SFDB framework (Ashton et al. 2005), both of them are based on the Virgo Rome Snag software. The Bayesian analysis uses `CWInPy` (Pitkin 2022), which uses `dynesty` (Skilling 2004, 2006) within `bilby` (Ashton et al. 2019). Plots are produced using `matplotlib` (Hunter 2007). Many pulsar ephemerides are produced with `Tempo` (Nice et al. 2015), `Tempo2` (Hobbs et al. 2006).

Table 2. Table of the results for the targeted search on the set of 45 known pulsars for the three considered pipelines described in Section 3.

Pulsar Name (J2000)	f_{rot} (Hz)	\dot{P}_{rot} (s s^{-1})	Distance (kpc)	h_0^{sd}	Analysis Method	$h_0^{95\%}$	$\varepsilon^{95\%}$	$Q_{22}^{95\%}$ (kg m^2)	$\frac{h_0^{95\%}}{h_0^{\text{sd}}}$	$C_{21}^{95\%}$	$C_{22}^{95\%}$	Statistic $l=2, m=1, 2$	Statistic # $l=2, m=2$
J0030+0451 α	205.5	-4.2×10^{-16}	0.3^a	3.5×10^{-27}	Bayesian \mathcal{F} -statistic $5n$ -vector	1.0×10^{-26} 1.4×10^{-26} 9.3×10^{-27}	1.9×10^{-8} 2.7×10^{-8} 1.7×10^{-8}	1.5×10^{30} $J0537 \ 2.1 \times 10^{30}$ 1.3×10^{30}	2.9 4.1 2.6	1.1×10^{-26} 1.6×10^{-26} 5.8×10^{-27}	5.2×10^{-27} 6.5×10^{-27} ...	-5.1 0.47 0.61	-10 0.04 0.038
J0058-7218 β	45.94	-6.1×10^{-11}	59.70^b	1.56×10^{-26}	Bayesian \mathcal{F} -statistic $5n$ -vector	8.8×10^{-27} 4.9×10^{-27} 6.5×10^{-27}	5.9×10^{-5} 3.3×10^{-5} 4.4×10^{-5}	4.5×10^{33} 2.5×10^{33} 3.4×10^{33}	0.56 0.31 0.41	2.4×10^{-26} 3.5×10^{-26} 9.4×10^{-27}	4.4×10^{-27} 6.2×10^{-27} ...	-5.3 0.32 1	-10 0.86 0.80
J0117+5914 γ	9.86	-5.69×10^{-13}	1.77^c	1.1×10^{-25}	Bayesian \mathcal{F} -statistic $5n$ -vector	1.7×10^{-25} 2.3×10^{-25} 3.2×10^{-25}	7.4×10^{-4} 1.0×10^{-3} 1.4×10^{-3}	5.8×10^{34} 7.8×10^{34} 1.1×10^{35}	1.6 2.2 2.9	7.7×10^{-23} 8.4×10^{-23} ...	8.8×10^{-26} 1.2×10^{-25} ...	-3.8 0.39 ...	-4.9 0.06 0.87
J0205+6449 δ	15.22	-4.49×10^{-11}	3.20^d	4.33×10^{-25}	Bayesian \mathcal{F} -statistic $5n$ -vector	$3.2(4.2) \times 10^{-26}$ $2.4(4.4) \times 10^{-26}$ $2.2(3.4) \times 10^{-26}$	$1.0(1.4) \times 10^{-4}$ $0.8(1.5) \times 10^{-4}$ $0.72(1.1) \times 10^{-4}$	$8.0(10) \times 10^{33}$ $6.0(10) \times 10^{33}$ $5.6(8.6) \times 10^{33}$	0.073(0.096) 0.055(0.10) 0.051(0.078)	$5.6(4.8) \times 10^{-25}$ $1.3(0.56) \times 10^{-24}$ $(5.7) \times 10^{-25}$	$1.5(2.0) \times 10^{-26}$ $1.1(2.2) \times 10^{-26}$...	-4.7(-4.5) 0.24(0.44) 0.86	-8.3(-8.3) 0.75(0.47) 0.84
J0437-4715 ϵ	173.69	-4.15×10^{-16}	0.16^e	7.95×10^{-27}	Bayesian \mathcal{F} -statistic $5n$ -vector	7.2×10^{-27} 9.0×10^{-27} 5.8×10^{-27}	8.8×10^{-9} 1.1×10^{-8} 7.1×10^{-9}	6.8×10^{29} 8.5×10^{29} 5.5×10^{29}	0.90 1.1 0.32	1.1×10^{-26} 1.5×10^{-26} 5.1×10^{-27}	3.4×10^{-27} 4.4×10^{-27} ...	-5.4 0.31 0.75	-10 0.26 0.38
J0534+2200 ζ	29.95	-3.78×10^{-10}	2.00^f	1.43×10^{-24}	Bayesian \mathcal{F} -statistic $5n$ -vector	$1.1(0.9) \times 10^{-26}$ $1.5(1.2) \times 10^{-26}$ $1.1(1.1) \times 10^{-26}$	$5.9(5.0) \times 10^{-6}$ $8.0(6.3) \times 10^{-6}$ $5.7(5.8) \times 10^{-6}$	$4.6(3.9) \times 10^{32}$ $6.3(4.9) \times 10^{32}$ $4.3(4.4) \times 10^{32}$	0.0078(0.0067) 0.011(0.0085) 0.0074(0.0075)	$6.6(6.0) \times 10^{-26}$ $9.4(7.0) \times 10^{-26}$ $2.6(2.6) \times 10^{-26}$	$5.4(4.5) \times 10^{-27}$ $8.8(6.1) \times 10^{-27}$...	-5.1(-5.2) 0.19(0.18) 0.97	-9.5(-9.2) 0.30(0.36) 0.44
J0537-6910 η	62.03	-1.99×10^{-10}	49.70^g	2.91×10^{-26}	Bayesian \mathcal{F} -statistic $5n$ -vector	$6.4(8.9) \times 10^{-27}$ $8.8(4.5) \times 10^{-27}$ $0.79(1.2) \times 10^{-26}$	$2.0(2.7) \times 10^{-5}$ $2.7(1.4) \times 10^{-5}$ $2.4(3.7) \times 10^{-5}$	$1.5(2.1) \times 10^{33}$ $2.0(1.0) \times 10^{33}$ $1.9(2.8) \times 10^{33}$	0.22(0.31) 0.29(0.15) 0.27(0.41)	$2.4(1.4) \times 10^{-26}$ $3.2(9.0) \times 10^{-26}$ $0.98(1.5) \times 10^{-26}$	$3.0(4.7) \times 10^{-27}$ $2.0(2.9) \times 10^{-27}$...	-5.5(-5.3) 0.24(0.25) 0.45	-10.2(-10.4) 1.00(0.92) 0.34
J0540-6919 θ	19.77	-1.87×10^{-10}	49.70^g	4.99×10^{-26}	Bayesian \mathcal{F} -statistic $5n$ -vector	$2.7(3.4) \times 10^{-26}$ $2.9(2.9) \times 10^{-26}$ $1.6(2.4) \times 10^{-26}$	$8.1(10) \times 10^{-4}$ $8.6(8.6) \times 10^{-4}$ $4.8(7.3) \times 10^{-4}$	$6.3(7.9) \times 10^{34}$ $6.7(6.7) \times 10^{34}$ $3.7(5.6) \times 10^{34}$	0.54(0.69) 0.58(0.58) 0.27(0.41)	$1.9(1.6) \times 10^{-25}$ $2.9(8.8) \times 10^{-25}$ $3.7(5.7) \times 10^{-25}$	$1.4(1.7) \times 10^{-26}$ $1.4(1.5) \times 10^{-26}$...	-4.6(-4.2) 0.53(0.34) 0.66	-8.5(-8.4) 0.32(0.45) 0.76
J0614-3329 ι	317.59	-1.76×10^{-15}	0.63^h	3.01×10^{-27}	Bayesian \mathcal{F} -statistic $5n$ -vector	1.1×10^{-26} 1.1×10^{-26} 8.0×10^{-27}	1.6×10^{-8} 3.1×10^{-8} 1.2×10^{-8}	1.2×10^{30} 2.4×10^{30} 9.1×10^{29}	3.6 3.6 2.7	8.9×10^{-27} 1.0×10^{-26} 7.3×10^{-27}	5.4×10^{-27} 5.3×10^{-27} ...	-5.1 0.66 0.15	-10 0.31 0.21
J0737-3039A κ	44.05	-3.41×10^{-15}	1.10^i	6.45×10^{-27}	Bayesian \mathcal{F} -statistic $5n$ -vector	8.9×10^{-27} 7.5×10^{-27} 6.2×10^{-27}	1.2×10^{-6} 1.0×10^{-6} 8.3×10^{-7}	9.2×10^{31} 7.6×10^{31} 6.4×10^{31}	1.4 1.2 0.96	1.8×10^{-26} 1.7×10^{-25} 1.4×10^{-26}	4.3×10^{-27} 6.4×10^{-27} ...	-5.3 0.99 0.49	-10 0.87 0.92
J0835-4510 λ	11.19	-1.57×10^{-11}	0.28^j	3.41×10^{-24}	Bayesian \mathcal{F} -statistic $5n$ -vector	$9.0(7.7) \times 10^{-26}$ $8.2(8.2) \times 10^{-26}$ $8.5(8.7) \times 10^{-26}$	$4.7(4.1) \times 10^{-5}$ $4.4(4.3) \times 10^{-5}$ $4.5(4.6) \times 10^{-5}$	$3.7(3.1) \times 10^{33}$ $3.4(3.3) \times 10^{33}$ $3.5(3.6) \times 10^{33}$	0.026(0.023) 0.024(0.024) 0.025(0.025)	$2.9(2.4) \times 10^{-24}$ $3.5(2.3) \times 10^{-24}$ $2.7(2.8) \times 10^{-24}$	$4.1(3.7) \times 10^{-26}$ $4.0(3.9) \times 10^{-26}$...	-4.1(-4.1) 0.65(0.81) 0.66	-7.1(-7.1) 0.45(0.19) 0.17
J1231-1411 μ	271.45	-5.92×10^{-16}	0.42^c	2.83×10^{-27}	Bayesian \mathcal{F} -statistic $5n$ -vector	1.2×10^{-26} 1.2×10^{-26} 6.6×10^{-27}	1.6×10^{-8} 1.6×10^{-8} 8.9×10^{-9}	1.2×10^{30} 1.2×10^{30} 6.9×10^{29}	4.1 4.1 1.4	1.2×10^{-26} 1.7×10^{-26} 5.4×10^{-27}	5.9×10^{-27} 5.9×10^{-27} ...	-4.6 0.14 0.68	-9.9 0.14 0.51

Table 2 continued

Table 2 (continued)

Pulsar Name (J2000)	f_{rot} (Hz)	\dot{P}_{rot} (s s^{-1})	Distance (kpc)	h_0^{ed}	Analysis Method	$h_0^{95\%}$	$\epsilon^{95\%}$	$Q_{22}^{95\%}$ (kg m^2)	$\frac{h_0^{95\%}}{h_0^{\text{ed}}}$	$C_{21}^{95\%}$	$C_{22}^{95\%}$	Statistic @ $l=2, m=1, 2$	Statistic # $l=2, m=2$
J1412+7922 β	17.18	-9.72×10^{-13}	3.30 j	5.81×10^{-26}	Bayesian \mathcal{F} -statistic 5 n -vector	3.1×10^{-26} 2.5×10^{-26} 2.3×10^{-26}	8.2×10^{-5} 6.6×10^{-5} 6.4×10^{-5}	6.3×10^{33} 5.1×10^{33} 4.9×10^{33}	0.53 0.43 0.4	9.9×10^{-25} 1.2×10^{-24} 4.0×10^{-25}	1.4×10^{-26} 1.3×10^{-26} ...	-4.7 0.17 1	-8.0 0.57 0.44
J1537+1155 α	26.38	-1.65×10^{-15}	0.93 k	6.82×10^{-27}	Bayesian \mathcal{F} -statistic 5 n -vector	1.3×10^{-26} 1.3×10^{-26} 1.6×10^{-26}	4.0×10^{-6} 4.0×10^{-6} 5.0×10^{-6}	3.1×10^{32} 3.1×10^{32} 3.9×10^{32}	1.8 1.8 2.3	8.5×10^{-26} 7.1×10^{-26} 3.3×10^{-26}	5.6×10^{-27} 6.4×10^{-27} ...	-5.2 0.62 0.90	-9.6 0.91 0.22
J1623-2631 γ	90.29	-5.26×10^{-15}	1.85 l	3.33×10^{-27}	Bayesian \mathcal{F} -statistic 5 n -vector	8.5×10^{-27} 1.0×10^{-26} 5.6×10^{-27}	4.6×10^{-7} 5.4×10^{-7} 3.0×10^{-7}	3.5×10^{31} 4.1×10^{31} 2.3×10^{31}	2.6 3.1 1.2	1.4×10^{-26} 1.2×10^{-26} 6.8×10^{-27}	4.1×10^{-27} 5.2×10^{-27} ...	-5.2 0.79 0.78	-10 0.19 0.68
J1719-1438 α	172.71	-2.22×10^{-16}	0.34 C	2.72×10^{-27}	Bayesian \mathcal{F} -statistic 5 n -vector	8.7×10^{-27} 7.4×10^{-27} 7.4×10^{-27}	2.3×10^{-8} 2.0×10^{-8} 2.0×10^{-8}	1.8×10^{30} 1.6×10^{30} 1.5×10^{30}	3.2 2.8 2.6	1.3×10^{-26} 2.0×10^{-26} 7.0×10^{-27}	3.7×10^{-27} 3.5×10^{-27} ...	-5.3 0.20 0.33	-10 0.51 0.14
J1744-1134 α	245.43	-4.34×10^{-16}	0.40 e	2.72×10^{-27}	Bayesian \mathcal{F} -statistic 5 n -vector	9.2×10^{-27} 1.4×10^{-26} 5.7×10^{-27}	1.4×10^{-8} 2.1×10^{-8} 8.8×10^{-9}	1.1×10^{30} 1.7×10^{30} 6.8×10^{29}	3.4 5.2 1.9	1.1×10^{-26} 1.2×10^{-26} 8.8×10^{-27}	4.4×10^{-27} 7.1×10^{-27} ...	-5.0 0.34 0.11	-10 0.02 0.69
J1745-0952 α	51.61	-2.3×10^{-16}	0.23 C	7.5×10^{-27}	Bayesian \mathcal{F} -statistic 5 n -vector	1.1×10^{-26} 8.6×10^{-27} 1.2×10^{-26}	2.1×10^{-7} 1.6×10^{-7} 2.5×10^{-7}	1.6×10^{31} 1.3×10^{31} 1.9×10^{31}	1.4 1.4 1.6	2.6×10^{-26} 1.6×10^{-26} 1.1×10^{-26}	5.0×10^{-27} 4.4×10^{-27} ...	-5.3 0.66 0.91	-9.7 0.62 0.023
J1756-2251 γ	35.14	-1.26×10^{-15}	0.73 m	6.6×10^{-27}	Bayesian \mathcal{F} -statistic 5 n -vector	1.1×10^{-26} 1.6×10^{-26} 1.0×10^{-26}	1.5×10^{-6} 2.2×10^{-6} 1.5×10^{-6}	1.2×10^{32} 1.7×10^{32} 1.1×10^{32}	1.6 2.3 1.6	5.6×10^{-26} 6.3×10^{-26} 3.1×10^{-26}	5.4×10^{-27} 7.1×10^{-27} ...	-5.1 0.17 0.031	-9.4 0.22 0.31
J1809-1917 γ	12.08	-3.73×10^{-12}	3.27 C	1.37×10^{-25}	Bayesian \mathcal{F} -statistic 5 n -vector	8.1×10^{-26} 7.9×10^{-26} 4.0×10^{-26}	4.3×10^{-4} 4.7×10^{-4} 2.1×10^{-4}	3.3×10^{34} 3.6×10^{34} 1.6×10^{34}	0.59 0.65 0.28	3.0×10^{-24} 4.3×10^{-24} 2.7×10^{-24}	3.9×10^{-26} 3.9×10^{-26} ...	-4.2 0.52 0.079	-7.0 0.05 0.64
J1811-1925 β	15.46	-1.05×10^{-11}	5.00 n	1.33×10^{-25}	Bayesian \mathcal{F} -statistic 5 n -vector	2.6×10^{-26} 3.3×10^{-26} 3.3×10^{-26}	1.3×10^{-4} 1.7×10^{-4} 1.6×10^{-4}	1.0×10^{34} 1.3×10^{34} 1.2×10^{34}	0.20 0.25 0.24	7.3×10^{-25} 4.3×10^{-25} 6.1×10^{-25}	1.3×10^{-26} 1.7×10^{-26} ...	-4.8 0.67 0.23	-8.1 0.85 0.23
J1813-1246 κ	20.80	-7.6×10^{-12}	2.63 O	1.85×10^{-25}	Bayesian \mathcal{F} -statistic 5 n -vector	1.5×10^{-26} 3.1×10^{-26} 1.6×10^{-26}	2.2×10^{-5} 4.7×10^{-5} 2.3×10^{-5}	1.7×10^{33} 3.4×10^{33} 1.8×10^{33}	0.082 0.055 0.087	1.4×10^{-25} 1.3×10^{-25} 7.7×10^{-26}	7.8×10^{-27} 1.5×10^{-26} ...	-5.0 0.72 0.73	-9.1 0.07 0.50
J1813-1749 θ	22.35	-6.34×10^{-11}	6.15 C	2.21×10^{-25}	Bayesian \mathcal{F} -statistic 5 n -vector	2.4×10^{-26} 3.1×10^{-26} 1.8×10^{-26}	6.9×10^{-5} 8.9×10^{-5} 5.3×10^{-5}	5.3×10^{33} 6.8×10^{33} 4.1×10^{33}	0.11 0.14 0.083	8.8×10^{-26} 5.3×10^{-26} 6.6×10^{-26}	1.2×10^{-26} 1.5×10^{-26} ...	-4.4 0.91 0.53	-8.7 0.02 0.12
J1823-3021A γ	183.82	-1.14×10^{-13}	8.02 l	2.5×10^{-27}	Bayesian \mathcal{F} -statistic 5 n -vector	7.5×10^{-27} 4.9×10^{-27} 4.5×10^{-27}	4.2×10^{-7} 2.7×10^{-7} 2.5×10^{-7}	3.3×10^{31} 2.2×10^{31} 1.9×10^{31}	3.0 2.0 1.8	1.6×10^{-26} 2.3×10^{-26} 6.5×10^{-27}	4.0×10^{-27} 3.5×10^{-27} ...	-5.2 0.12 0.40	-9.7 0.78 0.91

Table 2 continued

Table 2 (continued)

Pulsar Name (J2000)	f_{rot} (Hz)	\dot{P}_{rot} (s s^{-1})	Distance (kpc)	h_0^{ed}	Analysis Method	$h_0^{95\%}$	$\epsilon^{95\%}$	$Q_{22}^{95\%}$ (kg m^2)	$\frac{h_0^{95\%}}{h_0^{\text{ed}}}$	$C_{21}^{95\%}$	$C_{22}^{95\%}$	Statistic @ $l=2, m=1, 2$	Statistic # $l=2, m=2$
J1824–2452A \checkmark	327.41	-1.73×10^{-13}	$5.37 l$	3.45×10^{-27}	Bayesian \mathcal{F} -statistic $5n$ -vector	8.1×10^{-27} 7.0×10^{-27} 6.3×10^{-27}	9.6×10^{-8} 8.3×10^{-8} 7.4×10^{-8}	7.4×10^{30} 6.4×10^{30} 5.8×10^{30}	2.4 2.4 1.8	1.5×10^{-26} 2.2×10^{-26} 7.2×10^{-27}	3.7×10^{-27} 3.3×10^{-27} ...	-5.2 0.10 0.17	-10.0 0.70 0.64
J1826–1334 \checkmark	9.85	-7.31×10^{-12}	$3.61 C$	1.93×10^{-25}	Bayesian \mathcal{F} -statistic $5n$ -vector	1.5×10^{-25} 1.5×10^{-25} 4.3×10^{-25}	1.3×10^{-3} 1.3×10^{-3} 3.7×10^{-3}	1.0×10^{35} 1.0×10^{35} 2.9×10^{35}	0.79 0.79 2.2	4.9×10^{-23} 3.7×10^{-23} ...	7.0×10^{-26} 7.6×10^{-26} ...	-3.8 0.42 ...	-5.7 0.39 0.42
J1828–1101 \checkmark	13.88	-2.85×10^{-12}	$4.77 C$	7.67×10^{-26}	Bayesian \mathcal{F} -statistic $5n$ -vector	4.2×10^{-26} 3.5×10^{-26} 5.9×10^{-26}	2.5×10^{-4} 2.1×10^{-4} 3.5×10^{-4}	1.9×10^{34} 1.6×10^{34} 2.7×10^{34}	0.55 0.46 0.78	5.3×10^{-24} 3.1×10^{-24} 3.8×10^{-24}	2.1×10^{-26} 2.1×10^{-26} ...	-4.6 0.98 0.66	-7.4 0.75 0.19
J1831–0952 \checkmark	14.87	-1.84×10^{-12}	$3.68 C$	7.7×10^{-26}	Bayesian \mathcal{F} -statistic $5n$ -vector	4.2×10^{-26} 3.2×10^{-26} 2.9×10^{-26}	1.6×10^{-4} 1.2×10^{-4} 1.2×10^{-4}	1.3×10^{34} 0.99×10^{34} 9.0×10^{33}	0.54 0.41 0.38	6.4×10^{-25} 9.1×10^{-25} 5.2×10^{-25}	1.9×10^{-26} 2.1×10^{-26} ...	-4.6 0.44 0.85	-8.0 0.64 0.77
J1833–0827 \checkmark	11.72	-1.26×10^{-12}	$4.50 i$	5.88×10^{-26}	Bayesian \mathcal{F} -statistic $5n$ -vector	6.2×10^{-26} 5.4×10^{-26} 6.4×10^{-26}	4.8×10^{-4} 4.2×10^{-4} 4.9×10^{-4}	3.7×10^{34} 3.2×10^{34} 3.8×10^{34}	1.0 0.87 1.1	2.7×10^{-24} 3.5×10^{-24} 2.4×10^{-24}	3.0×10^{-26} 2.8×10^{-26} ...	-4.4 0.40 0.43	-7.2 0.66 0.35
J1837–0604 \checkmark	10.38	-4.84×10^{-12}	$4.78 C$	1.15×10^{-25}	Bayesian \mathcal{F} -statistic $5n$ -vector	7.8×10^{-26} 8.8×10^{-26} 9.3×10^{-26}	8.2×10^{-4} 9.3×10^{-4} 9.8×10^{-4}	6.3×10^{34} 7.1×10^{34} 7.6×10^{34}	0.68 0.77 0.80	5.6×10^{-24} 1.2×10^{-24} 4.7×10^{-24}	3.6×10^{-26} 3.6×10^{-27} ...	-4.4 0.97 0.98	-7.0 0.95 0.43
J1838–0655 β	14.18	-9.9×10^{-12}	$6.60 p$	1.02×10^{-25}	Bayesian \mathcal{F} -statistic $5n$ -vector	6.6×10^{-26} 7.1×10^{-26} 4.2×10^{-26}	5.1×10^{-4} 5.5×10^{-4} 3.3×10^{-4}	4.0×10^{34} 4.3×10^{34} 2.5×10^{34}	0.65 0.70 0.41	1.3×10^{-24} 2.6×10^{-24} 8.3×10^{-25}	3.4×10^{-26} 3.6×10^{-26} ...	-3.8 0.15 0.69	-6.7 0.04 0.29
J1849–0001 β	25.96	-9.54×10^{-12}	$7.00 q$	6.98×10^{-26}	Bayesian \mathcal{F} -statistic $5n$ -vector	1.4×10^{-26} 1.7×10^{-26} 1.4×10^{-26}	3.3×10^{-5} 4.0×10^{-5} 3.4×10^{-5}	2.6×10^{33} 3.2×10^{33} 2.6×10^{33}	0.19 0.23 0.2	1.3×10^{-25} 1.4×10^{-25} 6.3×10^{-26}	6.0×10^{-27} 8.1×10^{-27} ...	-5.2 0.18 0.078	-9.1 0.47 0.77
J1856+0245 \checkmark	12.36	-9.49×10^{-12}	$6.32 C$	1.12×10^{-25}	Bayesian \mathcal{F} -statistic $5n$ -vector	5.8×10^{-26} 5.3×10^{-26} 5.2×10^{-26}	5.7×10^{-4} 5.2×10^{-4} 5.1×10^{-4}	4.4×10^{34} 4.0×10^{34} 4.0×10^{34}	0.52 0.48 0.47	1.3×10^{-24} 1.8×10^{-24} 1.4×10^{-24}	2.9×10^{-26} 2.5×10^{-26} ...	-4.4 0.69 0.85	-7.8 0.66 0.40
J1913+1011 \checkmark	27.85	-2.62×10^{-12}	$4.61 C$	5.36×10^{-26}	Bayesian \mathcal{F} -statistic $5n$ -vector	1.1×10^{-26} 1.2×10^{-26} 1.2×10^{-26}	1.6×10^{-5} 1.7×10^{-5} 1.8×10^{-5}	1.2×10^{33} 1.3×10^{33} 1.4×10^{33}	0.21 0.23 0.23	6.5×10^{-26} 4.0×10^{-26} 3.6×10^{-26}	5.2×10^{-27} 5.8×10^{-27} ...	-5.2 0.96 0.89	-9.7 0.60 0.35
J1925+1720 \checkmark	13.22	-1.83×10^{-12}	$5.05 C$	5.94×10^{-26}	Bayesian \mathcal{F} -statistic $5n$ -vector	5.9×10^{-26} 5.4×10^{-26} 6.8×10^{-26}	4.1×10^{-4} 3.8×10^{-4} 4.6×10^{-4}	3.1×10^{34} 2.8×10^{34} 3.6×10^{34}	1.0 0.92 1.1	2.2×10^{-24} 4.2×10^{-24} 1.5×10^{-24}	2.8×10^{-26} 2.9×10^{-26} ...	-4.2 0.03 0.29	-6.2 0.33 0.014
J1935+2025 \checkmark	12.48	-9.47×10^{-12}	$4.60 C$	1.53×10^{-25}	Bayesian \mathcal{F} -statistic $5n$ -vector	5.5×10^{-26} 4.8×10^{-26} 3.7×10^{-26}	3.8×10^{-4} 3.3×10^{-4} 2.6×10^{-4}	3.0×10^{34} 2.6×10^{34} 2.0×10^{34}	0.36 0.31 0.24	1.5×10^{-24} 7.7×10^{-25} 1.6×10^{-24}	2.6×10^{-26} 2.3×10^{-26} ...	-4.6 0.98 0.57	-7.8 0.69 0.81

Table 2 continued

Table 2 (continued)

Pulsar Name	f_{rot} (Hz)	\dot{P}_{rot} (s s^{-1})	Distance (kpc)	h_0^{ed}	Analysis	$h_0^{95\%}$	$\epsilon^{95\%}$	$Q_{22}^{95\%}$ (kg m^2)	$\frac{h_0^{95\%}}{h_0^{\text{ed}}}$	$C_{21}^{95\%}$	$C_{22}^{95\%}$	Statistic @	Statistic #
(J2000)					Method							$l=2, m=1, 2$	$l=2, m=2$
J1952+3252 γ	25.30	-3.74×10^{-12}	$3.00 \hat{i}$	1.03×10^{-25}	Bayesian \mathcal{F} -statistic $5n$ -vector	$1.1(1.0) \times 10^{-26}$ 1.0×10^{-26} $1.1(1.1) \times 10^{-26}$	$1.2(1.1) \times 10^{-5}$ 1.1×10^{-5} $1.2(1.2) \times 10^{-5}$	$9.2(8.2) \times 10^{32}$ 8.4×10^{32} $9.1(9.5) \times 10^{32}$	$0.10(0.09)$ 0.091 $0.1(0.11)$	$1.9(68) \times 10^{-25}$ 2.2×10^{-25} $5.1(5.1) \times 10^{-26}$	$4.2(2.8) \times 10^{-27}$ 4.4×10^{-27} ...	$-5.3(-5.4)$ 0.03 0.54	$-8.6(-8.2)$ 0.77 0.72
J2016+3711 ζ	19.68	-2.81×10^{-11}	$6.10 \hat{T}$	1.58×10^{-25}	Bayesian \mathcal{F} -statistic $5n$ -vector	2.0×10^{-26} 3.2×10^{-26} 3.0×10^{-26}	7.4×10^{-5} 1.2×10^{-4} 2.4×10^{-4}	5.7×10^{33} 9.1×10^{33} 1.9×10^{34}	0.13 0.21 0.41	1.6×10^{-25} 1.2×10^{-25} 3.8×10^{-25}	8.8×10^{-27} 1.7×10^{-26} ...	-5.0 0.84 0.62	-9.1 0.07 0.020
J2021+3651 γ	9.64	-8.89×10^{-12}	$1.80 \hat{S}$	4.3×10^{-25}	Bayesian \mathcal{F} -statistic $5n$ -vector	$2.3(2.2) \times 10^{-25}$ $2.2(2.1) \times 10^{-25}$ $2.8(4.0) \times 10^{-25}$	$1.0(1.0) \times 10^{-3}$ $0.96(0.95) \times 10^{-3}$ $1.3(1.8) \times 10^{-3}$	$8.0(7.7) \times 10^{34}$ $7.7(7.4) \times 10^{34}$ $1(1.4) \times 10^{35}$	$0.53(0.51)$ $0.51(0.49)$ $0.66(0.93)$	$6.0(5.0) \times 10^{-23}$ $2.0(1.3) \times 10^{-22}$...	$1.1(1.1) \times 10^{-25}$ $1.1(1.1) \times 10^{-25}$...	$-3.1(-3.2)$ $0.09(0.65)$...	$-4.9(-5.2)$ $0.08(0.13)$ 1
J2022+3842 β	20.59	-3.65×10^{-11}	$10.00 \hat{t}$	1.07×10^{-25}	Bayesian \mathcal{F} -statistic $5n$ -vector	1.9×10^{-26} 1.7×10^{-26} 1.4×10^{-26}	1.0×10^{-4} 8.9×10^{-5} 7.5×10^{-5}	8.1×10^{33} 7.2×10^{33} 5.8×10^{33}	0.18 0.16 0.13	1.4×10^{-25} 8.0×10^{-26} 6.3×10^{-26}	8.6×10^{-27} 9.0×10^{-27} ...	-5.0 0.90 1	-9.1 0.60 0.77
J2043+2740 γ	10.40	-1.37×10^{-13}	$1.48 \hat{C}$	6.26×10^{-26}	Bayesian \mathcal{F} -statistic $5n$ -vector	1.1×10^{-25} 1.0×10^{-25} 7.9×10^{-26}	3.7×10^{-4} 3.4×10^{-4} 2.5×10^{-4}	2.8×10^{34} 2.5×10^{34} 2.0×10^{34}	1.8 1.6 1.2	1.2×10^{-23} 1.3×10^{-23} 6.9×10^{-24}	5.2×10^{-26} 4.4×10^{-26} ...	-4.1 0.42 0.26	-6.0 0.78 0.65
J2124-3358 α	202.79	-2.94×10^{-16}	$0.41 \hat{C}$	2.37×10^{-27}	Bayesian \mathcal{F} -statistic $5n$ -vector	9.2×10^{-27} 9.7×10^{-27} 5.4×10^{-27}	2.2×10^{-8} 2.3×10^{-8} 1.3×10^{-8}	1.7×10^{30} 1.8×10^{30} 9.8×10^{29}	3.9 4.1 1.3	9.9×10^{-27} 9.5×10^{-27} 5.1×10^{-27}	4.8×10^{-27} 4.8×10^{-27} ...	-5.0 0.78 0.73	-10 0.23 0.62
J2214+3000 η	320.59	-1.31×10^{-15}	$0.60 \hat{u}$	2.71×10^{-27}	Bayesian \mathcal{F} -statistic $5n$ -vector	9.0×10^{-27} 4.5×10^{-27} 5.4×10^{-27}	1.2×10^{-8} 0.60×10^{-8} 7.4×10^{-9}	9.6×10^{29} 4.8×10^{29} 5.7×10^{29}	3.3 1.7 1.8	8.6×10^{-27} 9.0×10^{-27} 7.5×10^{-27}	4.6×10^{-27} 5.8×10^{-27} ...	-5.3 0.81 0.11	-10 0.87 0.84
J2222-0137 α	30.47	-4.99×10^{-16}	$0.27 \hat{U}$	1.22×10^{-26}	Bayesian \mathcal{F} -statistic $5n$ -vector	1.3×10^{-26} 2.2×10^{-26} 1.3×10^{-26}	9.0×10^{-7} 1.5×10^{-6} 9.1×10^{-7}	6.9×10^{31} 1.2×10^{32} 7.0×10^{31}	1.1 1.9 3.3	4.1×10^{-26} 5.0×10^{-26} 4.9×10^{-26}	6.4×10^{-27} 1.1×10^{-26} ...	-5.1 0.93 0.016	-9.7 0.06 0.15
J2229+6114 γ	19.36	-2.9×10^{-11}	$3.00 \hat{W}$	3.29×10^{-25}	Bayesian \mathcal{F} -statistic $5n$ -vector	$1.5(0.9) \times 10^{-26}$ $1.5(0.63) \times 10^{-26}$ $1.3(0.99) \times 10^{-26}$	$2.8(1.8) \times 10^{-5}$ $2.9(1.2) \times 10^{-5}$ $2.4(1.9) \times 10^{-5}$	$2.2(1.4) \times 10^{33}$ $2.2(0.98) \times 10^{33}$ $1.8(1.4) \times 10^{33}$	$0.045(0.028)$ $0.046(0.032)$ $0.037(0.029)$	$1.8(1.6) \times 10^{-25}$ $2.9(2.5) \times 10^{-25}$ $3.9(3.2) \times 10^{-27}$	$6.8(4.6) \times 10^{-27}$ $4.7(2.5) \times 10^{-27}$...	$-5.1(-5.3)$ $0.24(0.41)$ 0.75	$-9.2(-9.4)$ $0.99(0.99)$ 0.88

References—The last two columns refers to the significance of the data against the noise hypothesis (@ for the dual-harmonic emission model, # for the single-harmonic emission model). For the Bayesian method, the columns show the base-10 logarithm of the Bayesian odds, comparing a coherent signal model modes to incoherent signal models. For the \mathcal{F} -statistic and the $5n$ -vector method, the columns show the p-value (for the $5n$ -vector method, considering a signal at just the $l = 2, m = 1$ mode for the dual-harmonic emission model).

References—The following is a list of references for pulsar ephemeris data used in this analysis: Nancay: α , NICER: β , JBO: γ , IAR: δ , Hobart: ϵ , FAST: ζ , CHIME: η , Chandra: θ , Fermi-LAT: κ .

References—The following is a list of references for pulsar distances and intrinsic period derivatives, and they should be consulted for information on the associated uncertainties on these quantities: (a) Ding et al. (2023), (b) Storm et al. (2004), (c) Yao et al. (2017), (d) Roberts et al. (1993), (e) Reardon et al. (2016), (f) Trimble (1968), (g) Walker (2012), (h) Bassa et al. (2016), (i) Verbiest et al. (2012), (j) Mereghetti et al. (2021), (k) Ding et al. (2021), (l) Baumgardt & Vasiliev (2021), (m) Ferdman et al. (2014), (n) Green et al. (1988), (o) Torres et al. (2019), (p) Lin et al. (2009), (q) H. E. S. S. Collaboration et al. (2018), (r) Liu et al. (2024), (s) Kirichenko et al. (2015), (t) Arzoumanian et al. (2011), (u) Guillemot et al. (2016), (v) Guo et al. (2021), (w) Halpern et al. (2001).

REFERENCES

- Aasi, J., Abadie, J., Abbott, B. P., et al. 2014, *ApJ*, 785, 119, doi: [10.1088/0004-637X/785/2/119](https://doi.org/10.1088/0004-637X/785/2/119)
- Abac, A. G., Abbott, R., Abouelfettouh, I., et al. 2024a, A search using GEO600 for gravitational waves coincident with fast radio bursts from SGR 1935+2154. <https://arxiv.org/abs/2410.09151>
- . 2024b, *The Astrophysical Journal Letters*, 970, L34, doi: [10.3847/2041-8213/ad5beb](https://doi.org/10.3847/2041-8213/ad5beb)
- Abadie, J., Abbott, B. P., Abbott, R., et al. 2011, *ApJ*, 737, 93, doi: [10.1088/0004-637X/737/2/93](https://doi.org/10.1088/0004-637X/737/2/93)
- Abbott, B. P., Abbott, R., Abbott, T. D., et al. 2017a, *PhRvD*, 96, 122006, doi: [10.1103/PhysRevD.96.122006](https://doi.org/10.1103/PhysRevD.96.122006)
- . 2017b, *ApJ*, 839, 12, doi: [10.3847/1538-4357/aa677f](https://doi.org/10.3847/1538-4357/aa677f)
- . 2019a, *PhRvD*, 100, 104036, doi: [10.1103/PhysRevD.100.104036](https://doi.org/10.1103/PhysRevD.100.104036)
- . 2019b, *PhRvD*, 99, 122002, doi: [10.1103/PhysRevD.99.122002](https://doi.org/10.1103/PhysRevD.99.122002)
- . 2019c, *ApJ*, 879, 10, doi: [10.3847/1538-4357/ab20cb](https://doi.org/10.3847/1538-4357/ab20cb)
- Abbott, R., Abbott, T. D., Abraham, S., et al. 2020, *ApJL*, 902, L21, doi: [10.3847/2041-8213/abb655](https://doi.org/10.3847/2041-8213/abb655)
- . 2021a, *PhRvX*, 11, 021053, doi: [10.1103/PhysRevX.11.021053](https://doi.org/10.1103/PhysRevX.11.021053)
- . 2021b, *ApJL*, 915, L5, doi: [10.3847/2041-8213/ac082e](https://doi.org/10.3847/2041-8213/ac082e)
- . 2021c, *ApJL*, 913, L27, doi: [10.3847/2041-8213/abffcd](https://doi.org/10.3847/2041-8213/abffcd)
- . 2021d, *ApJ*, 922, 71, doi: [10.3847/1538-4357/ac0d52](https://doi.org/10.3847/1538-4357/ac0d52)
- Abbott, R., et al. 2022, *Astrophys. J.*, 932, 133, doi: [10.3847/1538-4357/ac6ad0](https://doi.org/10.3847/1538-4357/ac6ad0)
- Abbott, R., Abe, H., Acernese, F., et al. 2022, *ApJ*, 935, 1, doi: [10.3847/1538-4357/ac6acf](https://doi.org/10.3847/1538-4357/ac6acf)
- Abbott, R., Abbott, T. D., Acernese, F., et al. 2023, *Physical Review X*, 13, 041039, doi: [10.1103/PhysRevX.13.041039](https://doi.org/10.1103/PhysRevX.13.041039)
- Amiri, M., Bandura, K. M., Boyle, P. J., et al. 2021, *ApJS*, 255, 5, doi: [10.3847/1538-4365/abfdcb](https://doi.org/10.3847/1538-4365/abfdcb)
- Andersson, N. 1998, *ApJ*, 502, 708, doi: [10.1086/305919](https://doi.org/10.1086/305919)
- Arzoumanian, Z., Gotthelf, E. V., Ransom, S. M., et al. 2011, *ApJ*, 739, 39, doi: [10.1088/0004-637X/739/1/39](https://doi.org/10.1088/0004-637X/739/1/39)
- Ashok, A., Beheshtipour, B., Papa, M. A., et al. 2021, *ApJ*, 923, 85, doi: [10.3847/1538-4357/ac2582](https://doi.org/10.3847/1538-4357/ac2582)
- Ashton, G., et al. 2019, *Astrophys. J. Suppl.*, 241, 27, doi: [10.3847/1538-4365/ab06fc](https://doi.org/10.3847/1538-4365/ab06fc)
- Astone, P., Colla, A., D’Antonio, S., et al. 2014a, *Phys. Rev. D*, 89, 062008, doi: [10.1103/PhysRevD.89.062008](https://doi.org/10.1103/PhysRevD.89.062008)
- . 2014b, *Phys. Rev. D*, 89, 062008, doi: [10.1103/PhysRevD.89.062008](https://doi.org/10.1103/PhysRevD.89.062008)
- Astone, P., D’Antonio, S., Frasca, S., & Palomba, C. 2010, *CQGra*, 27, 194016, doi: [10.1088/0264-9381/27/19/194016](https://doi.org/10.1088/0264-9381/27/19/194016)
- Astone, P., Frasca, S., & Palomba, C. 2005, *Class. Quant. Grav.*, 22, S1197, doi: [10.1088/0264-9381/22/18/S34](https://doi.org/10.1088/0264-9381/22/18/S34)
- Atwood, W. B., Abdo, A. A., Ackermann, M., et al. 2009, *ApJ*, 697, 1071, doi: [10.1088/0004-637X/697/2/1071](https://doi.org/10.1088/0004-637X/697/2/1071)
- Bassa, C. G., Antoniadis, J., Camilo, F., et al. 2016, *MNRAS*, 455, 3806, doi: [10.1093/mnras/stv2607](https://doi.org/10.1093/mnras/stv2607)
- Basu, A., Shaw, B., Antonopoulou, D., et al. 2022, *MNRAS*, 510, 4049, doi: [10.1093/mnras/stab3336](https://doi.org/10.1093/mnras/stab3336)
- Baumgardt, H., & Vasiliev, E. 2021, *MNRAS*, 505, 5957, doi: [10.1093/mnras/stab1474](https://doi.org/10.1093/mnras/stab1474)
- Bildsten, L. 1998, *ApJL*, 501, L89, doi: [10.1086/311440](https://doi.org/10.1086/311440)
- Bonazzola, S., & Gourgoulhon, E. 1996, *A&A*, 312, 675
- Brans, C., & Dicke, R. H. 1961, *PhRv*, 124, 925, doi: [10.1103/PhysRev.124.925](https://doi.org/10.1103/PhysRev.124.925)
- Capote, E., et al. 2024. <https://arxiv.org/abs/2411.14607>
- Ciolfi, R., & Rezzolla, L. 2013, *Mon. Not. Roy. Astron. Soc.*, 435, L43, doi: [10.1093/mnrasl/slt092](https://doi.org/10.1093/mnrasl/slt092)
- Cognard, I., & Backer, D. C. 2004, *ApJL*, 612, L125, doi: [10.1086/424692](https://doi.org/10.1086/424692)
- Cutler, C. 2002, *PhRvD*, 66, 084025, doi: [10.1103/PhysRevD.66.084025](https://doi.org/10.1103/PhysRevD.66.084025)
- Dall’Osso, S., & Perna, R. 2017, *MNRAS*, 472, 2142, doi: [10.1093/mnras/stx2097](https://doi.org/10.1093/mnras/stx2097)
- Ding, H., Deller, A. T., Fonseca, E., et al. 2021, *ApJL*, 921, L19, doi: [10.3847/2041-8213/ac3091](https://doi.org/10.3847/2041-8213/ac3091)
- Ding, H., Deller, A. T., Stappers, B. W., et al. 2023, *MNRAS*, 519, 4982, doi: [10.1093/mnras/stac3725](https://doi.org/10.1093/mnras/stac3725)
- D’Onofrio, L., De Rosa, R., & Palomba, C. 2024, in *Proceedings of XVIII International Conference on Topics in Astroparticle and Underground Physics — PoS(TAUP2023)*, Vol. 441, 109, doi: [10.22323/1.441.0109](https://doi.org/10.22323/1.441.0109)
- D’Onofrio, L., De Rosa, R., Palomba, C., et al. 2023, *Phys. Rev. D*, 108, 122002, doi: [10.1103/PhysRevD.108.122002](https://doi.org/10.1103/PhysRevD.108.122002)
- Dupuis, R. J., & Woan, G. 2005, *PhRvD*, 72, 102002, doi: [10.1103/PhysRevD.72.102002](https://doi.org/10.1103/PhysRevD.72.102002)
- D’Onofrio, L., Astone, P., Pra, S. D., et al. 2024, *Classical and Quantum Gravity*, 42, 015005, doi: [10.1088/1361-6382/ad94c5](https://doi.org/10.1088/1361-6382/ad94c5)
- Edwards, R. T., Hobbs, G. B., & Manchester, R. N. 2006, *MNRAS*, 372, 1549, doi: [10.1111/j.1365-2966.2006.10870.x](https://doi.org/10.1111/j.1365-2966.2006.10870.x)
- Espinoza, C. M., Kuiper, L., Ho, W. C. G., et al. 2024, *ApJL*, 973, L39, doi: [10.3847/2041-8213/ad778c](https://doi.org/10.3847/2041-8213/ad778c)

Table 3. Upper limits on the strain amplitude set with the narrowband search for each of the considered targets. As a reference, we list also the number of templates, N_{trials} , in the $f - \dot{f}$ plane. We report as well the lowest p-value found in the analysis with the corresponding threshold set after correcting a FAP of 10^{-2} for the trial factor. The nomenclature "pg" identifies the post-glitch analysis.

Pulsar Name (J2000)	N_{trials} $\times 10^6$	$h_0^{95\%}$ $\times 10^{-26}$	$h_0^{95\%}/h_0^{sd}$	Lowest p-value $\times 10^{-5}$	Threshold p-value $\times 10^{-11}$
J0205+6449	90	9.60	0.22	1.54	1.10
J0534+2200	1383	4.16	0.03	0.77	0.07
J0537-6910	298	3.52	1.21	0.13	0.33
J0537-6910 pg	119	3.75	1.29	$4 \cdot 10^{-4}$	0.84
J0540-6919	11	14.23	2.45	0.44	8.95
J0540-6919 pg	248	7.38	1.27	0.02	0.40
J0835-4510	23	21.53	0.06	8.50	4.18
J1811-1925	23	9.71	0.72	0.45	4.29
J1813-1246	24	5.81	0.31	4.07	4.03
J1813-1749	182	5.17	0.23	0.04	0.55
J1838-0655	21	12.98	1.27	2.93	4.68
J1913+1011	15	4.14	0.77	1.40	6.45
J1935+2025	16	17.84	1.17	0.63	5.94
J1952+3252	18	4.24	0.41	1.06	5.55
J2016+3711	73	6.31	0.40	1.37	1.37
J2021+3651	12	37.11	0.86	0.25	7.73
J2022+3842	99	5.80	0.54	0.25	1.01
J2229+6114	77	6.19	0.19	0.62	1.28

Espinoza, C. M., Lyne, A. G., Stappers, B. W., & Kramer, M. 2011, MNRAS, 414, 1679, doi: [10.1111/j.1365-2966.2011.18503.x](https://doi.org/10.1111/j.1365-2966.2011.18503.x)

Ferdman, R. D., Stairs, I. H., Kramer, M., et al. 2014, MNRAS, 443, 2183, doi: [10.1093/mnras/stu1223](https://doi.org/10.1093/mnras/stu1223)

Fesik, L., & Papa, M. A. 2020, ApJ, 895, 11, doi: [10.3847/1538-4357/ab8193](https://doi.org/10.3847/1538-4357/ab8193)

Friedman, J. L., & Morsink, S. M. 1998, ApJ, 502, 714, doi: [10.1086/305920](https://doi.org/10.1086/305920)

Fujisawa, K., Kisaka, S., & Kojima, Y. 2022, MNRAS, 516, 5196, doi: [10.1093/mnras/stac2585](https://doi.org/10.1093/mnras/stac2585)

Gancio, G., Lousto, C. O., Combi, L., et al. 2020, A&A, 633, A84, doi: [10.1051/0004-6361/201936525](https://doi.org/10.1051/0004-6361/201936525)

Gendreau, K. C., Arzoumanian, Z., Adkins, P., et al. 2016, SPIE Proceedings, 9905, 420, doi: [10.1117/12.2231304](https://doi.org/10.1117/12.2231304)

Ghosh, S. 2023, Monthly Notices of the Royal Astronomical Society, 525, 448, doi: [10.1093/mnras/stad2355](https://doi.org/10.1093/mnras/stad2355)

Ghosh, S., Pathak, D., & Chatterjee, D. 2023, The Astrophysical Journal, 944, 53, doi: [10.3847/1538-4357/acb0d3](https://doi.org/10.3847/1538-4357/acb0d3)

Gittins, F. 2024, Classical and Quantum Gravity, 41, 043001, doi: [10.1088/1361-6382/ad1c35](https://doi.org/10.1088/1361-6382/ad1c35)

Gittins, F., & Andersson, N. 2021, MNRAS, 507, 116, doi: [10.1093/mnras/stab2048](https://doi.org/10.1093/mnras/stab2048)

Glampedakis, K., & Gualtieri, L. 2018, Gravitational Waves from Single Neutron Stars: An Advanced Detector Era Survey, ed. L. Rezzolla, P. Pizzochero, D. I. Jones, N. Rea, & I. Vidaña, Vol. 457, 673, doi: [10.1007/978-3-319-97616-7_12](https://doi.org/10.1007/978-3-319-97616-7_12)

Glampedakis, K., Jones, D. I., & Samuelsson, L. 2012, PhRvL, 109, 081103, doi: [10.1103/PhysRevLett.109.081103](https://doi.org/10.1103/PhysRevLett.109.081103)

Green, D. A., Gull, S. F., Tan, S. M., & Simon, A. J. B. 1988, MNRAS, 231, 735, doi: [10.1093/mnras/231.3.735](https://doi.org/10.1093/mnras/231.3.735)

Guillemot, L., Smith, D. A., Laffon, H., et al. 2016, A&A, 587, A109, doi: [10.1051/0004-6361/201527847](https://doi.org/10.1051/0004-6361/201527847)

Guillemot, L., Cognard, I., van Straten, W., Theureau, G., & Gérard, E. 2023, A&A, 678, A79, doi: [10.1051/0004-6361/202347018](https://doi.org/10.1051/0004-6361/202347018)

Guo, Y. J., Freire, P. C. C., Guillemot, L., et al. 2021, A&A, 654, A16, doi: [10.1051/0004-6361/202141450](https://doi.org/10.1051/0004-6361/202141450)

Table 4. Limits on GW amplitude from dipole radiation in Brans-Dicke theory.

Pulsar Name	f_{rot}	\dot{f}_{rot}	Distance	$h_{0d}^{95\%}$	FAP
(J2000)	(Hz)	(Hz s ⁻¹)	(kpc)		
J0030+0451 ^{α}	205.53	-4.23×10^{-16}	0.33 ^{a}	8.77×10^{-27}	0.98
J0058-7218 ^{β}	45.94	-6.1×10^{-11}	59.70 ^{b}	3.02×10^{-26}	0.73
J0117+5914 ^{γ}	9.86	-5.69×10^{-13}	1.77 ^{c}	2.03×10^{-23}	1
J0205+6449 ^{γ}	15.22	-4.49×10^{-11}	3.20 ^{d}	$3.78(2.57) \times 10^{-25}$	0.99(0.79)
J0437-4715 ^{δ}	173.69	-4.15×10^{-16}	0.16 ^{e}	8.13×10^{-27}	0.98
J0534+2200 ^{γ}	29.95	-3.78×10^{-10}	2.00 ^{f}	$1.37(0.86) \times 10^{-25}$	0.46(0.99)
J0537-6910 ^{β}	62.03	-1.99×10^{-10}	49.70 ^{g}	$1.84(1.11) \times 10^{-26}$	0.98(0.60)
J0540-6919 ^{β}	19.77	-1.87×10^{-10}	49.70 ^{g}	$2.41(1.44) \times 10^{-25}$	0.92(0.36)
J0614-3329 ^{α}	317.59	-1.76×10^{-15}	0.63 ^{h}	1.78×10^{-26}	0.56
J0737-3039A ^{α}	44.05	-3.41×10^{-15}	1.10 ^{i}	4.08×10^{-26}	0.83
J0835-4510 ^{ϵ}	11.19	-1.57×10^{-11}	0.28 ^{i}	$4.12(2.73) \times 10^{-24}$	0.80(0.33)
J1231-1411 ^{α}	271.45	-5.92×10^{-16}	0.42 ^{c}	3.21×10^{-26}	1
J1412+7922 ^{β}	17.18	-9.72×10^{-13}	3.30 ^{j}	5.56×10^{-26}	0.93
J1537+1155 ^{α}	26.38	-1.65×10^{-15}	0.93 ^{k}	5.93×10^{-26}	0.97
J1623-2631 ^{γ}	90.29	-5.26×10^{-15}	1.85 ^{l}	3.10×10^{-25}	0.77
J1719-1438 ^{α}	172.71	-2.22×10^{-16}	0.34 ^{c}	5.44×10^{-27}	1
J1744-1134 ^{α}	245.43	-4.34×10^{-16}	0.40 ^{e}	1.60×10^{-26}	0.92
J1745-0952 ^{α}	51.61	-2.3×10^{-16}	0.23 ^{c}	4.30×10^{-26}	0.81
J1756-2251 ^{γ}	35.14	-1.26×10^{-15}	0.73 ^{m}	5.29×10^{-26}	0.64
J1809-1917 ^{γ}	12.08	-3.73×10^{-12}	3.27 ^{c}	3.25×10^{-24}	0.90
J1811-1925 ^{β}	15.46	-1.05×10^{-11}	5.00 ^{n}	6.20×10^{-25}	0.98
J1813-1246 ^{β}	20.80	-7.6×10^{-12}	2.63 ^{o}	3.60×10^{-25}	0.44
J1813-1749 ^{β}	22.35	-6.34×10^{-11}	6.15 ^{c}	1.09×10^{-25}	0.97
J1823-3021A ^{γ}	183.82	-1.14×10^{-13}	8.02 ^{l}	1.84×10^{-26}	0.58
J1824-2452A ^{α}	327.41	-1.73×10^{-13}	5.37 ^{l}	2.08×10^{-26}	0.49
J1826-1334 ^{γ}	9.85	-7.31×10^{-12}	3.61 ^{c}	3.69×10^{-25}	0.98
J1828-1101 ^{γ}	13.88	-2.85×10^{-12}	4.77 ^{c}	3.68×10^{-24}	1
J1831-0952 ^{γ}	14.87	-1.84×10^{-12}	3.68 ^{c}	1.13×10^{-24}	0.87
J1833-0827 ^{γ}	11.72	-1.26×10^{-12}	4.50 ^{i}	3.79×10^{-24}	0.82
J1837-0604 ^{γ}	10.38	-4.84×10^{-12}	4.78 ^{c}	9.77×10^{-24}	0.91
J1838-0655 ^{β}	14.18	-9.9×10^{-12}	6.60 ^{p}	2.91×10^{-24}	0.51
J1849-0001 ^{β}	25.96	-9.54×10^{-12}	7.00 ^{q}	1.70×10^{-25}	0.34
J1856+0245 ^{γ}	12.36	-9.49×10^{-12}	6.32 ^{c}	7.32×10^{-25}	1
J1913+1011 ^{γ}	27.85	-2.62×10^{-12}	4.61 ^{c}	8.43×10^{-26}	0.88
J1925+1720 ^{γ}	13.22	-1.83×10^{-12}	5.05 ^{c}	4.00×10^{-24}	0.70
J1935+2025 ^{γ}	12.48	-9.47×10^{-12}	4.60 ^{c}	1.57×10^{-24}	0.95
J1952+3252 ^{γ}	25.30	-3.74×10^{-12}	3.00 ^{i}	1.01×10^{-25}	0.78
J2016+3711 ^{ζ}	19.68	-2.81×10^{-11}	6.10 ^{r}	1.91×10^{-25}	0.90
J2021+3651 ^{γ}	9.64	-8.89×10^{-12}	1.80 ^{s}	$1.32(0.61) \times 10^{-22}$	0.39(0.08)
J2022+3842 ^{β}	20.59	-3.65×10^{-11}	10.00 ^{t}	7.44×10^{-24}	0.67
J2043+2740 ^{γ}	10.40	-1.37×10^{-13}	1.48 ^{c}	3.93×10^{-24}	0.97
J2214+3000 ^{η}	320.59	-1.31×10^{-15}	0.60 ^{u}	5.68×10^{-27}	1
J2222-0137 ^{α}	30.47	-4.99×10^{-16}	0.27 ^{v}	5.21×10^{-26}	0.96
J2229+6114 ^{γ}	19.36	-2.9×10^{-11}	3.00 ^{w}	$2.31(1.61) \times 10^{-25}$	0.86(0.25)

NOTE—For references and other notes see Table 2. Values in parentheses are those produced using the restricted orientation priors described in Section 3.1.1. The last column shows the false-alarm probability (FAP) for a signal, assuming that the $2\mathcal{D}$ value has a χ^2 distribution with 2 degrees-of-freedom.

- H. E. S. S. Collaboration, Abdalla, H., Abramowski, A., et al. 2018, *A&A*, 612, A2, doi: [10.1051/0004-6361/201629377](https://doi.org/10.1051/0004-6361/201629377)
- Halpern, J. P., Gotthelf, E. V., Leighly, K. M., & Helfand, D. J. 2001, *ApJ*, 547, 323, doi: [10.1086/318361](https://doi.org/10.1086/318361)
- Haskell, B., Andersson, N., Jones, D. I., & Samuelsson, L. 2007, *PhRvL*, 99, 231101, doi: [10.1103/PhysRevLett.99.231101](https://doi.org/10.1103/PhysRevLett.99.231101)
- Haskell, B., & Bejger, M. 2023, *Nature Astronomy*, 7, 1160
- Haskell, B., Samuelsson, L., Glampedakis, K., & Andersson, N. 2008, *MNRAS*, 385, 531, doi: [10.1111/j.1365-2966.2008.12861.x](https://doi.org/10.1111/j.1365-2966.2008.12861.x)
- Hobbs, G., Manchester, R., Teoh, A., & Hobbs, M. 2004, in *IAU Symposium*, Vol. 218, *Young Neutron Stars and Their Environments*, ed. F. Camilo & B. M. Gaensler, 139, doi: [10.48550/arXiv.astro-ph/0309219](https://doi.org/10.48550/arXiv.astro-ph/0309219)
- Hobbs, G., Jenet, F., Lee, K. J., et al. 2009, *MNRAS*, 394, 1945, doi: [10.1111/j.1365-2966.2009.14391.x](https://doi.org/10.1111/j.1365-2966.2009.14391.x)
- Hobbs, G. B., Edwards, R. T., & Manchester, R. N. 2006, *MNRAS*, 369, 655, doi: [10.1111/j.1365-2966.2006.10302.x](https://doi.org/10.1111/j.1365-2966.2006.10302.x)
- Hotan, A. W., van Straten, W., & Manchester, R. N. 2004, *PASA*, 21, 302, doi: [10.1071/AS04022](https://doi.org/10.1071/AS04022)
- Hunter, J. D. 2007, *CSE*, 9, 90, doi: [10.1109/MCSE.2007.55](https://doi.org/10.1109/MCSE.2007.55)
- Idrisy, A., Owen, B. J., & Jones, D. I. 2015, *Phys. Rev. D*, 91, 024001, doi: [10.1103/PhysRevD.91.024001](https://doi.org/10.1103/PhysRevD.91.024001)
- Iglewicz, B., & Hoaglin, D. 1993, *How to Detect and Handle Outliers*, ASQC basic references in quality control (ASQC Quality Press). <https://books.google.co.uk/books?id=siInAQAAIAAJ>
- Isi, M., Pitkin, M., & Weinstein, A. J. 2017, *PhRvD*, 96, 042001, doi: [10.1103/PhysRevD.96.042001](https://doi.org/10.1103/PhysRevD.96.042001)
- Jaranowski, P., & Królak, A. 2010, *CQGra*, 27, 194015, doi: [10.1088/0264-9381/27/19/194015](https://doi.org/10.1088/0264-9381/27/19/194015)
- Jaranowski, P., Królak, A., & Schutz, B. F. 1998, *PhRvD*, 58, 063001, doi: [10.1103/PhysRevD.58.063001](https://doi.org/10.1103/PhysRevD.58.063001)
- Johnson-McDaniel, N. K., & Owen, B. J. 2013, *PhRvD*, 88, 044004, doi: [10.1103/PhysRevD.88.044004](https://doi.org/10.1103/PhysRevD.88.044004)
- Jones, D. I. 2010, *MNRAS*, 402, 2503, doi: [10.1111/j.1365-2966.2009.16059.x](https://doi.org/10.1111/j.1365-2966.2009.16059.x)
- Karki, S., Tuyenbayev, D., Kandhasamy, S., et al. 2016, *Review of Scientific Instruments*, 87, 114503, doi: [10.1063/1.4967303](https://doi.org/10.1063/1.4967303)
- Keitel, D., Woan, G., Pitkin, M., et al. 2019, *Phys. Rev. D*, 100, 064058, doi: [10.1103/PhysRevD.100.064058](https://doi.org/10.1103/PhysRevD.100.064058)
- Kirichenko, A., Danilenko, A., Shternin, P., et al. 2015, *ApJ*, 802, 17, doi: [10.1088/0004-637X/802/1/17](https://doi.org/10.1088/0004-637X/802/1/17)
- Lander, S. K., & Jones, D. I. 2018, *MNRAS*, 481, 4169, doi: [10.1093/mnras/sty2553](https://doi.org/10.1093/mnras/sty2553)
- Leaci, P., Astone, P., D'Antonio, S., et al. 2017, *Physical Review D*, 95, doi: [10.1103/physrevd.95.122001](https://doi.org/10.1103/physrevd.95.122001)
- Leaci, P., & Prix, R. 2015, *Physical Review D*, 91, doi: [10.1103/physrevd.91.102003](https://doi.org/10.1103/physrevd.91.102003)
- Lewis, D. R., Dodson, R. G., Ramsdale, P. D., & McCulloch, P. M. 2003, in *Astronomical Society of the Pacific Conference Series*, Vol. 302, *Radio Pulsars*, ed. M. Bailes, D. J. Nice, & S. E. Thorsett, 121, doi: [10.48550/arXiv.astro-ph/0211010](https://doi.org/10.48550/arXiv.astro-ph/0211010)
- Lin, L. C.-C., Takata, J., Hwang, C.-Y., & Liang, J.-S. 2009, *MNRAS*, 400, 168, doi: [10.1111/j.1365-2966.2009.15468.x](https://doi.org/10.1111/j.1365-2966.2009.15468.x)
- Lin, R., van Kerkwijk, M. H., Kirsten, F., Pen, U.-L., & Deller, A. T. 2023, *ApJ*, 952, 161, doi: [10.3847/1538-4357/acdc98](https://doi.org/10.3847/1538-4357/acdc98)
- Liu, Q.-C., Zhong, W.-J., Chen, Y., et al. 2024, *MNRAS*, 528, 6761, doi: [10.1093/mnras/stae351](https://doi.org/10.1093/mnras/stae351)
- Lorimer, D. R., & Kramer, M. 2004, *Handbook of Pulsar Astronomy*, Vol. 4
- Lu, N., Wette, K., Scott, S. M., & Melatos, A. 2023, *Monthly Notices of the Royal Astronomical Society*, 521, 2103, doi: [10.1093/mnras/stad390](https://doi.org/10.1093/mnras/stad390)
- Luo, J., Ransom, S., Demorest, P., et al. 2019, *PINT: High-precision pulsar timing analysis package*, *Astrophysics Source Code Library*, record ascl:1902.007
- . 2021, *ApJ*, 911, 45, doi: [10.3847/1538-4357/abe62f](https://doi.org/10.3847/1538-4357/abe62f)
- Mastrogiovanni, S., Astone, P., D'Antonio, S., et al. 2017, *Class. Quant. Grav.*, 34, 135007, doi: [10.1088/1361-6382/aa744f](https://doi.org/10.1088/1361-6382/aa744f)
- McKee, J. W., Janssen, G. H., Stappers, B. W., et al. 2016, *MNRAS*, 461, 2809, doi: [10.1093/mnras/stw1442](https://doi.org/10.1093/mnras/stw1442)
- Melatos, A., & Payne, D. J. B. 2005, *ApJ*, 623, 1044, doi: [10.1086/428600](https://doi.org/10.1086/428600)
- Mereghetti, S., Rigoselli, M., Taverna, R., et al. 2021, *ApJ*, 922, 253, doi: [10.3847/1538-4357/ac34f2](https://doi.org/10.3847/1538-4357/ac34f2)
- Morales, J. A., & Horowitz, C. J. 2022, *MNRAS*, 517, 5610, doi: [10.1093/mnras/stac3058](https://doi.org/10.1093/mnras/stac3058)
- Ng, C.-Y., & Romani, R. W. 2004, *ApJ*, 601, 479, doi: [10.1086/380486](https://doi.org/10.1086/380486)
- . 2008, *ApJ*, 673, 411, doi: [10.1086/523935](https://doi.org/10.1086/523935)
- Nice, D., Demorest, P., Stairs, I., et al. 2015, *Tempo: Pulsar timing data analysis*, *Astrophysics Source Code Library*, record ascl:1509.002
- Nieder, L., Clark, C. J., Bassa, C. G., et al. 2019, *ApJ*, 883, 42, doi: [10.3847/1538-4357/ab357e](https://doi.org/10.3847/1538-4357/ab357e)
- Nieder, L., Clark, C. J., Kandel, D., et al. 2020, *ApJL*, 902, L46, doi: [10.3847/2041-8213/abb02](https://doi.org/10.3847/2041-8213/abb02)
- Owen, B. J. 2005, *Physical Review Letters*, 95, 211101, doi: [10.1103/PhysRevLett.95.211101](https://doi.org/10.1103/PhysRevLett.95.211101)
- Philippov, A., & Kramer, M. 2022, *Annual Review of Astronomy and Astrophysics*, 60, 495, doi: <https://doi.org/10.1146/annurev-astro-052920-112338>

- Piccinni, O. J., Astone, P., D'Antonio, S., et al. 2018, *Classical and Quantum Gravity*, 36, 015008, doi: [10.1088/1361-6382/aaefb5](https://doi.org/10.1088/1361-6382/aaefb5)
- Pitkin, M. 2022, *Journal of Open Source Software*, 7, 4568, doi: [10.21105/joss.04568](https://doi.org/10.21105/joss.04568)
- Pitkin, M., Gill, C., Jones, D. I., Woan, G., & Davies, G. S. 2015, *MNRAS*, 453, 4399, doi: [10.1093/mnras/stv1931](https://doi.org/10.1093/mnras/stv1931)
- Rajbhandari, B., Owen, B. J., Caride, S., & Inta, R. 2021, *Phys. Rev. D*, 104, 122008, doi: [10.1103/PhysRevD.104.122008](https://doi.org/10.1103/PhysRevD.104.122008)
- Ransom, S. 2011, PRESTO: Pulsar Exploration and Search TOolkit, Astrophysics Source Code Library, record ascl:1107.017
- Reardon, D. J., Hobbs, G., Coles, W., et al. 2016, *MNRAS*, 455, 1751, doi: [10.1093/mnras/stv2395](https://doi.org/10.1093/mnras/stv2395)
- Riles, K. 2023, *Living Reviews in Relativity*, 26, 3, doi: [10.1007/s41114-023-00044-3](https://doi.org/10.1007/s41114-023-00044-3)
- Roberts, D. A., Goss, W. M., Kalberla, P. M. W., Herbstmeier, U., & Schwarz, U. J. 1993, *A&A*, 274, 427
- Shamohammadi, M., Bailes, M., Flynn, C., et al. 2024, *MNRAS*, 530, 287, doi: [10.1093/mnras/stae016](https://doi.org/10.1093/mnras/stae016)
- Shklovskii, I. S. 1970, *Soviet Ast.*, 13, 562
- Sieniawska, M., & Jones, D. I. 2022, *MNRAS*, 509, 5179, doi: [10.1093/mnras/stab3315](https://doi.org/10.1093/mnras/stab3315)
- Singhal, A., Leaci, P., Astone, P., et al. 2019, *Classical and Quantum Gravity*, 36, 205015, doi: [10.1088/1361-6382/ab4367](https://doi.org/10.1088/1361-6382/ab4367)
- Skilling, J. 2004, in *American Institute of Physics Conference Series*, Vol. 735, *Bayesian Inference and Maximum Entropy Methods in Science and Engineering: 24th International Workshop on Bayesian Inference and Maximum Entropy Methods in Science and Engineering*, ed. R. Fischer, R. Preuss, & U. V. Toussaint (AIP), 395–405, doi: [10.1063/1.1835238](https://doi.org/10.1063/1.1835238)
- Skilling, J. 2006, *Bayesian Analysis*, 1, 833, doi: [10.1214/06-BA127](https://doi.org/10.1214/06-BA127)
- Smits, R., Lorimer, D. R., Kramer, M., et al. 2009, *A&A*, 505, 919, doi: [10.1051/0004-6361/200911939](https://doi.org/10.1051/0004-6361/200911939)
- Smits, R., Tingay, S. J., Wex, N., Kramer, M., & Stappers, B. 2011, *A&A*, 528, A108, doi: [10.1051/0004-6361/201016141](https://doi.org/10.1051/0004-6361/201016141)
- Soni, S., Berger, B. K., Davis, D., et al. 2024, LIGO Detector Characterization in the first half of the fourth Observing run. <https://arxiv.org/abs/2409.02831>
- Storm, J., Carney, B. W., Gieren, W. P., et al. 2004, *A&A*, 415, 531, doi: [10.1051/0004-6361:20034634](https://doi.org/10.1051/0004-6361:20034634)
- Torres, D. F., Viganò, D., Coti Zelati, F., & Li, J. 2019, *MNRAS*, 489, 5494, doi: [10.1093/mnras/stz2403](https://doi.org/10.1093/mnras/stz2403)
- Trimble, V. 1968, *AJ*, 73, 535, doi: [10.1086/110658](https://doi.org/10.1086/110658)
- Tuo, Y., Serim, M. M., Antonelli, M., et al. 2024, *ApJL*, 967, L13, doi: [10.3847/2041-8213/ad4488](https://doi.org/10.3847/2041-8213/ad4488)
- Ushomirsky, G., Cutler, C., & Bildsten, L. 2000, *MNRAS*, 319, 902, doi: [10.1046/j.1365-8711.2000.03938.x](https://doi.org/10.1046/j.1365-8711.2000.03938.x)
- van Straten, W., Demorest, P., & Osłowski, S. 2012, *Astronomical Research and Technology*, 9, 237, doi: [10.48550/arXiv.1205.6276](https://doi.org/10.48550/arXiv.1205.6276)
- Verbiest, J. P. W., Weisberg, J. M., Chael, A. A., Lee, K. J., & Lorimer, D. R. 2012, *ApJ*, 755, 39, doi: [10.1088/0004-637X/755/1/39](https://doi.org/10.1088/0004-637X/755/1/39)
- Verbiest, J. P. W., Bailes, M., van Straten, W., et al. 2008, *ApJ*, 679, 675, doi: [10.1086/529576](https://doi.org/10.1086/529576)
- Verma, P. 2021, *Universe*, 7, 351, doi: [10.3390/universe7070235](https://doi.org/10.3390/universe7070235)
- Viets, A. D., Wade, M., Urban, A. L., et al. 2018, *Classical and Quantum Gravity*, 35, 095015, doi: [10.1088/1361-6382/aab658](https://doi.org/10.1088/1361-6382/aab658)
- Walker, A. R. 2012, *Ap&SS*, 341, 43, doi: [10.1007/s10509-011-0961-x](https://doi.org/10.1007/s10509-011-0961-x)
- Weisskopf, M. C., Brinkman, B., Canizares, C., et al. 2002, *PASP*, 114, 1, doi: [10.1086/338108](https://doi.org/10.1086/338108)
- Wette, K. 2023, *Astroparticle Physics*, 153, 102880, doi: <https://doi.org/10.1016/j.astropartphys.2023.102880>
- Woan, G., Pitkin, M. D., Haskell, B., Jones, D. I., & Lasky, P. D. 2018, *ApJL*, 863, L40, doi: [10.3847/2041-8213/aad86a](https://doi.org/10.3847/2041-8213/aad86a)
- Yao, J. M., Manchester, R. N., & Wang, N. 2017, *ApJ*, 835, 29, doi: [10.3847/1538-4357/835/1/29](https://doi.org/10.3847/1538-4357/835/1/29)
- Yu, M., Manchester, R. N., Hobbs, G., et al. 2013, *MNRAS*, 429, 688, doi: [10.1093/mnras/sts366](https://doi.org/10.1093/mnras/sts366)
- Zimmermann, M., & Szedenits, Jr., E. 1979, *PhRvD*, 20, 351, doi: [10.1103/PhysRevD.20.351](https://doi.org/10.1103/PhysRevD.20.351)